ADDIS ABABA UNIVERSITY
SCHOOL OF GRADUATE STUDIES
DEPARTMENT OF EARTH SCIENCE

HYDROGEOCHEMICAL AND ISOTOPE HYDROLOGY IN INVESTIGATING GROUNDWATER RECHARGE AND FLOW PROCESSES, SOUTH AFAR EASTERN ETHIOPIA

A THESIS SUBMITTED TO THE SCHOOL OF GRADUATE STUDIES OF ADDIS ABABA UNIVERSITY IN PARTIAL FULFILLMENT OF THE REQUIREMENTS FOR THE DEGREE OF MASTER OF SCIENCE IN HYDROGEOLOGY

By: ADDISU DERESSA GELETA

JUNE, 2012
Addis Ababa

HYDROGEOCHEMIAL AND ISOTOPE HYDROLOGY IN INVESTIGATING GROUNDWATER RECHARGE AND FLOW PROCESSES; LOWER AFAR, EASTERN ETHIOPIA

A THESIS SUBMITTED TO THE SCHOOL OF GRADUATE STUDIES ADDIS ABABA UNIVERSITY IN PARTIAL FULFILLMENT OF THE REQUIREMENTS FOR THE DEGREE OF MASTER OF SCIENCE IN HYDROGEOLOGY

BY
ADDISU DERESSA GELETA
JUNE, 2012

ADDIS ABABA UNIVERSITY
SCHOOL OF GRADUATE STUDIES

HYDROGEOCHEMICAL AND ISOTOPE HYDROLOGY IN INVESTIGATING GROUNDWATER RECHARGE AND FLOW PROCESSES; SOUTH AFAR, EASTERN ETHIOPIA

BY: Addisu Deressa Geleta

APPROVED BY BOARD OF EXAMINERS:-

Dr. Seifu Kebede: _____

Chair Man

Dr. Seifu Kebede: _____

Advisor

EXAMINERS:

Dr. Dereje Ayalew: _____

Internal Examiner

Ato Tesfaye Tadesse: _____

External Examiner

DECLARATION

I, the undersigned, declare that this thesis is my original work, has not been presented for a degree in any other university and that all sources of materials used for the thesis have been duly acknowledged.

Addisu Deressa Geleta
Signature_____
Submission date _____

The thesis has been submitted for examination with my approval as university advisor
Dr. Seifu Kebede
Signature_____
Date _____

Place and date of submission:
Addis Ababa University, School of Graduate Studies,
June, 2012

ACKNOWLEDGEMENT

I would like to express my appreciation and gratitude to my advisor and instructor Dr. Seifu Kebede for his professional advice, guidance, support and provision of relevant reference materials for this research work.

I am thankful to Oromia Water Works Design and Supervision Enterprise (OWWDSE), for providing me secondary data, for facilitating and attaching me to the Somali Project for primary data collection for this research.

I am grateful to Prof. Tenalem Ayenew for his nice teaching of conceptual hydrogeology and provision of related references, to Dr. Tarun K.Raghuvanshi for his valuable and nice teaching of research methodology. My sincere thanks and appreciation goes to Ato Abenezer Kefeni and the current PhD students: Ato Tilahun Azagegn, Ato Gadisa Deyassa, Ato Silesh Mamo who assisted me a lot by sharing their valuable knowledge and assisting me to master different application soft wares. Ato Bereket Fentaw and Yonas Mulugeta from Ethiopian Institute of Geological Survey, Hydrogeology department, helped me to get the hydrogeological and hydrochemical data and maps of Harar sheet which partly covers the southeastern part of this research area.

I am also grateful to Water Works Design and Supervision Enterprise (WWDSE) Geological Survey of Ethiopia (GSE) and National Meteorological Services Agency for providing me the necessary data. I gratefully acknowledge all organizations and individuals who directly or indirectly supported me in this research work.

My appreciation and thanks is also goes to my friends Likisa Fanta and Roba Edao for their valuable experiences in sharing ideas and comments.

Finally, I would like to express my grateful thanks and appreciation to all my families and relatives for their heartfelt encouragement, best wishes and support both directly and indirectly.

ABSTRACT

The research area includes the eastern part of the lower Awash Basin and Aysha Basin located in the eastern part of Ethiopia (South Afar). The areas have two physiographic regions the Rift and the Eastern Escarpment. Stable environmental isotopes ($\delta^{18}O$ and $\delta\ ^{2}H$) and hydrogeochemistry of precipitation and groundwater are used for the eastern lower Awash basin. However, only hydrogeochemistry is used for Aysha basin due to unreliability of isotopic laboratory results.

The main objective of this research is to investigate groundwater recharge and flow processes in the area. The integrated application of hydrogeochemistry and stable isotope of water (^{2}H and ^{18}O) for investigating the recharge and flow processes is a new approach for the area under consideration compared to the previous works in the area. The methodologies applied to achieve the objectives set are sampling and analysis, hierarchical cluster analysis (HCA), inverse geochemical modeling, the plot of $\delta^{18}O$ vs $\delta\ ^{2}H$ and chloride mass balance (CMB). Analyses of the water samples collected for physico-chemical and isotope were conducted at the laboratory of Water Works Design and Supervision Enterprise (WWDSE) and Addis Ababa University (AAU) respectively.

Prior to using the water chemistry results for the intended application, charge balance evaluation is done and those with an error greater than 10% are rejected from the data set. Then hydrochemical facies analysis was conducted to identify the major water types. Accordingly, four major water types in the eastern lower Awash Basin: Ca-Mg-HCO3, Na-$HCO3^{-}$, Na-Cl-$SO4^{2-}$, or Na- $SO4^{2}$-Cl and Ca-Mg-Cl-SO4 or Ca-Mg-$SO4^{2}$-Cl and two major water types in the Aysha Basin: Ca- $(HCO3)_{2,}$ and Na-Ca- SO4 or Cl were identified. Bicarbonate type water represent recharge area groundwater in topographically higher areas and fast moving discharge area groundwater in the rift. However, as groundwater moves toward rift it evolves to chloride or sulfate water type. HCA also classified the groundwaters of eastern lower Awash basin in to two major groups and eight subgroups and that of Aysha basin in to two major groups and five subgroups. The spatial distribution map of HCA in the basins clearly indicated the groundwater flow directions. Based on the clustering results inverse geochemical modelings are carried out along five selected flow paths in the Awash Basin and along one path in the Aysha Basin. Accordingly, the results indicate dissolution of halite, anhydrite, silicate minerals, consumption of CO2 during silicate hydrolysis, cation-exchange, and precipitation of calcite and clay minerals along the flow path toward the rift.

For the eastern part of lower Awash Basin, the plot of $\delta^{18}O$ vs $\delta^{2}H$ for groundwater identified three recharge mechanisms using local meteoric water line (LMWL) derived from Addis Ababa rainfall: recharge from local rainfalls, recharge from evaporated flood waters or mixing, and regional groundwater which are most likely recharged by lateral infiltration of meteoric water. The integrated analysis of salinity (TDS) and $\delta^{18}O$ also identified two major processes for the origin of salinity: evaporation and dissolution. The annual recharge rates computed using CMB method for the eastern lower Awash and Aysha Basins are 29.15 and 58.24 mm/year respectively. However, the figure is extremely over estimated for the Aysha Basin due to fast selective recharge. The average annual rainfall amount and average Cl concentration in rainfall accounted for the CMB method are 662.81mm/year and 0.91 mg/l respectively. Ninety nine (99) groundwater Cl concentrations (93 from Awash and 6 from Aysha basin) are used.

Keywords: Groundwater, recharge, flow processes, hydrogeochemistry, environmental isotopes

Table of Contents

1. INTRODUCTION……1

1.1 BACKGROUND 1

1.2 STATEMENTS OF THE PROBLEM 2

1.3 OBJECTIVES 2

1.3.1 GENERAL OBJECTIVE 2

1.3.2 SPECIFIC OBJECTIVES 2

1.4 RELAVANCE OF THE RESEARCH 3

1.5 RESEARCH DESIGN 3

1.5.1 APPROACHES 3

1.5.1.1 DESK STUDY 3

1.5.1.2 FIELD WORK 4

1.5.2 LITERATURE REVIEW 4

1.5.3 MATERIALS AND DATA INPUT 7

1.6 THESIS OUTLINE 7

2. AREA DESCRIPTIONS……9

2.1. LOCATION AND ACCESSIBILITY 9

2.2. PHYSIOGRAPHY 9

2.3 CLIMATE 10

2.3.1 SPATIAL DISTRIBUTION OF RAINFALL USING THIESSON POLYGON METHOD 12

2.3.2 SPATIAL DISTRIBUTION OF RAINFALL USING ISOHYETAL METHOD 14

2.4 LAND USE-LAND COVER 15

2.5 GEOLOGY 17

2.5.1 GENERAL 17

2.5.2. PRECAMBRIAN ROCKS 17

2.5.2. MESOZOIC SEDIMENTARY ROCKS 18

2.5.3. CENOZOIC FORMATIONS....19
2.6 HYDROGEOLOGY....23
2.6.1 GENERAL....23
2.6.2 AQUIFER PRODUCTIVITY AND PROPERTIES....23
2.7 STRUCTURES....26
2.7.1 REGIONAL STRUCTURES....26
2.7.2 RESEARCH AREA GEOLOGICAL STRUCTURES....27
3. METHODOLOGY....29
3.1 GENERAL....29
3.2 SAMPLING AND ANALYSIS....29
3.3 HYDROGEOCHEMICAL METHODS....31
3.3.1 GENERAL....31
3.3.1 HIERARCHICAL CLUSTER ANALYSIS (HCA)....31
3.3.2 INVERSE GEOCHEMICAL MODELLING....32
3.3.3 CORRELATION OF MAJOR ION AND TOTAL DISSOLVED ION....33
3.3.4 GROUNDWATER RECHARGE ESTIMATION....33
3.3.4.1 CHLORIDE MASS BALANCE (CMB) METHOD....34
3.4 ISOTOPE HYDROLOGY....34
3.4.1 OXYGEN (δ18O) AND DEUTRIUM (δ2H) ISOTOPES....35
3.4.2 INTEGRATION OF STABLE ISOTOPE AND HYDROGEOCHEMISTRY....35
4. HYDROGEOCHEMICAL METHOD....36
4.1 GENERAL....36
4.2 PHYSICAL PROPERTIES....36
4.2.1 TEMPERATURE....36
4.2.2 HYDROGEN-ION ACTIVITY (PH)....37
4.2.3 TOTAL DISSOLVED SOLIDS (TDS)....37

4.2.4 ELECTRICAL CONDUCTIVITY (EC) 38
4.3 CHEMICAL PROPERTIES 40
4.3.1 HYDROCHEMICAL FACIES 40
4.3.2 HYDROGEOCHEMISTRY OF GROUNDWATER 42
4.3.3 HYDROGEOCHEMISTRY OF SURFACE WATER 45
4.4 CORRELATION OF MAJOR ION AND TOTAL DISSOLVED ION 46
4.6 HIERARCHICAL CLUSTER ANALYSIS (HCA) 50
4.7 INVERSE GEOCHEMICAL MODELING 59
4.8 GOUNDWATER QUALITY 65
4.8.1 DRINKING WATER QUALITY 66
4.8.1 IRRIGATION WATER QUALITY 66
5. STABLE ISOTOPES OF WATER 69
5.1 ISOTOPIC COMPOSITION OF THE RESEARCH AREA RAIN WATER 70
5.2 OXYGEN (δ18O) AND DEUTRIUM (δ2H) ISOTOPES 71
5.3 ISOTOPIC COMPOSITION OF GROUNDWATER 74
5.4 ISOTOPIC SIGNATURE OF SURFACE WATER 75
6. RECHARGE PROCESSES 78
6.1GENERAL 78
6.2 HYDROGEOCHEMICAL EVIDENCES 79
6.2.1EQUILIBRIUM CONDITIONS OF GROUNDWATER 79
6.2.2 CALCIUM TO MAGNESIUM RATIO (Ca/Mg) IN GROUNDWATER 82
6.3 ISOTOPIC EVIDENCES 83
6.3.1 DEUTRIUM (^{2}H) vs OXYGEN (^{18}O) 83
6.3.2 ALTITUDE EFFECT 85
6.4 INTEGRATION OF STABLE ISOTOPE AND HYDROGEOCHEMISTRY 86
6.5. GROUNDWATER RECHARGE ESTIMATION 87

6.5.1 CHLORIDE MASS BALANCE (CMB) METHOD 87

6.5.2 RELATIONSHIP OF GROUNDWATER CHLORIDE AND RECHARGE RATE 91

7. CONCLUSIONS AND RECOMMENDATIONS……...93

7.1 CONCLUSIONS 93

7.2 RCOMMENDATIONS 95

REFERENCES……..97

ANNEXES……....101

List of Figures

Figure 1.1 Flow charts of data input and methodologies applied for the research 8

Figure 2.1 Location map of the area 10

Figure 2.3 Graphs showing: Mean Min, Mean Max and average temperature and variation of precipitation with altitude 11

Figure 2.4 Thiesson polygon map of the area 13

Figure 2.5 Rainfall isohyetal map of the area 15

Figure 2.6 Land use-land cover map 16

Figure 2.7 Some geological structures & units in the area 19

Figure 2.8 Young formations and dikes 21

Figure 2.9 Geological map of the area 22

Figure 2.10 Discharge of Boreholes and transmissivity in different formations at the foot of the Escarpment 25

Figure 2.11 Hydrogeological Map of the area. 26

Figure 2.12 Structural Map of the area superimposed on the geology 28

Figure 3.1 Location of total samples used for analysis 30

Figure 4.1 A graph showing correlation between TDS and EC of Eastern Lower Awa……38

Figure 4.2 Spatial distribution map of TDS 38

Figure 4.3 Spatial distribution map of Electrical conductivity (EC) 39

Figure 4.4 Piper plot of water samples from eastern lower Awash Basin 40

Figure 4.5 Piper plot of water samples from Aysha Basin 41

Figure 4.6 Hydrochemical representations of groundwaters 44
Figure 4.7 Hydrochemical representations of surface water 45
Figure 4.8 Composition diagrams of the major ions plotted against total dissolved ions (TDI) for the eastern lower Wash Basin 47
Figure 4.9 Dendrogram of Hierarchical Cluster Analysis (HCA) for Eastern Lower Awash Basin 52
Figure 4.10 Dendrogram of Hierarchical Cluster Analysis (HCA) for Aysha Basin 53
Figure 4.11 Spatial Distribution Map of Groundwater clusters for eastern lower Awash and Aysha Basins 58
Figure 4.12 Selected flow paths for inverse geochemical modeling 61
Figure 4.13 Wilcox diagram of Sodium Adsorption Ratio (SAR); A) Awash and B) Aysha groundwater in the investigation area 68
Figure 5.1 Scatter plot of deutrium (^{2}H) vs oxygen (^{18}O) monitored at Addis Ababa station by IAEA from 1961-2007 69
Figure 5.2 Location of sampling points for isotope data 70
Figure 5.3 Plot of Isotopic signature of summer rainfall of 2011 from inside and around the investigation area 71
Figure 5.4 A plot of Deuterium (^{2}H) and Oxygen 18 isotopes of water samples 73
Figure 5.5 Spatial distribution map of d18O in the eastern lower Awash Basin over classified DEM 74
Figure 5.6 Graph showing Isotopic compositions of groundwater 75
Figure 5.7 Graph showing isotopic compositions of surface water 77
Figure 6.1 The various mechanisms of recharge in a (semi-)arid area (after Lerner, 1990). 78
Figure 6.2 Graph of Saturation Indices (SI) of common minerals in eastern lower Awash Basin 80
Figure 6.3 Graph of Saturation Indices (SI) of common minerals in Aysha Basin 81
Figure 6.4 Spatial distribution map of Ca to Mg ratio in groundwater of the investigation area 83

Figure 6.5 The plot of $\delta^{18}O$ vs $\delta^{2}H$ for the eastern part of lower Awash Basin groundwater 84
Figure 6.6 A scatter diagram showing a relationship between groundwater $\delta^{18}O$ and altitude 86
Figure 6.7 Relationship between salinity and stable isotope concentration for salinization processes identification in groundwater 87
Figure 6.8 Spatial distribution map of Recharge rate estimated using CMB for Awash and Aysha Basins 91
Figure 6.9 The curve showing the relationship between groundwater chloride and recharge rate 92

List of Tables

Table 4.1 Min and Max TDS values (Mg/L) recorded in the Basins from different sources 38
Table 4.2 Correlation matrices for eastern lower Awash Basin groundwater data 49
Table 4.3 Correlation matrices for Aysha Basin groundwater data 50
Table 4.4 Clusters Mean Values of parameters for eastern lower Awash Basin 54
Table 4.5 Clusters Mean Values of Compositions for Aysha Basin..... 54
Table 4.6 Descriptions for Eastern Lower Awash Basin groundwater clusters using (HCA) 55
Table 4.7 Groundwater chemistry data used for the Modeling 60
Table 4.8 Summary of petrographic analysis of some rocks in the area (source: WWDSE, 2003) 60
Table 4.9 Comparisons of min. and max. recorded parameters in the area with guidelines of WHO (2011) 66

ACRONYM

AAU – Addis Ababa University

CMB – Chloride Mass Balance

DEM - Digital Elevation Map

DDAC - Dire Dawa Administrative Council

EC – Electrical Conductivity

GMWL – Global Meteoric Water Line

GNIP-Global Networking of Isotopes in Precipitation

GSE – Geological Survey of Ethiopia

HCA – Hierarchical Cluster Analysis

IAEA – International Atomic Energy Agency

IGM – Inverse Geochemical Modeling

ITCZ - Inter-Tropical Convergence Zone

LMWL – Local Meteoric Water Line

MER – Main Ethiopian Rift

OWWDSE – Oromia Water Works Design and Supervision Enterprise

SAR – Sodium Adsorption Ratio

SMOW –Standard Mean Oceanic Water

TDS – Total Dissolved Solids

TDI - Total Dissolved Ions

VSMOW – Vienna Standard Mean Oceanic Water

WHO – World Health Organization

WWDSE – Water Works Design and Supervision Enterprise

1. INTRODUCTION

1.1 BACKGROUND

Groundwater is the only source of water for domestic and irrigation purposes in the investigation area due to lack of adequate surface water flows. Modern drought is also expanding in an alarming rate in the arid and semi-arid parts of the area beside an increasing demand of groundwater development. Realizing these facts, starting from 2003 the Federal Government has been planning and supporting the study and development of groundwater resources conducted by Water Works Design and Supervision Enterprise (WWDSE) in the area for Dire Dawa and Harar town water supply. In addition, the government has been involving in groundwater potential assessment and water supply projects of Shinille Zone, which have been carrying out by Oromia Water Works Design and Supervision Enterprise (OWWDSE) since 2009. Currently, based on the good result of potential assessment medium to large scale groundwater based irrigation projects are under construction in Shinille zone. Even though, the assessment result revealed the potentiality of the area from groundwater resource perspectives, it did not account the Escarpment zone and Dire Dawa Administrative council which are helpful to get the complete information about recharge processes and groundwater evolution.

Therefore, the successfulness and sustainability of such large projects should require good investigations of the isotope hydrology and hydrogeochemistry of the area in complement to hydrogeology and geology. That is because new findings and investigations can be an input for better and sustainable groundwater development and management of the Basins.

The purpose of this research is to investigate the groundwater recharge and flow processes of the area. Moreover, identifications of the recharge source and mechanism, processes and source of salinity in the area have a significant value for the community of the area, due to increasing demand of groundwater for irrigation and domestic water supply. It is also helpful from Basin development and management perspectives. The investigation is approached through the use of hydrogeochemical and stable environmental isotope data collection, analysis and interpretation.

1.2 STATEMENTS OF THE PROBLEM

In the research area groundwater is the only source of domestic water supply. It is because of the majority of the area is characterized by semi-arid climate which has low rainfall amount, frequency and spatial distribution, and scarce surface water. In addition, currently the demand for medium to large scale groundwater based irrigation is also getting increased in the rift which has not ever practiced. Harar and Dire Dawa towns' water supply is also from the investigation area. To supply these alarming demands of water in the area, groundwater potential assessment and development has been carrying out since 2003.

However, further beyond the groundwater potential assessment and development there are some problems which were not answered. The problems are lack of scientific and evidential information about the sources of recharge and mechanism; the major processes for the source of salinity; non-availability of geochemical modeling results that show the flow processes from recharge to discharge area; lack of possible estimated recharge rate over the basins and no availability of previous generated isotopic data.

Therefore, the understandings of the groundwater recharge sources and mechanisms, the types of chemical reactions that took place and the minerals that dissolve/precipitate as the water moves from recharge to discharge area as well as the identification of salinity sources, processes and the determination of recharge rates are very essential for effective, well managed and sustainable use and development of water resources.

1.3 OBJECTIVES

1.3.1 GENERAL OBJECTIVE

The main objective of the research is to investigate groundwater recharge and flow processes using hydrogeochemistry and stable environmental isotope hydrology (^{2}H & ^{18}O).

1.3.2 SPECIFIC OBJECTIVES

The specific objectives of the research are as follows:

- ❖ To identify isotopic composition of rain water and groundwater in the area

- ❖ To identify the sources and mechanisms of groundwater recharge
- ❖ To determine the major processes for the origin of salinity
- ❖ To model the geochemical evolution of the groundwater along its flow path. This is to determine the type and amount (in moles) of mineral species that dissolve/precipitate along the selected flow paths
- ❖ To estimate groundwater recharge rates over the basins

1.4 RELAVANCE OF THE RESEARCH

The integrated utilization of hydrogeochemistry and stable isotope of water (^{2}H and ^{18}O) for investigating the recharge processes and salinity origins are the new approaches for the area under consideration compared to the previous works in the area. The result of this research could be an input for the limited fresh water resource development and management of the basins. Especially, not only in filling the data gaps concerning the sources of recharge and mechanism, but also in identifying the different flow processes that result in the origins of salinity. The result can also be used as a data source for future researchers and for both governmental and non-governmental organizations who/which are interested in water related works of the area.

In the last few years the demand for groundwater exploration in the region is also becoming increased for water supply and irrigation purposes. This is as a result of scarce surface water and expansion of the modern drought in the area. Therefore, the final result of this research can also be used as an input for further and sustainable groundwater exploitation and management.

1.5 RESEARCH DESIGN

1.5.1 APPROACHES

The research approaches followed are as summarized below:

1.5.1.1 DESK STUDY

- ➢ Gathering and reviewing of available previous works within and around the study area from different sources for instances, water supply and irrigation study

reports, meteorological data, geological, hydrochemical and hydro geological maps and reports from various sectors

- Delineating the study area with the help of Global Mapper and Arc GIS, to determine the boundary of research area considering basin water divide
- Plotting the collected secondary data on DEM (Digital Elevation Map) or Base Map to identify data gaps
- Understanding the geological and hydro geological set up of the research area using gathered maps and reports

1.5.1.2 FIELD WORK

Field survey is conducted to obtain primary data and observation for the research.

- Georeferencing and sampling the representative water sources along the traverses made
- Collection of well completion reports with their water quality from zonal water offices and NGOs
- Sampling rainwater both from highland and low land for both physico-chemical and isotope analsis
- Observation and description of geologic units, structures, grain size and geomorphology
- Observation of land cover and land use practice of the area

1.5.2 LITERATURE REVIEW

Almost no water related studies have been conducted in the northern and northeastern part of the research area previously. All previous works are concentrated around Dire Dawa town and the Escarpment. However, starting from 2009 Oromia Water Works Design and Supervision Enterprise (OWWDSE) has been carrying out groundwater potential assessment projects for water supply and irrigation purposes for the entire shinille zone of Awash and Aysha Basins. Some of the relevant literatures reviewed are as follows:

Andarge and Jiri (2010), Hydrogeological and Hydrochemical Maps of Harar NC 38-9 and NC 38-10, Geological Survey of Ethiopia

The authors produced water quality data base, hydrogeological and hydrochemical maps with a scale of 1:250,000, which cover a few portion of the research area in the southeastern part.

Jiri and Habteab (1986), Hydrogeology and Hydrochemistry of the Dire Dawa Area, NC 37-12 Sheet, Geological Survey of Ethiopia, Addis Ababa, unpublished report

They indicated as the surface water divide between the Awash and Wabe Shebelle basins roughly corresponds with the boundary between the Eastern Plateau and the Eastern Escarpment. Runoff and base flow on this plateau drain relatively slowly southwards in contrast to the ones of the escarpment which flow rapidly northwards until it reaches the plain of Afar, where it quickly lose its water in to the alluvium. The work also indicated the general increase of TDS of groundwater northwards through the alluvial sediments and the occurrence of basic groundwater -Ca-HCO_3 type with TDS less than 1000mg/l at plateau and escarpment areas and transitional Na-HCO_3 and Ca-Na-HCO_3 types at the foot of the escarpment with TDS ranging from 500-1000mg/l. The groundwater is warm and of basic Na-HCO_3 type at the Alledeghe plain and emerges from faulted basalt.

OWWDSE (2011), Shinille groundwater potential assessment project, Addis Ababa, Inception report

The study suggested that the major recharge inducing to the groundwater of rift plain comes from the southern highlands which are experienced by regular precipitation. This work supports the hypothesis by the dissection, shuttering, and structurally controlled geology that receives prolonged annual rainfall of significant amount due to its distinct elevated topography. The study also addressed the tectonic dynamicity of the region to trigger the onset of networked geological structures that could allow the groundwater flow path to the low land of the rift. The same work pointed out that groundwater flow direction in the Awash Basin of the area converges to the NNW direction which the seasonal streams ultimately follow; salinity behavior of groundwater also increases along the flow direction and the water type is dominantly Ca-Na-HCO3-SO4-Cl. Some times SO4 and Cl concentration rule out.

WWDSE (2004), Dire Dawa Administrative Council Integrated Resource Development Master Plan Study Project, Part 2-Hydrogeology

This study identified the existence of highest TDS in the alluvial sediments at the foot of the Escarpment relative to the other formations. This work also characterized the upper sandstone as the highest potential aquifer followed by limestone and alluvium. However, the study distinguished the basaltic aquifers as the least productive aquifers near the Escarpment.

Seifu et al. (2004), Groundwater recharge circulation and geochemical evolution in the source region of the Blue Nile River, Applied Geochemistry

The authors identified two major structurally deformed regions with distinct groundwater circulation and evolution history. These are Lake Tana graben and Yerer Tuluwolel Volcanic lineaments. The basaltic plateau aquifers outside these regions are a source of rapid recharge through fractures because of their low TDS. The authors pointed out the difference between isotopic signature of waters of the rift and plateau, rift ward movement of ground water from the plateau zone.

Seifu (2004), Environmental isotopes and geochemistry in investigating groundwater and lake hydrology: cases from the Blue Nile basin & the Ethiopian Rift, Ethiopia, PhD dissertation

The use of geochemical and isotope hydrological data helped him to identify two types of groundwater systems in the upper Blue Nile basin. These are the low salinity, Ca-Mg-HCO3 type, isotopically relatively enriched cold (13-25°C) groundwaters from the basaltic plateau and the high TDS, Na-HCO3 type, isotopically relatively depleted low temperature (25-40 °C) thermal groundwater systems from the deeply faulted grabens.

Tenalem et al. (2009), Hierarchical cluster analysis of hydrochemical data as a tool for assessing the evolution and dynamics of groundwater across the Ethiopian rift, International Journal of Physical Sciences Vol. 4 (2)

The authors distinguished the existence of different hydrochemical facies corresponding to various hydrogeological regimes across the rift valley using the conventional hydrochemical data analysis and Q-mode hierarchical cluster analysis.

Tesfamikael (1974), Hydrogeology of Dire Dawa Area, Geological Survey of Ethiopia, Addis Ababa, Unpublished report No. 11

His investigation suggested as the infiltrated water rapidly joins the regional groundwater body which is at a minimum depth of 25m, in the escarpment zone and in the southern edge of the plains area where rocks of relatively higher infiltration capacities occur. The infiltration occurs through the fissures (cracks) in limestone while concentrated infiltration occurs along the river beds through the gravels and exposed limestones and sandstones. His potential evapotranspiration estimation at Dire Dawa showed 1984mm.

1.5.3 MATERIALS AND DATA INPUT

- Digital Elevation Map (30m resolution)
- Geological and hydrogeological maps, reports and raw data from various sectors
- Meteorological data records from National Meteorological Agency
- GPS for georeferencing the water points
- Hand held EC and PH meter kits to take in-situ measurements in the field
- Capped plastic bottles (1liter volume) to take water samples for physico-chemical analysis
- Capped glass bottles (25ml) for taking water samples for isotope analysis
- Arc GIS soft ware version 9.3, Global Mapper 8, Aquachem 4, Statistica, Surfer 8, PHREEQC Interactive 2.8, Microsoft Excel and Access 2007

1.6 THESIS OUTLINE

The thesis is structured in to 7 chapters. The first chapter contains introduction, statements of the problem, objectives and literature review. The second chapter deals with the general descriptions of the area such as climate, land use-land cover, geology and hydrogeology. The third chapter explains the different methodologies applied to achieve the objectives set. The fourth chapter presents the hydrogeochemical properties of the Basins. The fifth chapter talks about the isotopic compositions of rainwater, surface water and groundwater. The sixth chapter discusses about the various recharge processes. Finally, the seventh chapter draws conclusions and recommendations.

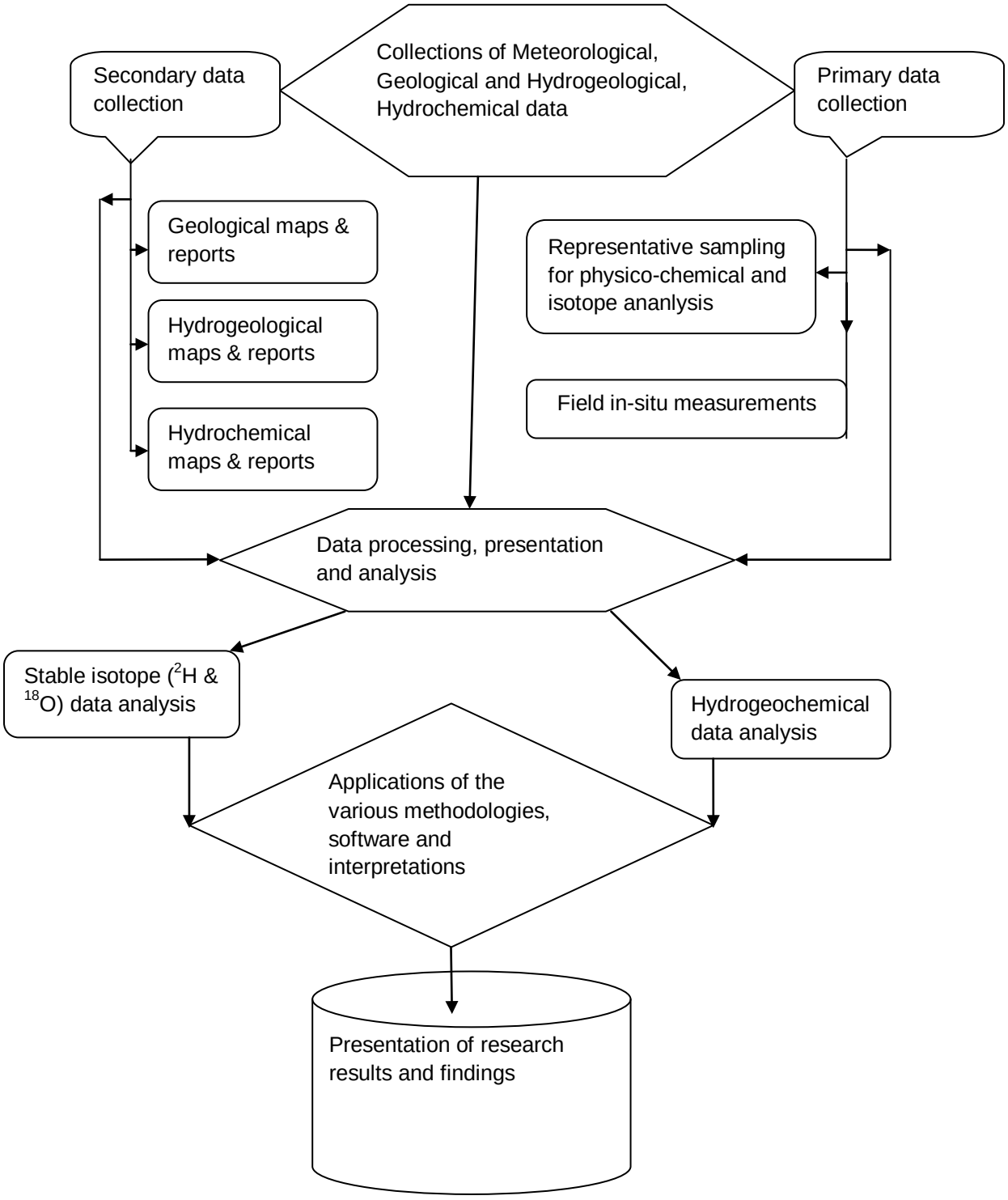

Figure 1.1 Flow charts of data input and methodologies applied for the research

2. AREA DESCRIPTIONS

2.1. LOCATION AND ACCESSIBILITY

The research area includes two basins namely: the eastern part of Lower Awash Basin and the Aysha Basin located in the Eastern part of Ethiopia. The area is bounded by Eastern Ethiopian Escarpment in the south, the Ethio-Somali political boundary in the east, Ethio-Djibouti border and Afar Depression in the north and Awash River water divide in the west. Its total areal coverage is estimated to be 45,979 km^2. Out of the total area Awash basin constitutes 41,887Km^2 (91%) while the Aysha Basin covers only 4,092 km^2 (9%). The area covers Dire Dawa Administrative Council (DDAC), Shinille Zone and very limited parts of East and West Hararghe Zones along the Eastern Escarpment.

The area is found between an elevation of approximately 3,000 and 230m above m.s.l and between 40^0 16' – 43^0 22' longitude and 8^0 56' - 11^0 11' latitude. The maximum elevation belongs to the highlands of the Escarpment while the minimum elevation belongs to the rift around Lake Abbe. It can be accessed by the Addis Ababa - Dire Dawa main asphalt road and Ethio-Djibouti railway. Additionally, it can also be reached by Dire Dawa - Djibouti and Dire Dawa - Miesso, through Erer, all weather roads (fig.2.1) and a number of dry weather road networked on the alluvial plains.

2.2. PHYSIOGRAPHY

There are two major physiographic subdivisions in the area under investigation. The first physiographic feature is the Rift valley, which mainly constitutes the research area, while the second feature is the Eastern Escarpment which bounds this area at the south.

The physiographic features of the research area are formed by the volcanic activities, erosional and depositional processes, and tectonic influences. The area is constituted by repetitive down thrown fault blocks (composed of volcanic rocks, Mesozoic sedimentary formations and basements) to the north around Dire Dawa due to ENE-WSW aligned faults in the south, Tadesse (1972). Whereas the flat plain that extends from the foot of the escarpment toward north is covered by alluvium. However, there are some acidic volcanic cones through the alluvium and basaltic ridges at the northern

extreme of the research area. The elevation of the area ranges from about 3,000m to 230m above m.s.l and have a significant drop of 2,750 meters within 190km from south to north.

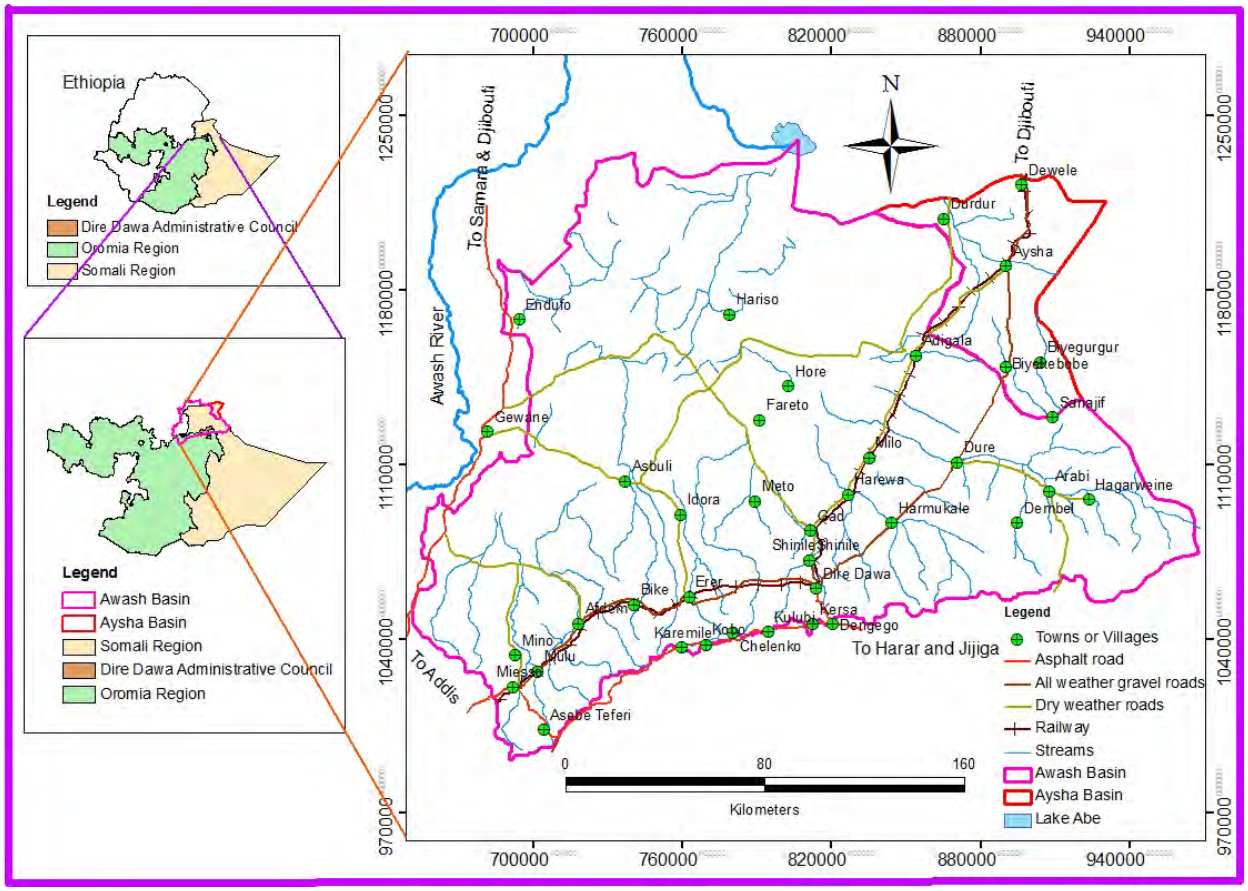

Figure 2.1 Location map of the area

2.3 CLIMATE

The climate of the area varies significantly as one goes from the escarpment, where the climate is moderate, to the northern extreme of the area toward the Afar Depression. The Afar low land is characterized by arid to semi-arid climate and recurrent drought. The drought is due to lack of adequate rainfall and limited availability of perennial fresh surface water bodies in the Rift. These facts cause the local population to rely mainly on groundwater as a major source of water supply.

The average minimum and maximum temperature of the area is 16 and 30 ^{0}C respectively (Fig 2.3). Potential evapotranspiration estimated by Tesfamikael (1974) was 1984mm at Dire Dawa.

Rainfall in Ethiopia is controlled primarily by monsoon winds either from the Atlantic or from the Indian oceans depending on the season. Seventy five percent (75%) of annual rainfall on the NWP (Northwestern Plateau) and in the MER occurs during the summer (June-September) when the Inter-Tropical Convergence Zone (ITCZ) is located north of Ethiopia. During this period, the Indian and the Atlantic Ocean monsoons converge in the ITCZ. The other 25% of rainfall occurs in Spring (March-April) when the ITCZ passes southwards. During this period, the north Indian Ocean is believed to be the main source of moisture (Seifu, 2004).

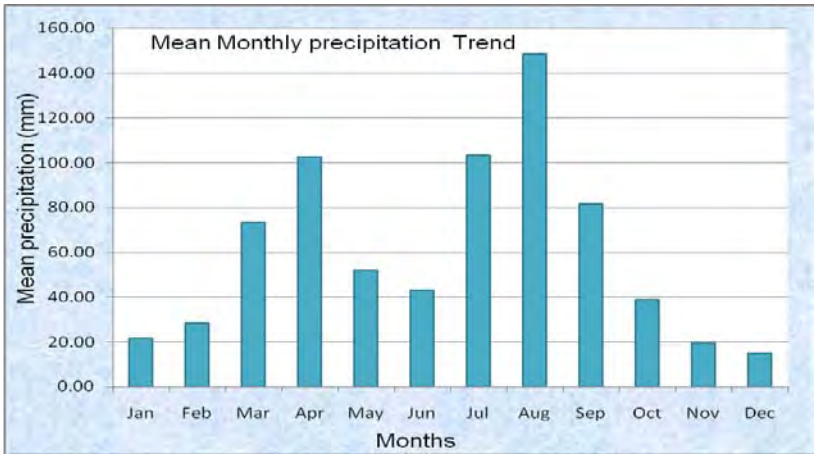

Figure 2.2 Mean monthly precipitation graph

Accordingly, the study area is characterized by its nearly bimodal (two peak) type of rainfall. The area gets the first major rainy season during summer period with peak in August and the second minor rainy season during spring with peak in April (Fig 2.2).

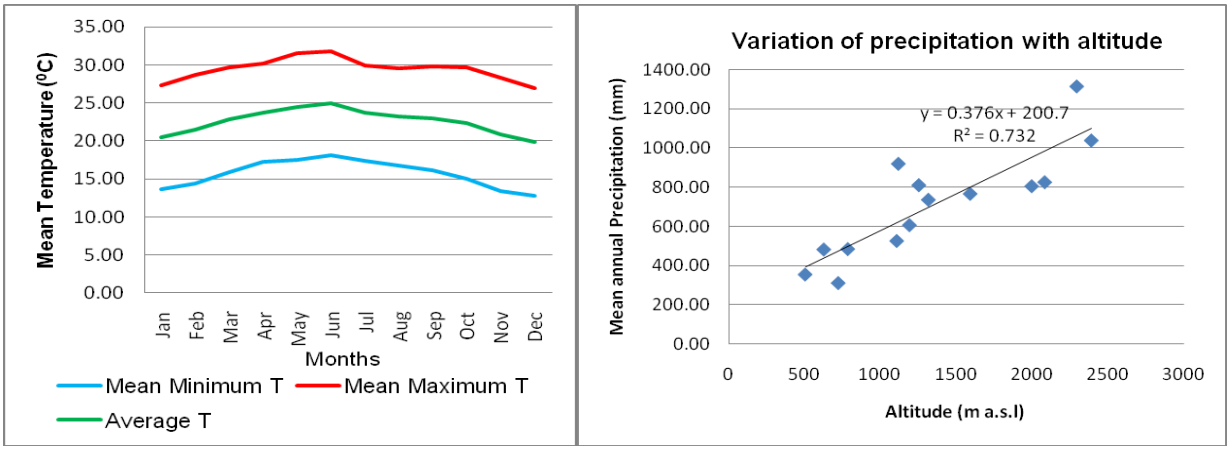

Figure 2.3 Graphs showing: Mean Min, Mean Max and average temperature and variation of precipitation with altitude

The spatial distribution of mean annual rainfall in the area generally decreases from the escarpment toward the Afar depression (Fig 2.3). This may be due to the blocking of the moisture carrying wind by the Eastern Plateau and Escarpment in addition to elevation and slope differences. Hence, this causes the leeward side to get minimum amount of precipitation relative to the plateau and the escarpment (windward side). For instance, in the study area Bike gets greater annual precipitation than Kulubi and Lange regardless of elevation due to its exposure to rain carrying winds. In general the spatial and temporal distribution of rainfall tends to decrease with decreasing altitude.

2.3.1 SPATIAL DISTRIBUTION OF RAINFALL USING THIESSON POLYGON METHOD

Thiesson polygon is one of the methods to determine the areal depth of precipitation for the catchment under consideration from several point rainfall data records. This method involves determining the area of influence for each station after locating all available rainfall stations and amount within and surrounding the catchment on a base map. Then, it draws perpendicular bisectors of lines connecting adjacent stations to form a series of irregular polygons. Each polygon indicates the area of influence for each precipitation stations. The Thiesson method uses the following relations to get the weighted average of each precipitation stations;

$$P_A = \frac{\sum_{i=1}^{n} p_i a_i}{A_t}$$

, where P_A is average precipitation (mm), P_i is observed precipitation (mm), a_i is area of influence of a station (km^2), A_t is total area of the catchment under consideration (km^2). The area of each station and the total area of the catchment are calculated using Arc GIS Version 9.3. The limitation of this method is its accuracy in mountainous areas due to unaccountability of the altitude effect unlike the isohyetal method. To estimate areal depth of precipitation using this method, 11 metrological stations from within the catchment and 3 stations from outside the catchment are used. The stations from outside the catchment are used for an extrapolation purposes instead of scarce gauging stations in the catchment. The annual

average depth of precipitation estimated for the catchment under consideration by using Thiesson polygon method is 553mm/year.

Table 2.1 Weighted annual rainfall of research area using Thiesson Polygon method

Stations	Enclosed Area by Polygon (Km^2)	Weighed Area (%)	Mean Annual Rainfall (mm)	Annual Weighted Rainfall (mm)
Adaitu	4357.00	9.48	354.01	33.55
Aysha	8807.00	19.16	310.32	59.45
Bike	3751.00	8.16	918.97	74.98
Dengego	1105.00	2.40	824.98	19.83
D/Dawa	824.00	1.79	605.98	10.86
Gewane	5508.00	11.98	481.43	57.68
Harewa	10297.00	22.40	483.77	108.36
Hurso	2309.00	5.02	525.24	26.38
Kara Mile	745.00	1.62	1313.89	21.29
Kulubi	314.00	0.68	1038.07	7.09
Lange	133.00	0.29	804.64	2.33
Mieso Mission	1640.00	3.57	735.32	26.23
Mullu	2069.00	4.50	809.98	36.45
TeferiBer	4113.00	8.95	765.83	68.52
Total	**45972.00**	**100.00**		**553.00**

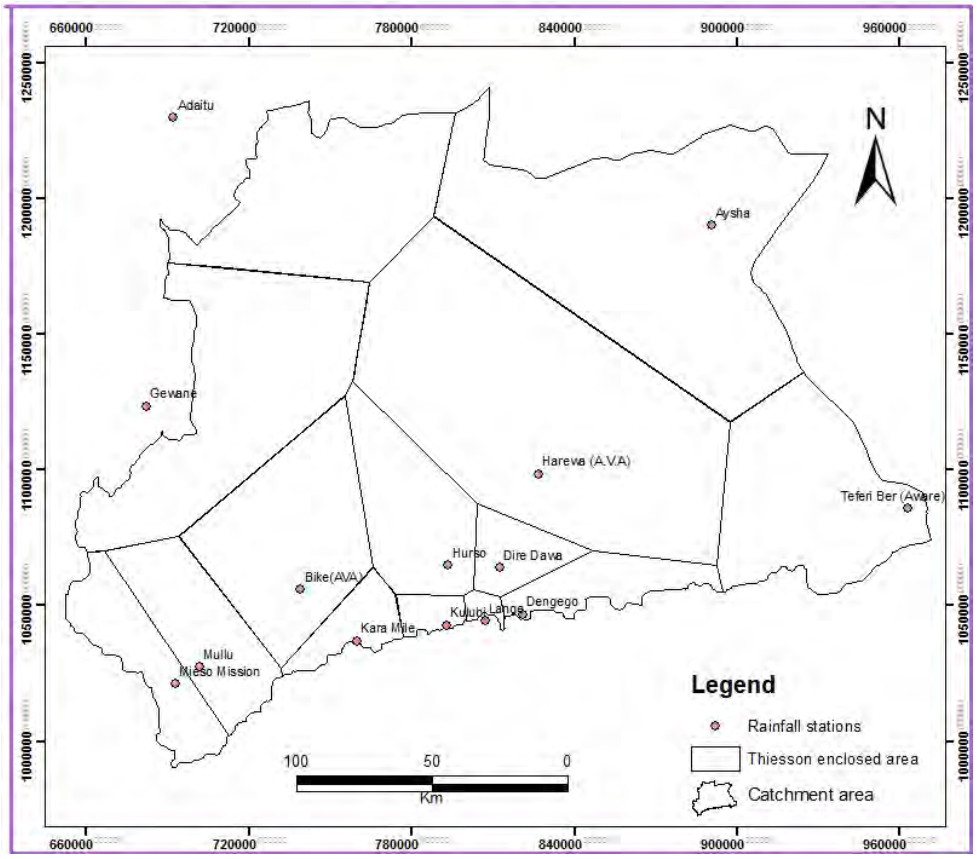

Figure 2.4 Thiesson polygon map of the area

2.3.2 SPATIAL DISTRIBUTION OF RAINFALL USING ISOHYETAL METHOD

Isohyetal method is the most basic and accurate method of representing the spatial distribution of rainfall by taking in to account the orographic effects. The method involves drawing lines of equal rainfall (isohyets) by interpolating between observed rainfalls depths according to the contour interval assigned. The drawing of the isohyets (contours) are made using Arc GIS 9.3. The value of rainfall depth between two consecutive isohyets is an average between the two. In order to construct the isohyetal lines 11 metrological stations from within and 3 stations from outside the catchment are used. This method based on the following formula to calculate an average areal depth of precipitation for the catchment under consideration;

$$\bar{P} = \frac{\sum_{r=1}^{n} P_i A_i}{\sum_{r=1}^{n} A_i}$$

Where, $\bar{P}$ = Average precipitation over the catchment; A_i= Areas between successive isohyets; P_i= Average rainfall between successive isohyetes (i=1, 2, 3,..)

According to the isohyetal method the average depth of precipitation estimated for the catchment is 662.81mm/year.

Table 2.2 Weighted annual rainfall of the research area using Isohyetal method

Range of Isohyets (mm)	Average values of isohyets (mm)	Enclosed area between isohyets (Km^2)	Weighed area (%)	Weighted rainfall (mm)
< 400	400	2145.00	4.67	18.66
400-500	450	2554.20	5.56	25.00
500-600	550	8825.8	19.20	105.59
600-700	650	15508.50	33.73	219.28
700-800	750	11617.00	25.27	189.52
800-900	850	3443.00	7.49	63.66
900-1000	950	1262.00	2.75	26.08
1000-1100	1050	324.10	0.70	7.40
1100-1200	1150	161.00	0.35	4.03
1200-1300	1250	118.00	0.26	3.21
> 1300	1300	13.40	0.03	0.38
Total		**45972.00**	**100.00**	**662.81**

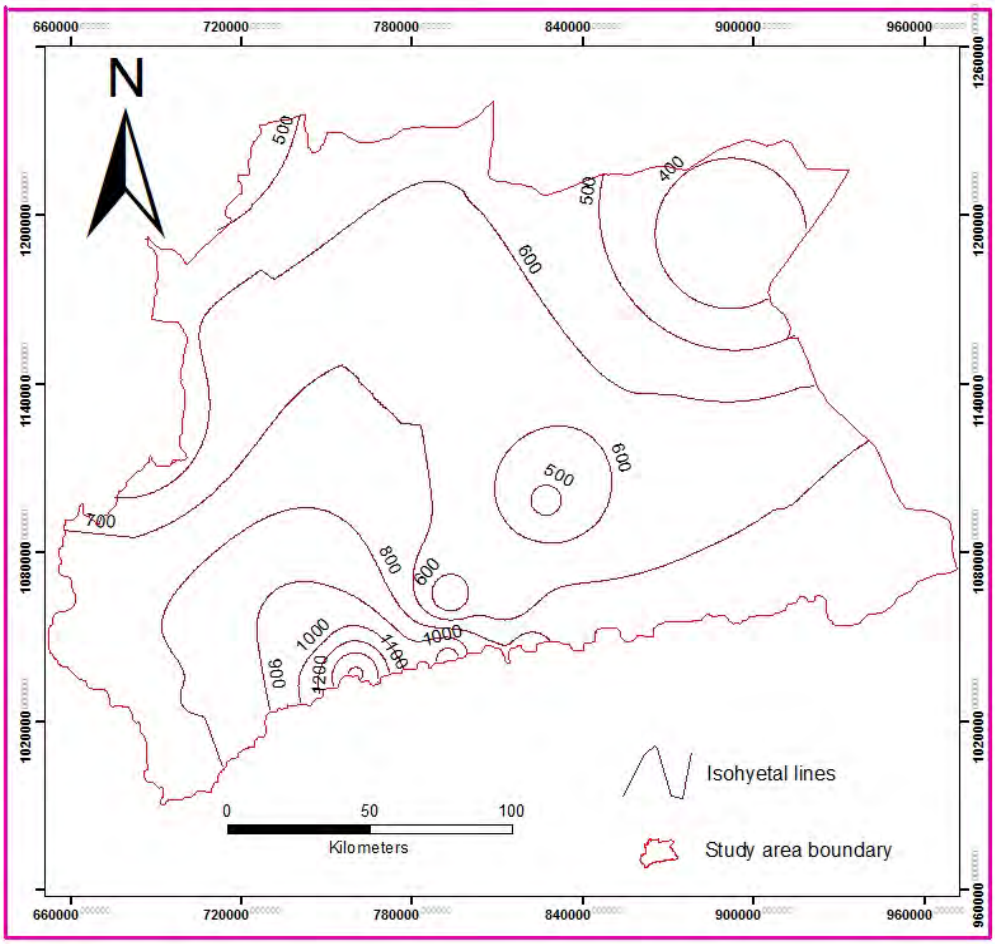

Figure 2.5 Rainfall isohyetal map of the area

2.4 LAND USE-LAND COVER

The land cover of an area is based on its geographic situation, climate and availability of water to the root zone. Since the investigation area is characterized by arid to semi-arid climate the vegetations of the area mainly comprise bushes and shrubs. Approximately more than 40% of the area is covered by rocky surface, while open grass land constitutes approximately greater than 30%. Only the southern margin of the area is predominantly cultivated along the east west Escarpment, which is approximately less than 10%. In contrast to the southern boundary, which is cultivated, the northern part of the area is the untouched part due to the economic dependence of the community on animal production (such as camels, goats and sheep) and scarcity of surface water

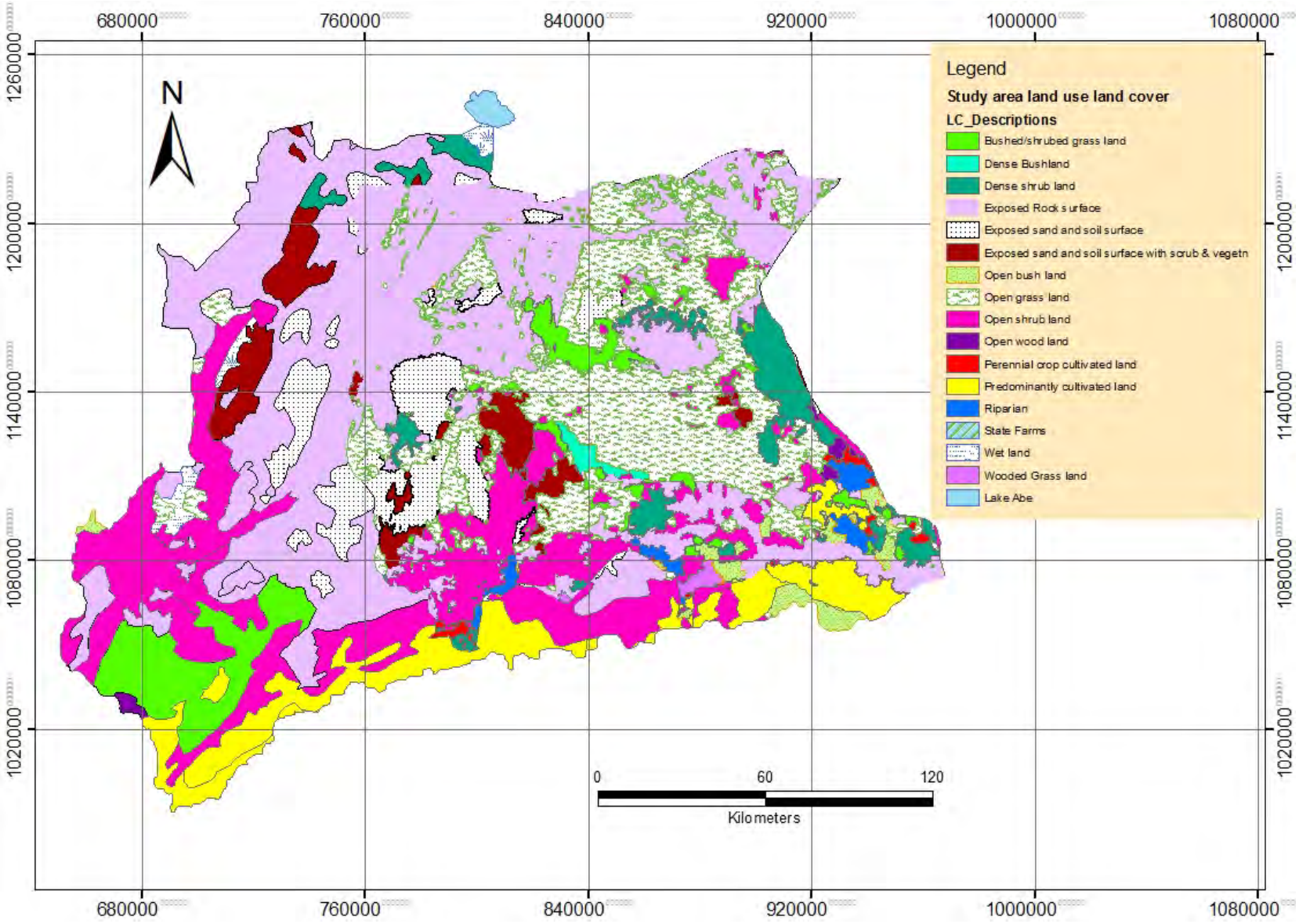

Figure 2.6 Land use-land cover map (modified and composed from Shinille land use-land cover map compiled by OWWDSE, 2010 and FAO, 1984)

2.5 GEOLOGY

2.5.1 GENERAL

The study of the geology of the southern part of the investigation area has been carried out by various authors and a few water sectors. Hailemeskel (1964) established the geology of Eastern Harar sheet which partly covers the present study area at the southeastern part; the regional work of Mohr (1973) summarized the structural geology of the African Rift System and Mohr (1962) explained about the Ethiopian Rift System; Shachnai (1972) described the geology of NC37-12 (Dire Dawa) and NC38-9 (Harar) sheets; Canuti et al., (1972) investigated volcanic intercalation in the Mesozoic sediments of the Kulubi area; Water Works Design and Supervision Enterprise (WWDSE, 2003) Conducted Dire Dawa Administrative Council (DDAC) integrated resource development master plan study project. The geological and geomorphological mapping at 1:500,000, 1:250,000 and 1:50,000 scales were conducted by OWWDSE (2011) for Shinille groundwater potential assessment. This study covers a significant portion of the research area as well as extending in to the northern extreme part of the area.

The investigation area is characterized by its complex geology and tectonic structure because of its proximity to the Afar depression where the three Rift structures, the Main Ethiopian Rift (MER), the Gulf of Aden Rift and the Red Sea Rift converge (the triple junction). The geology of the area dominantly comprises Precambrian basement rocks, Mesozoic sedimentary rocks, tertiary and quaternary volcanic rocks and quaternary to recent alluvial and lacustrine deposits.

2.5.2. PRECAMBRIAN ROCKS

These rocks are the oldest rocks of the area under consideration. The Precambrian basement exposures are found in areas not intensively affected by Cenozoic volcanism and rifting and where the phanerozoic cover have been eroded away (Mengesha et al., 1996). The basement rock outcrops are exposed at the southern, southeastern and eastern part. For instance, these rock outcrops are exposed along the Dire Dawa-Dengego main high way. The Precambrian rocks of the area are composed of granulites, migmatites and gneisses (biotite and hornblende) (Mengesha et al., 1996).

They are high grade metamorphic rocks exposed as discontinuous lenses along the eastern escarpment mainly as a result of regional uplift and subsequent step faulting (OWWDSE, 2011).

2.5.2. MESOZOIC SEDIMENTARY ROCKS

The Mesozoic sedimentary formations are the result of the transgression and regression events caused by the fluctuations and denudations of the ancient Indian Ocean which passed over the area from SSE and ESE to different extents (Shachnai, 1972). The process resulted in the sedimentary sequence which thins toward the NNW. The stratigraphic succession of these formations is categorized in to three. The arrangement of the succession from bottom to top is the Lower Adigrat Sandstone, Hamaneli Limestone and the Upper Amba Aradam Sandstone.

Lower sandstone- unconformably overlying the basement complex is exposed mainly in the southern parts of the area and underlying the Hamaneli formation. This sandstone beds are dipping 16-26^{o} due south and southeast. Petrographic analysis of the Adigrat sandstone shows that it is composed of 30-39% quartz, up to 35% calcite cement, 15-62% potassium feldspar 4% plagioclase 2% muscovite, 2% zircon and 2% opaque minerals (WWDSE, 2003). Shachnai (1972) and various investigators cited there in reported different values (20-150m) for the thickness of the Adigrat sandstone in the region.

Hamanlei formation - found overlying the Adigrat sandstone. It constitutes Jurassic fossiliferous limestone (OWWDSE, 2011) and exposed in the southern part of the area along the East-West Esacrpment and in the Northeastern extreme around Aysha-Dewele. It forms different step like blocks extended in the east-west direction and decreasing topographic elevation from south towards the rift. It is intercalated with thin beds of shale (Fig 2.7 b). In the absence of the Adigrat sandstone, it unconformably overlies the Precambrian basement rocks. The limestone beds are generally dipping due south and southeast with varying dip angles ranging from 10 ^{o} to 27 ^{o} (WWDSE, 2003). Due to the repetition of the limestone by the step faults and the basal transition zone from the Adigrat sandstone, it is difficult to determine the exact thickness of the Hamanlei formation. However, Greitzer (1970) and WWDSE (2003) reported that the

thickness of the limestone in the Dire Dawa area is in the range of 100-275m. The limestone is highly fractured and cavernous (fig 2.7 d) represented by caves in areas like Lega Oda. Petrographic analysis of the gray color limestone, which is the dominant type in Dire Dawa area, is composed of 80-98% calcite, 2-17% quartz, 1-3% plagioclase and 0-1% opaque minerals. The brown color variety of the limestone is composed of 84% calcite like that of the gray color, 15% opaque (Fe-oxides) and 1% plagioclase.

Upper san dstone- The Hamanlei formations are overlain by the upper sandstone (Amba Aradom formation). This formation is exposed at the southern part of the area along the East-West Escarpment and at the Northeastern region around Aysha - Dewele. The cretaceous upper sandstone has a thickness of about 200m as reported by Tesfamikael (1974). It is fine to medium grained, not well bedded, compacted near the bottom while the upper part is usually friable. The friable and immature upper sandstone outcrops are exposed around Kulubi area. The sandstone beds are dipping 23-52^{o} due south and southeast. It is highly fractured and the fractures have similar trends with the main faults in the area. Petrographic analysis of the rock shows that it is composed of 40-90% quartz, up to 60% potassium feldspar, 5-15% plagioclase feldspar, 3-13% clay cement, 5% calcite cement and 1% opaque (WWDSE, 2003).

Figure 2.7 Some geological structures & units in the area a) Down thrown sub horizontal limestone units due to NE striking fault structure b) Limestone beds with thin intercalation of shale c) Interconnected NE and WNW fractures and cracks in grey limestone at 15 km from D/Dawa on the way to Djibouti d) cavernous limestone due to solution opening

2.5.3. CENOZOIC FORMATIONS

Tertiary volcanic rocks- the trap series extruded during the tertiary period and referred to as the trap series. The series is a succession of flood volcanics comprising many basic and acidic variants reaching around 2000m in the western part (around Asebe Teferi) and thinning out or absent towards the east and south Shachnai (1972). According to the author the succession of a section around Asebe Teferi from bottom to

top constitutes vesicular and amgdaloidal olivine basalt (about 600m thick), porphyritic plagioclase basalt (400m), acidic sequence (tuff, breccias, ignimbrites) (200-400m thick), dense vesicular olivine basalts with pyroclastic basaltic breccias and trachytes and ignimbrites (about 400m).

The volcanic rocks of the Trap Series rest over the upper sandstone along the escarpment area. It also exists as dolerite sills and dikes in basement and Mesozoic rocks (Fig 2.8 c and d). The series are also indicated to constitute Alajae Formation (Seife, 1985). They represent the oldest volcanic rock in the area (Oligocene in age). However, Canuti et al., (1972) reported the existence of pre-trappean volcanic flows inter bedded in the Mesozoic rocks around Kulubi. According to the detail geological study of WWDSE (2003), the petrographic analysis of the alajae basalt is composed of 53-55% plagioclase, 25% pyroxene, 5-15% olivine, 3-8% devitrified glass, 10% oxides and trace of carbonte and apatite.

Quaternary formations- the quaternary formations cover a significant portion of the area under consideration relative to the other formations. The formations include alluvial and lacustrine deposits as well as rhyolitic and trachytic volcanic centers, obsidian pitchstone, scoria, ignimbrite, elluvium, calcrete, upper and lower Afar stratoid basalts. The superficials of the escarpment zone are mainly colluviums comprising of talus (Tesfamikael, 1974; Habteab and Jiri, 1986) and fluviates whereas that of rift plain consists of alluvium (composed of sand, clay, and silt), river gravels, fans and travertine. For instance, typical alluvial fans are clearly seen around Harmukale area on the way from Dire Dawa to Djibouti very close to the Escarpment. The superficial deposits also cover beds of river valleys. Moreover, all rivers descending from the Escarpment have built enormous thickness of the alluvial deposits.

The alluvium becomes finer in grain size (silty to clayey) in the northern part of the extensive plains (Fig 2.8 b). The general decrease in grain size of the alluvial sediments could be explained in terms of distance of transportation from the escarpment. The longer the distance of travel, the finer the grain size. The thickness of the alluvial deposits of the study area is estimated to be 100 meters (Katema, 1982) and 400 m (Tesfamikael, 1974). However, water-well drilling supervision reports of Oromia Water

Works Design and Supervision Enterprise (OWWDSE, 2011) indicated the partial thickness of the alluvial deposits encountered is 250m around Aydora area. According to the drilling report even at 250m depth the bed rock was not intercepted. The drilling supervision report of OWWDSE (2011 and 2012) also indicated as the thickness of the alluvium varies from 122-170m around Gabi artesian wells in the east.

In addition to the above formations, the area comprises the recent Cenozoic rocks. These rocks include basalts, gravelly materials and talus. The recent volcanic rocks occur in the southwestern and southeastern parts of the study area. In all cases, the recent (Holocene) volcanic rocks occur in association with trachytic to rhyolitic rocks and scoriaceous cones and flows. In the southwestern part, the recent volcanic rocks extruded at the intersections of the NNE, NW and EW faults. These rocks are basaltic in composition and appear as fresh lava flows which are devoid of any soil or vegetation (OWWDSE, 2011). At some places the Holocene basalts are found overlying the quaternary alluvial deposits, for instance Harmukale and Bokoli (north of Bike) (Fig 2.8a).

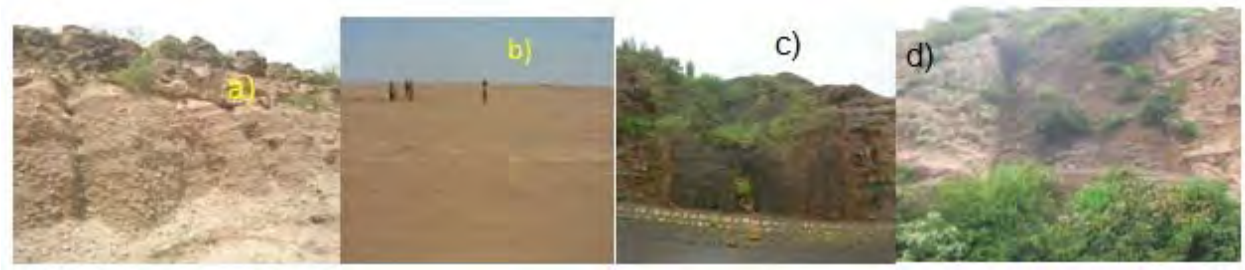

Figure 2.8 Young formations and dikes: a) Alluvial deposits overlain by basaltic flows (Harmukale) b) Very fine grained clayey alluvial deposits around Idora-Asbuli flat plain c) N-S striking basaltic dike within Mesozoic formation exposed around Kersa on the way to Addis d) NW running basaltic dike exposed within the basement rock near Dengego

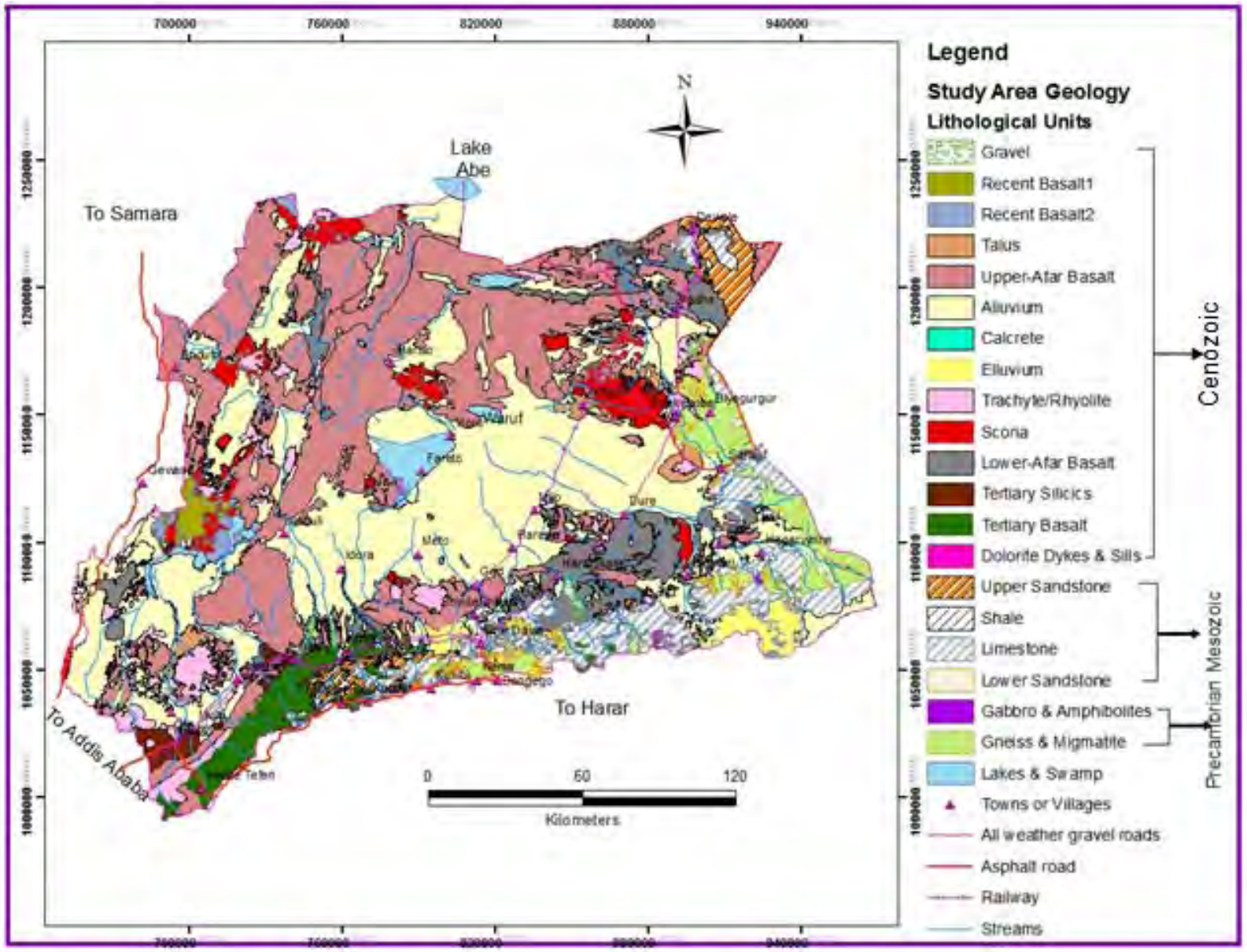

Figure 2.9 Geological map of the area (modified from Shinille and adjoining areas geological map compiled by OWWDSE, 2011)

2.6 HYDROGEOLOGY

2.6.1 GENERAL

The surface water divide between the Awash and Wabe Shebelle basins roughly corresponds with the boundary between the Eastern Plateau and the Escarpment. Runoff and base flow on this plateau drain relatively slowly southwards in contrast to the ones of the Escarpment which flow vigorously northwards until it reaches the plain of Afar, where it quickly lose its water into the alluvium (Habteab and Jiri, 1986; Andarge and Jiri, 2010). Due to this fact neither the perennial nor the intermittent streams reach their final out let (i.e. Awash River or Lake Abe).

The hydrogeological study of WWDSE (2003) and OWWDSE (2011) in the study area distinguished that the Mesozoic sedimentary formations (particularly upper sandstone and limestone) and the alluvial deposits are the major water bearing formations with a yield of more than 20 L/S and 5 L/S respectively from a well depth ranging from 150-250m at the foot of the Escarpment (Fig 2.11). For the case studies of WWDSE Aseliso well fields can be good examples while Biyobahay well fields can be mentioned as case studies for OWWDSE.

In the Escarpment zone and in the southern edge of the plains area where rocks of relatively higher infiltration capacities occur, infiltrated water rapidly joins the regional groundwater body which is at minimum depth of 25m (Tesfamikael, 1974). According to this author the main mechanism of infiltration suggested was selective infiltration through cracks (fractures) in limestone while concentrated infiltration occurs along the river beds through gravels and exposed limestone and sandstones. Habteab and Jiri (1986) also considered sedimentary and volcanic rocks in the escarpment area with karastic and fissured permeability to have good groundwater resource.

2.6.2 AQUIFER PRODUCTIVITY AND PROPERTIES

Groundwater resource potential assessment in Shinille and adjoining areas by OWWDSE (2011) classified aquifer productivity of the area in to low, moderate to high and high productive aquifers. Meta sediments, granite intrusions, non-fractured and non-weathered metamorphic rocks, trachytic and rhyolitic volcanic flows and domes are categorized in to low productive aquifers or aquiclude. In contrast, basaltic rocks of the

catchment are presented as moderate to high productive aquifers. Whereas aquifer materials characterized by noticeable karastic permeability and fracture, intergranular porosity and vesicular openings are grouped in to high productivity aquifers and compositionally comprises Mesozoic sedimentary rocks (sandstone and limestone), alluvial deposits and scoriacious basalt.

Habteab and Jiri (1986) pointed out as the discharge of the sedimentary rocks on the southeastern part of the area, the dominant volcanic rocks in the southwestern part, the Afar depression alluvial sediments with porous permeability and Afar volcanic rocks with fissured permeability vary from 1-50 l/s, 0.5-10 l/s, 2-8 l/s and 1- 5 l/s respectively. The authors also specify the average transmissivity of limestone blocks at the foot of the escarpment is 2.8 x 10-3 m2/s that of alluvium as 6.1 x 10-3 m2/s and Afar depression volcanic rocks 2.1 x 10-3 m2/s.

However, free flowing artesian wells with discharges of approximately greater than 50 l/s are recently tapped from Afar volcanic aquifers at the northern part (Gabi irrigation well fields). An attempt was made to conduct the pumping test of Gabi Test well with a discharging of 32 l/s by fixing the pump position at 9m below ground level. But this pumping rate could not stop the well from free flowing. The sound hydrogeological reason for this condition might be an increase in degree of fractures as one move toward the Afar Depression in the rift. The basalts are overlain by alluvium as an upper confining layer at the northern and central part of the study area (i.e. Gabi and Mete artesian wells with depth ranging from 158-250m) according to the water well drilling supervision reports of OWWDSE, 2011 and 2012 and field observation made.

The test well drilling and pumping test results of Afdem/Shake test well in the western part of the investigation area also showed the potentiality of the volcanic aquifers. According to the pumping test result, the well has static water level of 32.9m b.g.l and total draw down of 4.3m with a yield of 22 l/s within 24 hrs. This well is drilled in the rift closer to the Afdem Mountain, which is mainly composed of acidic rocks. Unlike the volcanic rocks of Awash Basin, the yield of the volcanic aquifers of the Aysha Basin is low, ranging from dry to 1.8 l/s as observed during drilling and pumping test supervision work and analyzed from well completion reports. The maximum drilled depth (350m) is in this basin but the well is dry.

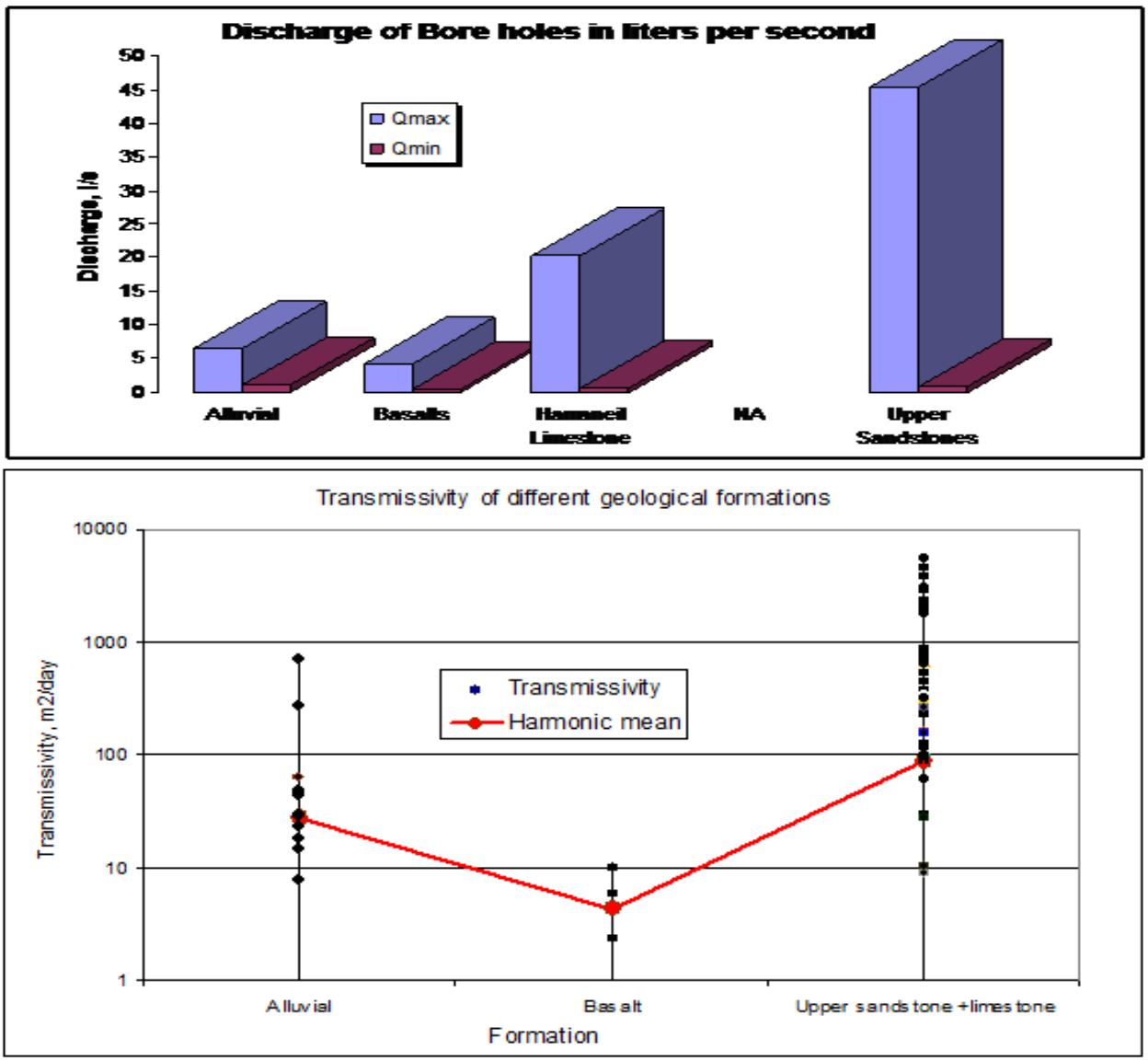

Figure 2.10 Discharge of Boreholes and transmissivity in different formations at the foot of the Escarpment (Source: WWDSE, 2003)

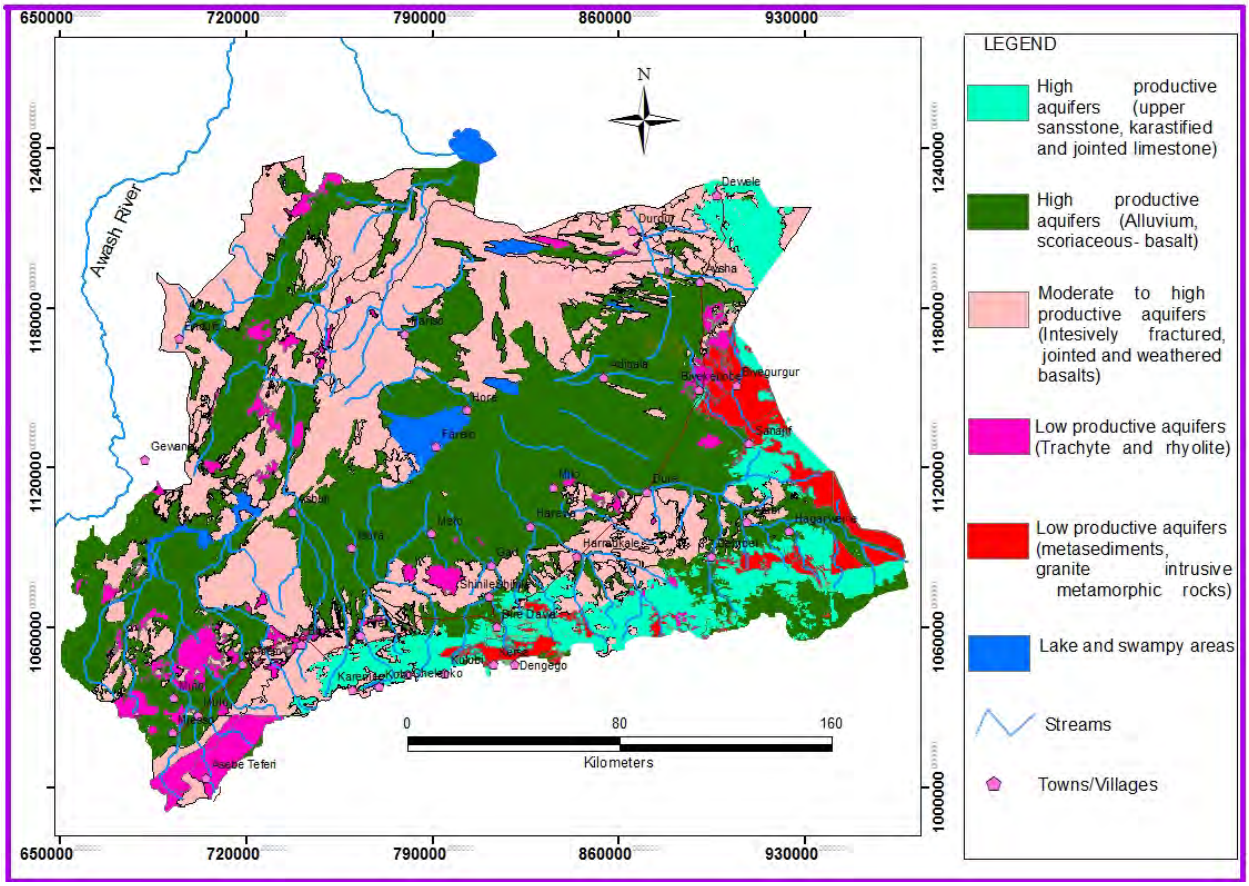

Figure 2.11 Hydrogeological Map of the area (Source: modified from OWWDSE, 2011 inception report). It is again under modification based on recent data.

2.7 STRUCTURES

2.7.1 REGIONAL STRUCTURES

The geological structures of the investigation area are studied by various authors and a few water sectors. Some of these studies include Mohr (1962) explained the Ethiopian Rift System; Mohr (1973) summarized Structural Geology of African Rift System; Shachnai (1972) produced the geology of NC37-12 and NC38-9 sheets; Mezmure (1964) compiled the geology of Eastern Harar sheets; Tesfamikael (1974) investigated hydrogeology of Dire Dawa area; and Habteab and Jiri (1986) worked on the hydrogeology and hydrochemistry of Dire Dawa sheet (NC37-12); OWWDSE (2011) mapped the geology and geomorphology of Shinille zone and adjoining areas.

2.7.2 RESEARCH AREA GEOLOGICAL STRUCTURES

The area consists of two structural units: the Escarpment and the Afar plain (the Rift). The Afar plain of the research area constitutes the southern part of the Triple Junction (where the three rifts-East African Rift, Red Sea Rift and Gulf of Aden Rift converge). The major trends of the faults in the area are EW, NW, NE and NS. Many of the tilted limestone blocks strike EW and dip 20^0 S along the Escarpment (Shachnai, 1972).

Among the major structural trends the most prominent one is the EW. Even the volcanic cones aligned in the EW direction in the rift reflect a line of weakness along this trend (Hailemeskel, 1964). The structural trends of the escarpment follow the Gulf of Aden trend (EW). The major preferred orientations of Stream and River valleys of the area are toward NW in the east and NE and/or NS in the West. It is assumed that stream orientation is geologically controlled. Moreover, the stream trend in the east is the Red Sea trend (NW) (Shachnai, 1972).

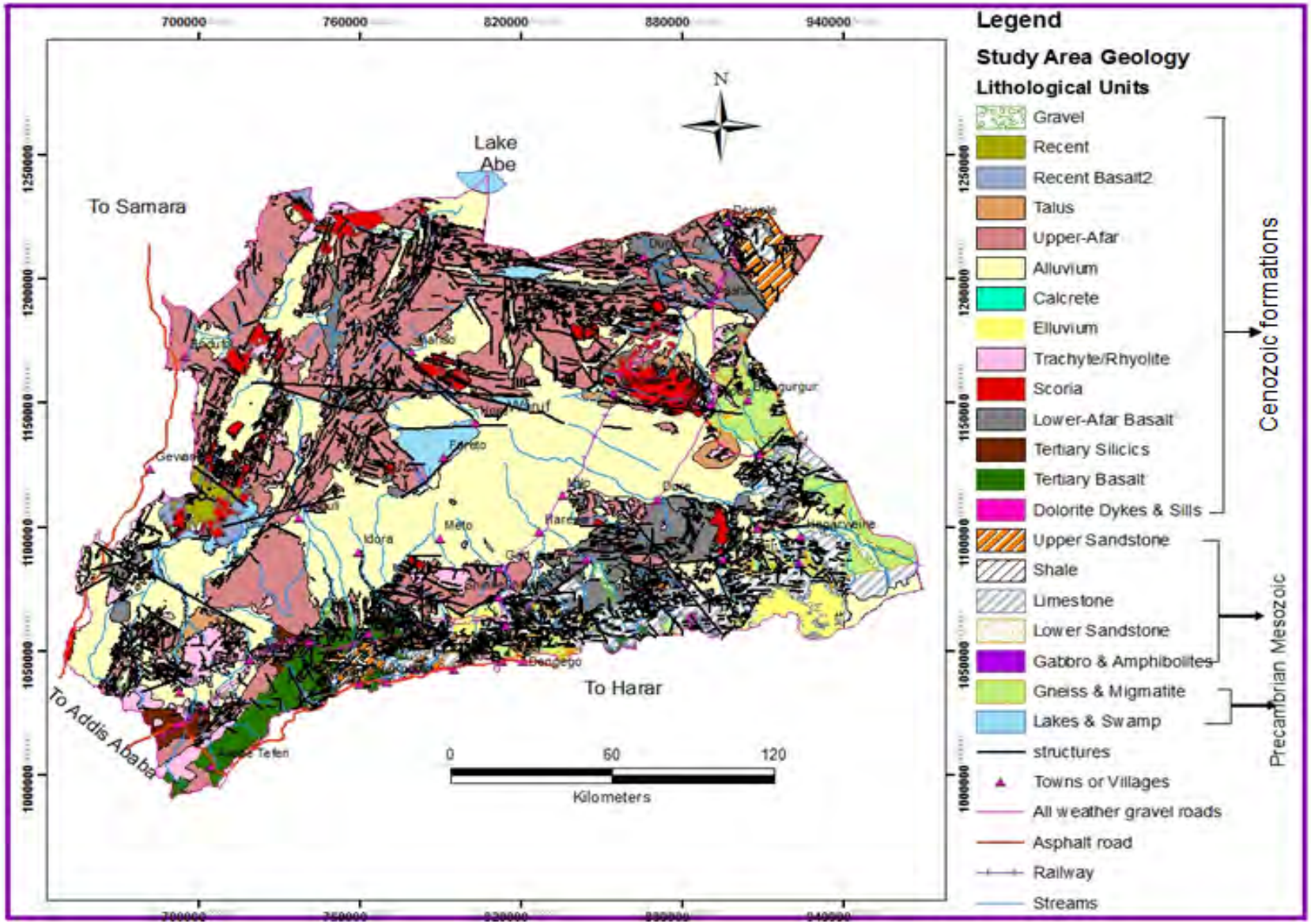

Figure 2.12 Structural Map of the area superimposed on the geology (source: OWWDSE, 2011)

3. METHODOLOGY

3.1 GENERAL

In many cases conventional hydrogeochemical studies only are not sufficient enough to characterize groundwater hydrodynamics or to investigate recharge sources and mechanisms and source of salinity. Since the isotopic compositional signatures of $\delta^{18}O$ and $\delta^{2}H$ in groundwater do not change as a result of rock–water interactions at low temperatures, it provides a helpful means to bridge this knowledge gap (Sidle, 1998). The application of isotope-based methods has become well established for water resource assessment, development and management in the hydrological sciences, and is now an integral part of many water quality and environmental studies (Clark and Fritz, 1997; and Cook and Herczeg, 1999). However, the conjunctive use of hydrogeochemistry and environmental isotope to investigate groundwater recharge and flow processes has never been applied in the investigation area up to the end of this work.

3.2 SAMPLING AND ANALYSIS

In order to investigate the groundwater recharge and flow processes in the research area, three field trips were conducted. The first trip was conducted at the end of August, 2011 to install rainfall sampling bucket at 4 stations. The second trip was at the end of September, 2011 to collect the gathered rainfall samples. The third trip was carried out at the beginning of Dec. 2011 to generate 45 and 14 representative primary data for isotope and phsico-chemical analysis respectively (annex 2 and 3). The water samples were collected from shallow and deep boreholes, dug wells, springs, surface water and summer rainfall.

Rain water sampling has been conducted for complete one month from 26, August to 26, September 2011 at 4 stations during summer rain in order to get the cumulative and reliable information about its isotopic signature and chloride (Cl) concentration. During this time, the rain water collected in the bucket has been protected from evaporation by adding 400ml of paraffin in to 20 liter bucket to produce a film of paraffin cover over the collected rain.

The paraffin is added in to the bucket prior to a drop of rain. In addition to the 4 stations, one day direct precipitation sampling was also conducted at 2 stations during the second trip.

During the third field trip in-situ physical properties such as Electrical Conductivity (EC), Total Dissolved Solids (TDS), PH values and temperature (T) are measured using hand held EC and PH meters. Prior to field work the PH meter is calibrated to PH values=4 and 7 using buffer solutions at Water Works Design and Supervision Enterprise (WWDSE) laboratory. Fourteen (14) representative water samples are collected in 1 liter capped plastic bottles for physico-chemical analysis (annex 3) and in 25 ml capped glass bottle for stable environmental isotope analysis (^{18}O and ^{2}H) (annex 2). The total numbers of water quality results used for the analysis are 210 (Fig 3.1). Out of these water quality data 196 of them are from secondary sources (182 samples from Awash and 14 samples from Aysha basins) (annex 4). Totally there was no secondary data of isotopes.

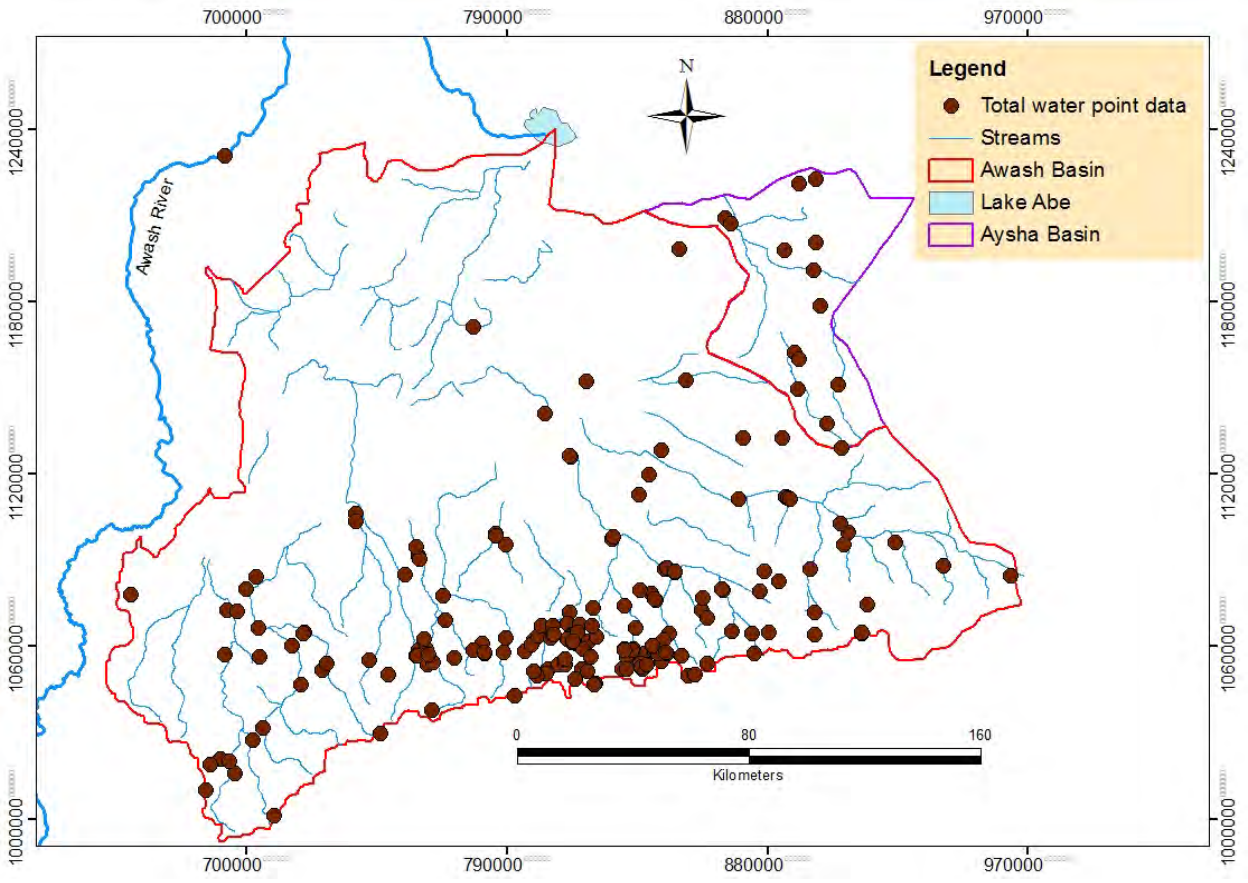

Figure 3.1 Location of total samples used for analysis

3.3 HYDROGEOCHEMICAL METHODS

3.3.1 GENERAL

Hydrogeochemical methods include the use of physical and chemical properties of water to identify the various hydrochemical processes controlling water chemistry, to cluster the groundwater data in to distinct groups on which inverse geochemical modeling is conducted to determine the phase mole transfers (flow processes) and to understand the hydrochemical evolutions of groundwater along flow path or flow dynamics. In addition, hdrogeochemistry can provide information that can distinguish recharge zone water from transition and discharge ones based on the chemical composition of water type. Moreover, in hydrogeochemistry major cations (Ca^{+2}, Mg^{+2}, Na^{+}, K^{+}) and major anions ($HCO3^{-}$, $CO3^{-2}$, $SO4^{-2}$, Cl^{-}) are the most widely and frequently used parameters for characterization of the various water types and deduction of the flow processes and origin of salinity.

3.3.1 HIERARCHICAL CLUSTER ANALYSIS (HCA)

Hierarchical cluster analysis (HCA) is a powerful statistical tool which has been employed for partitioning the analysis results of the water samples into hydrochemical facies, also known as water groups or water types. Statistical classifications of geochemical data by Q-mode hierarchical cluster analysis (HCA) provide a suitable mechanism for objective classification of water composition into hydrochemical facies and for geochemical modeling (Swanson et al, 2001; Guler et al., 2002; Seifu et al, 2005; Tenalem et al. 2009; Addis, 2011 and Bizuneh, 2011).

HCA do not necessarily establish cause-and-effect relationships, but do present the information in a compact format as the first step in the complete analysis of the data and can assist in generating hypothesis for the interpretation of hydrochemical processes. It can be used to test water quality data and determine if samples can be grouped into distinct populations (hydrochemical groups or sub groups) that are significant in the geologic and hydrogeologic context. The characteristics of the groups or sub groups are not pre determined but can be obtained after the classification. This classification is useful especially to understand geological controls on water chemistry under conditions where useful geochemical data are available but clear hydrogeologic models have not

yet been developed (Swanson et al., 2001). The advantage of HCA is that many variables such as physical, chemical or isotopic composition can be used to classify waters (Seifu et al, 2005).

The assumptions of cluster analysis techniques include equal variance and normal distribution of the variables (Alther, 1979). Equal weighing of all variables requires the log-transformation and standardization of the raw data. This restricts the influence of or the biases caused by the variables that have the greatest or the smallest variances or magnitudes on the clustering results.

3.3.2 INVERSE GEOCHEMICAL MODELLING

Inverse geochemical modeling is commonly used to reconstruct geochemical evolution of groundwater from one point in an aquifer to another point located in the inverse direction along the groundwater flow path. Recently, inverse geochemical modeling has been used to investigate the chemical evolution of groundwater along the flow path by various investigators (Plummer et al., 1990; Guler et al., 2002).

It is a useful approach to determine the type and amount in moles of minerals that dissolve or precipitate (flow processes) along a groundwater flow path. In the cases where information is available on the hydrogeology of the basin, the flow paths can be selected based on the hydrogeological knowledge. The initial and the final member can be chosen by taking into account the location of the point, the hydraulic heads of the aquifer system and observed trends in chemical evolution of the water (Hidalgo and Cruz-Sanjulian, 2001).

In areas where information on groundwater flow direction is lacking, the initial and final waters can be selected from the HCA groups. This is based on the logical assumption that waters which fall in a statistical group may have similar residence time, similar recharge history, and identical flow paths or reservoir (Guler and Thyne, 2004). The PHREEQC interactive 2.8 computer program (Parkhurst and Appelo, 1999) is used to simulate the geochemical evolution from initial to final member between different groups of statistical clusters. A number of assumptions are inherent in the application of inverse geochemical modeling: (1) the two groundwater analyses from the initial and final water-wells should represent groundwater that flows along the same flow path, (2) dispersion and diffusion do not significantly affect groundwater chemistry, (3) a chemical steady-

state prevails in the groundwater system during the time considered, and (4) the mineral phases used in the inverse calculation are present in the aquifer (Zhu and Anderson, 2002). The soundness or validity of the results in the inverse modeling depends on a valid conceptualization of the groundwater system, validity of the basic hydrogeochemical concepts and principles, accuracy of input data into the model, and level of understanding of the geochemical processes in the area (Guler and Thyne, 2004).

3.3.3 CORRELATION OF MAJOR ION AND TOTAL DISSOLVED ION

Total dissolved ion (TDI) is the sum of major cations and anions. This method involved the plot of major ions (Ca^{+2}, Mg^{+2}, Na^{+}+K^{+} , $HCO3^{-}$, $SO4^{-2}$, Cl^{-}) against TDI in which both axes represent concentration in meq/l to detect whether there are compositional differences (water types) in the sample set. Data that plot in linear trends represent mixing of water with low dissolved ion concentrations and water with higher dissolved ion concentrations. While data that plot as more than one cluster indicate separate types of water that are not mixed. A random distribution of data indicates that many individual, unrelated water types exist or that the analytical quality of the data is poor (Mazor, 2004). This method can also indicate major elements contributing to groundwater salinity.

3.3.4 GROUNDWATER RECHARGE ESTIMATION

Groundwater recharge may be defined as the downward flow of water reaching the water table, forming an addition to the groundwater reservoir (Lerner et al, 1990). Reliable estimates of groundwater recharge are needed for a number of reasons;

1) quantifying groundwater resources which can be utilized without detrimental effects on environment 2) assessing the surface water – ground water interactions and total availability of water resources and groundwater vulnerability (for both quantity and quality aspects) 3) identifying implications of changes in land use and/or climate on water resources 4) ground water management and planning – funding of ground water development projects 5) formulation of regional scale artificial recharge and rainwater harvesting programmes 6) regulation of ground water development

3.3.4.1 CHLORIDE MASS BALANCE (CMB) METHOD

The selection of recharge estimation method based on the different climatic and hydrogeologic conditions. Accordingly, the chloride mass balance (CMB) method is selected to estimate recharge and has been applied in many different countries and environments (Eriksson & Khunakasem, 1969). Moreover, it has been most widely applied for estimating low recharge rates in arid and semi-arid regions where other suitable methods are lacking. The method assumes that the only source of chloride in groundwater is via deposition in rainfall, that the rate of chloride accession to the landscape is constant, and there are no sources or sinks of chloride in the subsurface. The following steady state mass balance equation can be used to estimate recharge (R):

$$R = \frac{(P-Ro)*Cl_p}{Cl_{GW}}$$

Where P is the mean annual precipitation rate, Ro is the annual surface runoff rate, Clp is the chloride concentration in the precipitation, and Cl_{GW} is the chloride concentration in recharge water (groundwater). However, for the research area under investigation surface runoff was not accounted since the sporadic surface runoff disappears in to the alluvium before it reaches its final destination. Therefore, the above equation is more simplified to:

$$R = \frac{P*Cl_p}{Cl_{GW}}$$

3.4 ISOTOPE HYDROLOGY

Environmental isotopes now routinely contribute to groundwater investigations, complementing geochemistry and physical hydrogeology. The stable isotopic compositions of water, for instance is modified by meteoric processes, and so the recharge waters in a particular environment will have a characteristic isotopic signature (Clark and Fritz, 1997). This signature then serves as a natural tracer for the provenance of groundwater. Looking at isotopes in water, reveals about groundwater quality, geochemical evolution, recharge processes, rock-water interaction, the origin of salinity and contaminant processes.

3.4.1 OXYGEN (δ18O) AND DEUTRIUM (δ2H) ISOTOPES

Oxygen ($\delta^{18}O$) and deuterium ($\delta^{2}H$) are the most widely used stable environmental isotopes in various hydrological sciences for investigating water resource development and management.

The stable isotope content of water molecule $^{2}H/^{1}H$ and $^{l8}O/^{16}O$ is expressed by convention as parts per thousand (‰) deviations relative to the standard VSMOW (Vienna Standard Mean Oceanic Water). VSMOW is standard water prepared from distilled seawater that was modified to have an isotopic composition close to SMOW (Standard Mean Oceanic Water) by IAEA (Clark and Fritz, 1997). This reference is identified as VSMOW and defining the value of δ (delta) = 0 and provide an appropriate reference for meteoric waters, as the oceans are the basis of the meteorological cycle. Delta notation (δ), which is commonly used to report isotopic concentrations of the analyzed water samples, is defined as:

$$\delta = \left(\frac{R_{\text{SAMPLE}}}{R_{\text{STANDARD}}} - 1 \right) \times 1000 ; [‰]$$

Where, R_{SAMPLE} and $R_{STANDARD}$ refer to the isotopic ratios of $^{2}H/^{1}H$ and $^{18}O/^{16}O$.

A plot of $\delta^{18}O$ vs $\delta^{2}H$ for sampled waters readily identifies the influence of evaporation and the effects of mixing from different sources within the hydrologic system. Un evaporated meteoric waters are generally recognized by their proximity to the Global Meteoric Water Line **(**GMWL**;** Craig, 1961) whereas waters altered directly by evaporation or mixed with evaporatively enriched water plot to the right of the GMWL ($\delta^{2}H=8\ \delta^{18}O + 10$ ‰ SMOW).

3.4.2 INTEGRATION OF STABLE ISOTOPE AND HYDROGEOCHEMISTRY

The integration of stable environmental isotopes such as $\delta^{2}H$, $\delta^{18}O$ and geochemical techniques are used for the investigation of the sources of saline water intrusion into potable fresh groundwater in various parts of the world (IAEA, 1997). During the processes of leaching salt formations or mineral dissolution, the stable isotope content of the water is not affected while the salinity of water increases. This is a unique feature which will enable identification of such processes based on isotopic and chemical data.

4. HYDROGEOCHEMICAL METHOD

4.1 GENERAL

In order to point out the hydrochemical composition, flow processes and evolution of groundwater in the investigation area, a systematic survey and analyses of both the physical (EC, TDS, PH and T) and chemical properties of water (major cations and anions) are conducted to fill the data gaps of the secondary data.

In arid and semi-arid areas where hydrological and hydrogeological data are scarce and difficult to access, hydrochemical and isotopic data can be used as a valuable tool to investigate recharge and flow processes. Moreover, in this research, hydrochemical investigations are conducted to identify the type of hydrochemical facies, to model the type and amount of minerals that will dissolve and/or precipitate along flow path. Water chemistry data can also be used to infer groundwater flow directions, identify sources of recharge, estimate groundwater flow rates, and define local, intermediate, and regional flow systems (Anderson and Woessner, 1992).

Hydrogeochemistry has been applied by various investigators for different purposes. For instance, in the determination of groundwater recharge, in the identifications of chemical evolution and dynamics of groundwater along its flow path at different places using various techniques (Plummer et al., 1990; Guler and Thyne, 2004; Tenalem et al., 2009; Seifu et al., 2005). Among the various techniques applied, piper plot, Hierarchical Cluster Analysis (HCA) and Inverse Geochemical Modeling (IGM) are the major techniques employed by the investigators.

4.2 PHYSICAL PROPERTIES

4.2.1 TEMPERATURE

The temperature of groundwater of the investigation area ranges from a minimum of 16.4ºC to a maximum of 72ºC. The minimum temperature is obtained from cold spring around the Escarpment (AW-SP3) while the maximum temperature is associated with hot spring of Arabi (AW-SP11) around rift margin. Both the maximum and minimum temperatures are observed in the Awash Basin. The spatial variation of temperature reflects that the southern part of the area (the recharge area) is characterized by relatively lower temperature and the temperature increases gradually towards the rift.

4.2.2 HYDROGEN-ION ACTIVITY (PH)

The PH is a term used universally to express the intensity of the acid or alkaline condition of water. It is defined as the negative logarithm of hydrogen ion. Most of the waters are slightly alkaline due to the presence of bicarbonates. The PH of the area varies from 6.56 to 8.82 and 97% of the total samples used are within the permissible range of WHO (2011), which is 6.5-8.5.

The hydrogen-ion activity in an aqueous solution is controlled by interrelated chemical reactions that produce or consume hydrogen ions. The dissociation equilibrium for water is always applicable to any aqueous solution, but many other equilibrium and non-equilibrium reactions that occur in natural water among solute, solid and gaseous, or other liquid species also involve hydrogen ions. The pH of natural water is a useful index of the status of equilibrium reactions in which the water participates (Hem, 1985).

4.2.3 TOTAL DISSOLVED SOLIDS (TDS)

Total Dissolved Solids (TDS) signifies the salinity behavior of water because it is the index of the concentration of the dissolved ion in the water. There is also a relationship between TDS and Electrical Conductivity (EC). This relation is used to estimate TDS after having field EC measurement or vice versa and it also helps to check the reliability of laboratory result using certain constant (A). A is mostly between 0.55 and 0.75; the higher values generally being associated with water high in sulfate concentration (Hem, 1985). In this case A=0.714 (fig 4.1) for eastern lower Awash Basin;

$$TDS = 0.714 * EC$$

The minimum recorded TDS in the area is 190 (mg/l) which corresponds to the spring (AW-SP32) around the Escarpment and the maximum one is 10,700 (mg/L) measured from a borehole drilled in the alluvium around Harey village (AW-BH49). Both the minimum and maximum values are recorded in the eastern lower Awash Basin (ELAB). The graph of TDS versus EC also depicted a unique TDS concentration for Harey borehole in contrast to all other samples which showed a good correlation between TDS and EC (Fig 4.1). Out of 196 samples including both the primary and secondary data about 77% of them fall within the range of WHO allowable concentration and only 23% are above the maximum range of WHO (1,000mg/L) concentration in the ELAB.

However, out of 14 samples only 43% are within the range of WHO allowable concentration while 57% are above the range for Aysha Basin.

The spatial distribution map of TDS (Fig. 4.2) depicted a significant increment from the south to the north along the flow direction toward the rift floor in the eastern lower Awash Basin except along Kulen valley, Mete and Chiro to Butuji/Afdem which is mainly characterized by low TDS. However, low TDS value is measured at Durdur spring in the Aysha Basin at the northern extreme near Ethio-Djibouti border, which is likely the result of local recharge.

Table 4.1 Min and Max TDS values (Mg/L) recorded in the Basins from different sources

S/N	Data Source	Awash Basin		Aysha Basin		Fetter, 1994 TDS Classification of water	
		TDS Min	TDS Max	TDS Min	TDS Max		
1	Boreholes	332	10,700	1642	2780	0-1,000	Fresh
2	Hand-dugwells	246	4,360	2860	220	1,000-10,000	Brackish
3	Springs	190	4,204	360		10,000-100,00	Saline
4	Rivers	280	4,213	All intermittent		>100,000	Brine

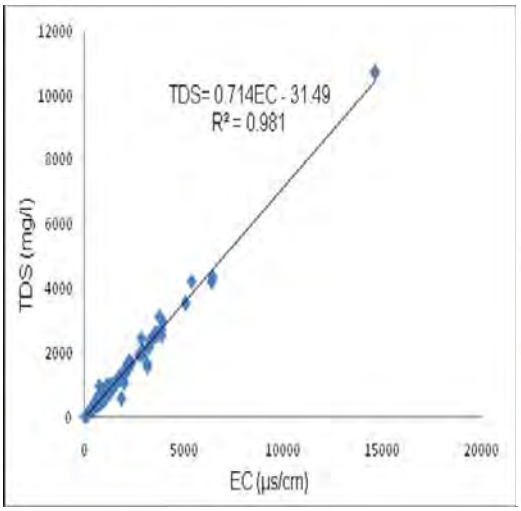

Figure 4.1 A graph showing correlation between TDS and EC of Eastern Lower Awash

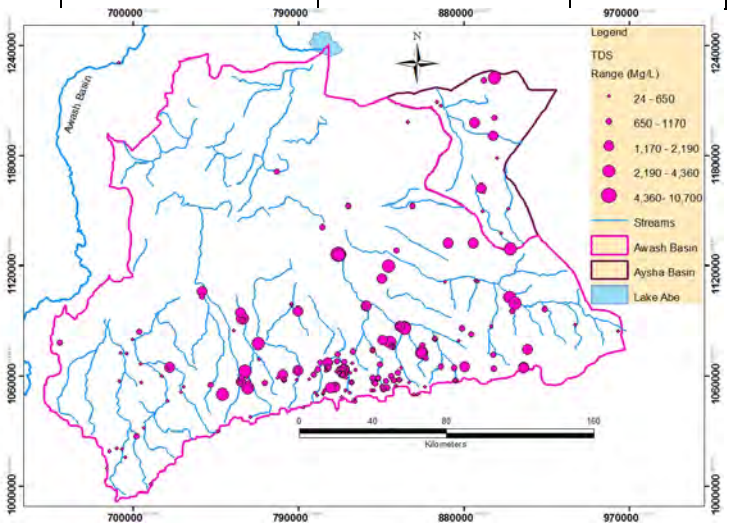

Figure 4.2 Spatial distribution map of TDS

4.2.4 ELECTRICAL CONDUCTIVITY (EC)

Electrical conductivity of water is the ability of the water to conduct an electric current. The presence of charged ionic species in water makes the water conductive. As ion

concentrations increase, conductance of the water increases. Therefore, the conductance measurement provides an indication of ion concentration in the water (Hem, 1985).

EC values of the water samples of the investigation area are in the range of 314 µs/cm to 14,620 µs/cm. The optimum values are much higher than the maximum permissible range of the standard EC value set by World Health Organization (WHO, 2011) for drinking water, which is 1,400 µs/cm.

The electrical conductivity (EC) values in the investigation area showed an increasing trend from recharge to discharge area as depicted on the spatial distribution map of EC (Fig 4.3). The groundwater sample gathered from the escarpment or recharge area indicate the least EC values. Therefore, this shows that the modification and increment of EC values comes after series of interaction of water with different lithologies along the flow path depending on various controlling factors such as the residence time, temperature, PH, the type of chemical reactions, silicate weathering and erosion of rocks and soils. The other factor is evaporation effect.

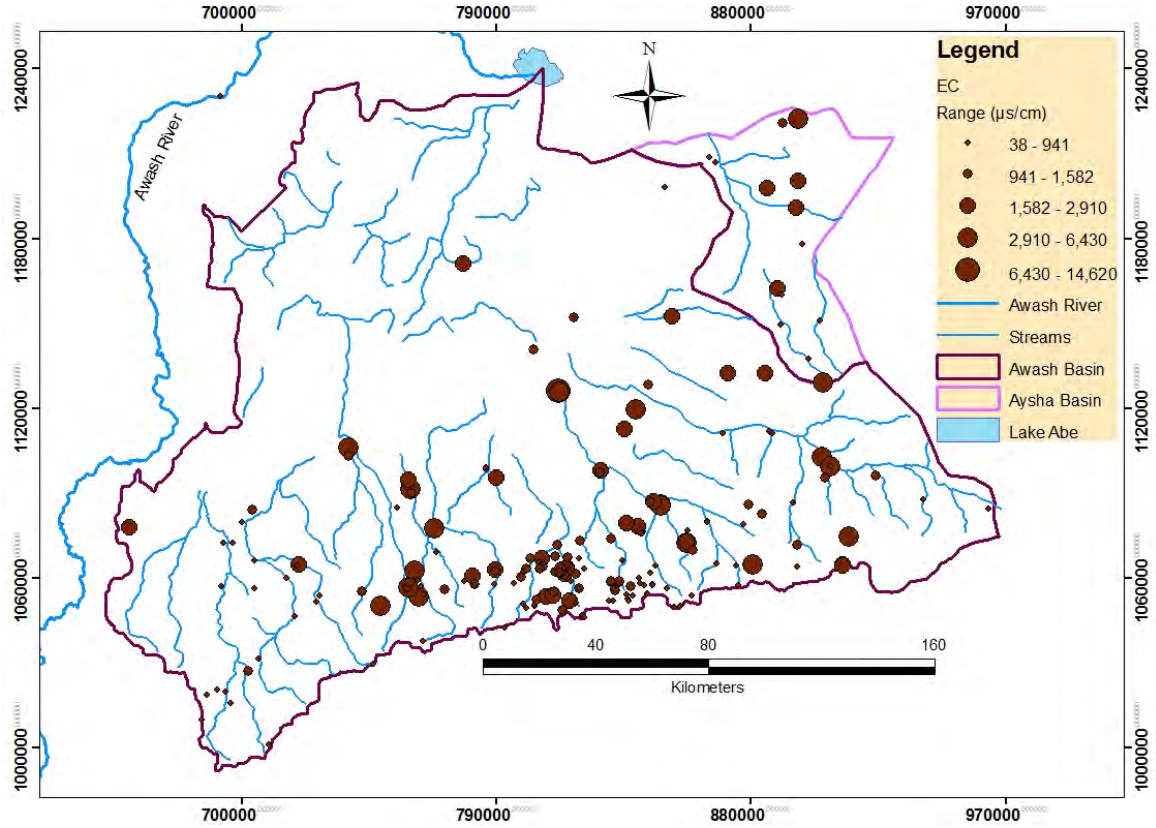

Figure 4.3 Spatial distribution map of Electrical conductivity (EC)

4.3 CHEMICAL PROPERTIES

4.3.1 HYDROCHEMICAL FACIES

Prior to use the water quality results for hydrochemical facies analysis and cluster analysis charge balance error or electro neutrality evaluation is performed for both primary and secondary data, and those with an error of more than 10 % are rejected from the data set. Then after, based on the major cation and anion analysis, four major water types are identified in the eastern lower Awash Basin using Aquachem version 4 Piper plot (Fig. 4.4). The chemical water types are distinguished and grouped by their position on a Piper diagram (Piper, 1944; Ophori and Toth, 1988; Kirchner, 1994).The identified water types are: (I) Ca-Mg-$HCO3^-$, (II) Na-$HCO3^-$ (III) Na-Cl-$SO4^{2-}$, or Na-$SO4^{2-}$-Cl and (IV) Ca-Mg-Cl-SO4 or Ca-Mg-$SO4^{2-}$-Cl.

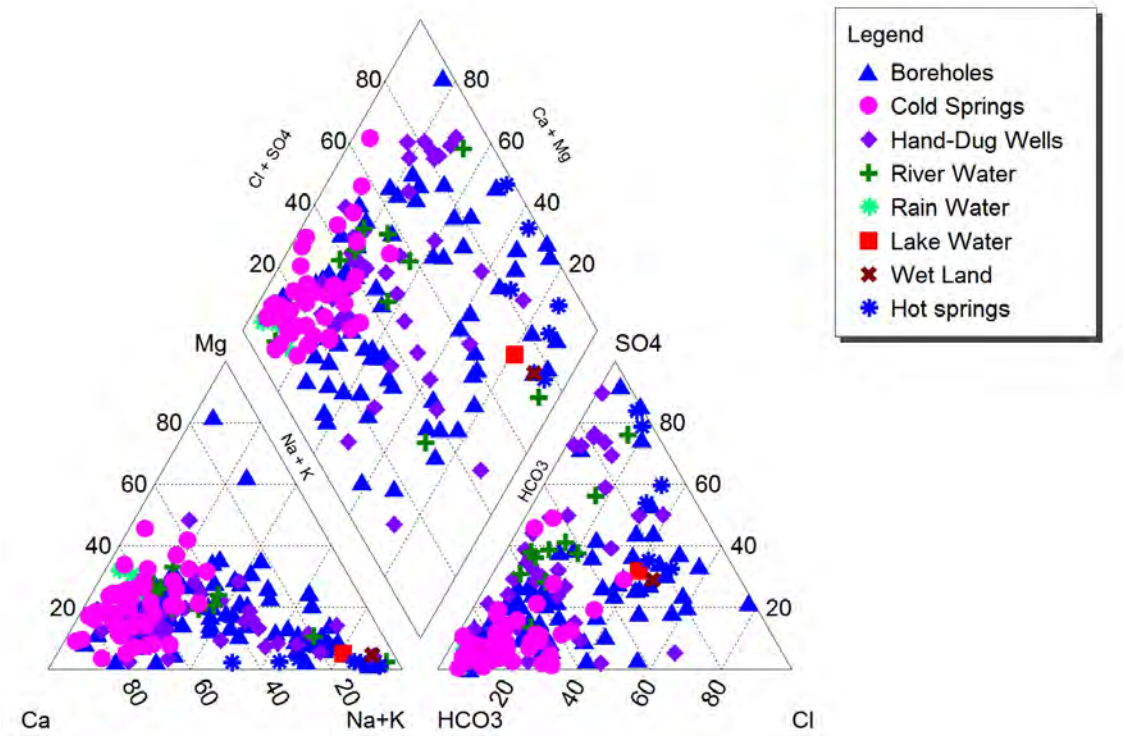

Figure 4.4 Piper plot of water samples from eastern lower Awash Basin

The analysis of water chemistry result showed that calcium (Ca^{++}) and magnesium (Mg^{++}) ions are the dominant cations while bicarbonate is the dominant anion for the majority of cold springs, boreholes, dug wells and river water samples of the eastern lower Awash Basin. Sodium (Na^+) ion is the next dominant cation with the corresponding chloride (Cl^-) and sulphate ($SO4^{2-}$) anions. However, in all of the hot

springs Na^{+} cation dominates in association with the corresponding (Cl^{-}) and sulphate ($SO4^{2-}$) anions (Fig. 4.4).

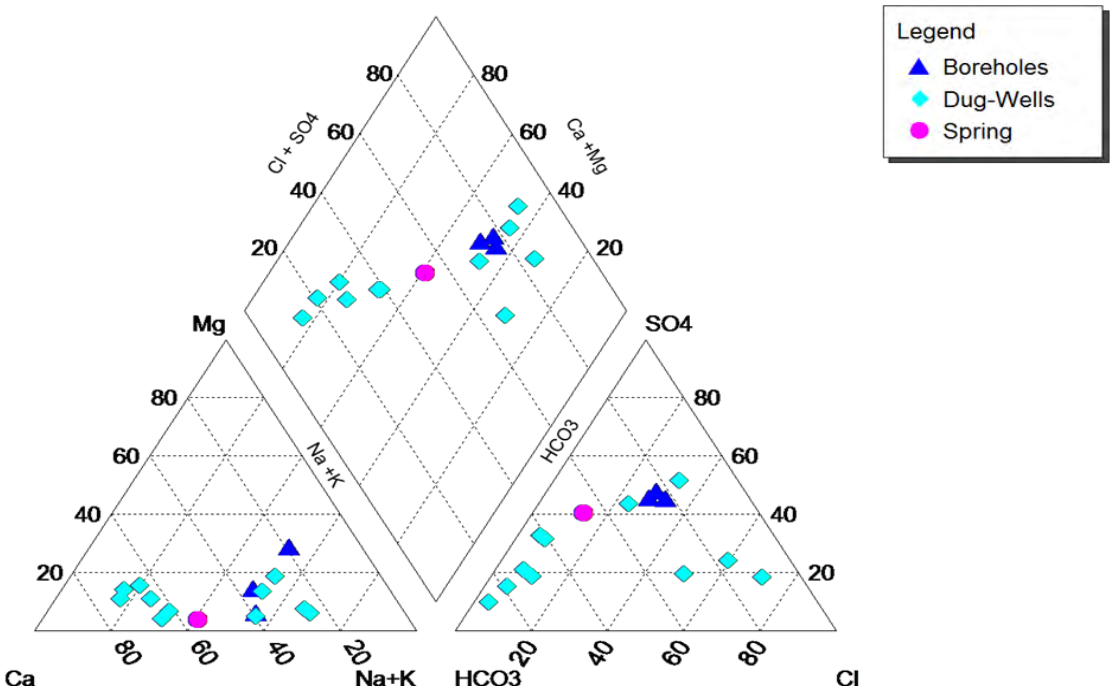

Figure 4.5 Piper plot of water samples from Aysha Basin

Unlike the eastern lower Awash Basin, the piper plot of groundwater samples of the Aysha Basin depicted the presence of two major water types/groups (Fig 4.5). These water types are: Group1) Ca-HCO3, and Group 2) Na-Ca- SO4 or Cl. Group1 comprised shallow circulating groundwater with low TDS (majorities are dug-wells from near the water divide between the Awash Basin and Aysha Basin). However, Durdur spring shows more or less a mixture of fresh and brackish water which is dominated by Ca (HCO3)2 water type followed by SO4 ions. Finally, the second group contained the entire bore holes sampled from the basin and 5 dug-wells. Two of the boreholes are tapped from volcanic rocks over lain by alluvium (Degago and Aysha boreholes) and one is from sedimentary succession around Sanajif. The source of sulphate ions in the Aysha Basin is most probably the dissolution of gypsum intercalated in the sedimentary rocks in addition to evaporate.

4.3.2 HYDROGEOCHEMISTRY OF GROUNDWATER

In the research area, Ca-Mg-HCO3 type waters occur mainly in topographically higher areas. The formation of Ca-Mg-HCO3 waters is primarily a result of the dissolution of carbonate minerals, whereby surface water charged with atmospheric and biogenic CO2 infiltrates into the subsurface (Adams et al, 2001). Rapidly circulating groundwaters in regional fractures which have not undergone a pronounced water-rock interaction have also similar water types in the rift (e.g. Kulen valley groundwater). Whereas those groundwaters characterized by Ca-Mg-SO4 or Cl are discharged from limestone and low land alluvium aquifers (fig.4.6 a, b & c). These water are evolved from Ca-Mg-HCO3 type waters in geological formations with very low/no Na (sodium) constituent. One of the most sulfate (SO4) rich route identified in the investigation area is the Erer-Idora- Asbuli flow path. The high salinity (TDS, 2610 mg/l) and temperature of Kantras (the former Erer palace) hot spring (AW-SP7) can testify the existence of deep groundwater circulation due to deep seated geological structures.

Groundwaters which fall in the Ca-Na-HCO3 type waters in the Piper plot characterize groundwater discharging from crystalline rocks (volcanic and basement rocks) around the southern escarpment (e.g. AW-SP1, AW-SP3, and Butuji-AW-BH36) (fig. 4.6 a, b). The low TDS, the enrichment of sodium and the decline of Ca^{2+} testify that the water represents transition zone groundwater.

Those Groundwaters which fall in the Na-HCO3 type waters in the Piper plot represent groundwater discharging from volcanic rock aquifers found at the margin of the rift and alluvium/elluvium that occur at the foot of the escarpment. This is because with further hydrolysis of silicate minerals by the Ca-Mg-HCO3 type waters from the escarpment, the concentration of sodium, potassium, magnesium and bicarbonate increase but Ca2+ enrichment is limited by an earlier saturation and precipitation of carbonates (Seifu, 2004).

The Na-HCO3 type groundwaters are further evolved to Na-Cl or SO4 as the groundwater moves toward the rift as observed in most of boreholes and dug wells from volcanic and alluvium aquifers in the rift.

Generally, the dominant anion of the groundwater evolves from bicarbonate in the recharge area to sulphate or chloride based on the flow path with a corresponding increase in TDS toward the rift.

$$Ca\text{-}(HCO_3)_2 \longrightarrow Ca\text{-}Mg\text{-}Na\text{-}HCO_3 \longrightarrow Na\text{-}HCO_3 \longrightarrow Na\text{-}Cl/SO_4 \quad or$$

$$Ca/Mg\text{-}HCO_3 \longrightarrow Ca\text{-}Cl/SO_4$$

This is generally related to the types of geological formations encountered and chemical reactions that took place along the flow paths. In addition, the relative age and the length of the groundwater flow paths as well as depth of groundwater circulation and exposure of water to evaporation prior to infiltration are also the determinant factors for the geochemical evolutions. The water types that are dominated by sulphates and chlorides occur in areas where there is greater water rock interaction at depth (e.g. hot springs and deep wells) due to long residence time. In the areas under considerations, the NaCl water types are also common in the discharge regimes (i.e. the lower lying areas) where salt accumulation due to high evaporation of recharged water exist (e.g. Harey borehole, AW-BH49).

a)

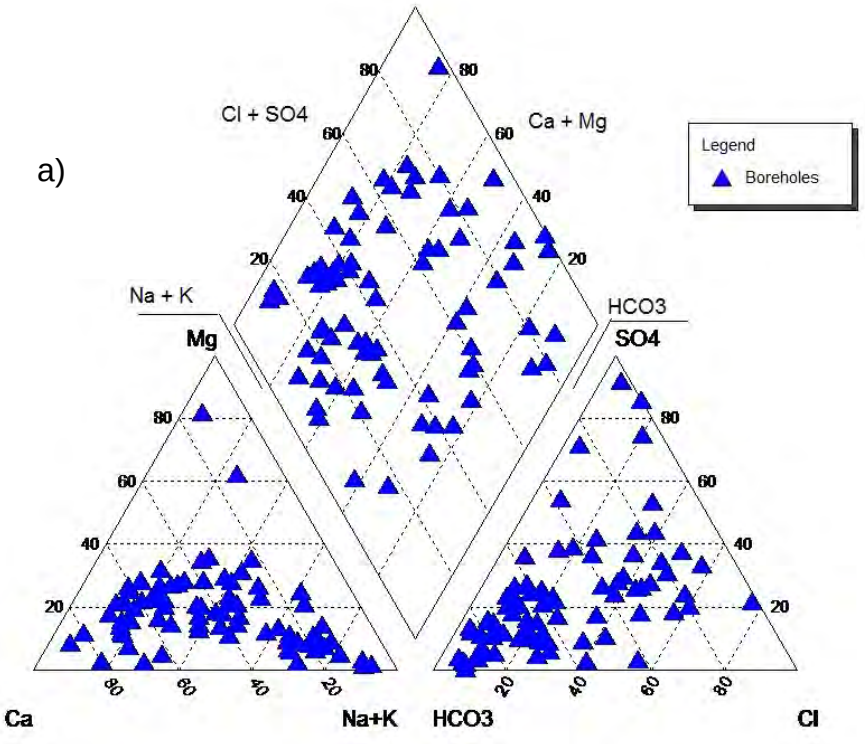

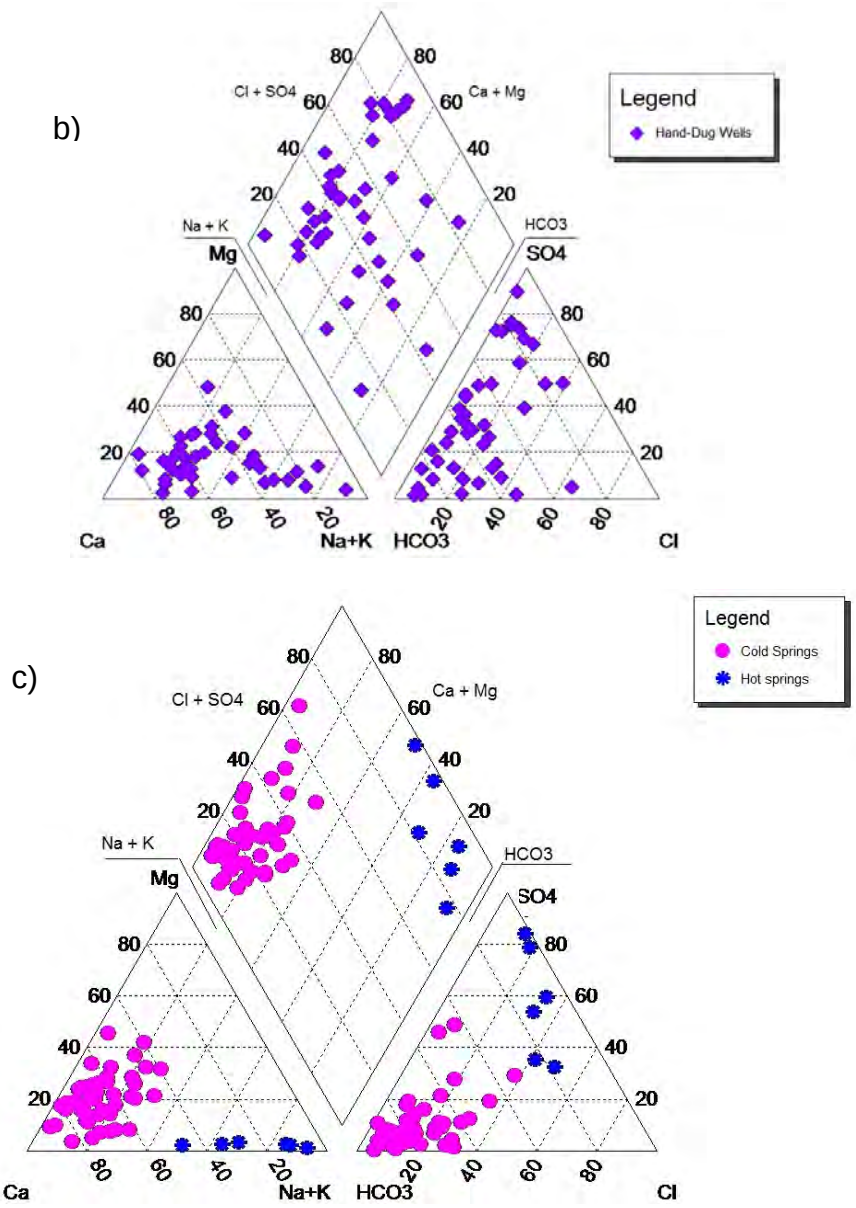

Figure 4.6 Hydrochemical representations of groundwaters: (a) boreholes (b) hand dug wells and (c) springs in the eastern lower Awash Basin using piper plot

The hot springs characterized by Na-Ca-SO4 water type are discharging from the upper sandstone and tertiary basalt where NNE aligned fault is situated (AW-SP7 and AW-SP9) at the margin of the rift. However, those characterized by Na-SO4-Cl are emerging from faulted upper Afar basalt by NNW structure (AW-SP11) and from faulted lower Afar basalt by EW running structure (AW-SP20) (fig. 4.6 c) in the rift. Their average TDS is 2470 mg/l. Generally, the entire hot springs plot as an outlier relative to the cold springs due to the effect of these structures. These structures cause deep circulation of

groundwater which brings the enrichment of Sodium (Na) and chloride (Cl) or sulfate (SO4) ions concentration.

4.3.3 HYDROGEOCHEMISTRY OF SURFACE WATER

Medisa River (AW-RW1) sampled at the top of the escarpment around Karamile on the main Asphalt road from Addis Ababa to Dire Dawa represent Ca-(HCO3)2 water types. The source of the river is spring emerging from around the water divide. This shows that groundwater and surface water are inseparable entities and they recharge each other alternatively based on hydrogeological conditions. This river base flow has a similar chemical composition with rainwater on a piper plot (Fig 4.7). That means it is not further evolved and represented by low TDS (280 mg/l). In contrast to this river, Bona stream and Chirmite Rivers which are characterized by very high TDS of 2748 and 4213 mg/l respectively testify that the rivers are the base flow of deep circulating groundwater. This fact can be confirmed by Bona stream which is the base flow of the former Erer palace hot spring (AW-SP7). The water type of Bona stream is Ca-Na-SO4 while that of Chirmite is Na-SO4-HCO3 type. The stream bed of Bona is also constituted by white salt stains which reveal the precipitation of salts. All the rivers including the Ca-Mg-Na-HCO3 river waters are also originating from the escarpment in the form of springs and disappear into the alluvium within 10-15 kilometers from the foot of the escarpment. The wet land and lake water characterized by Na-Cl-SO4-HCO3 water type denote the effect of evaporation.

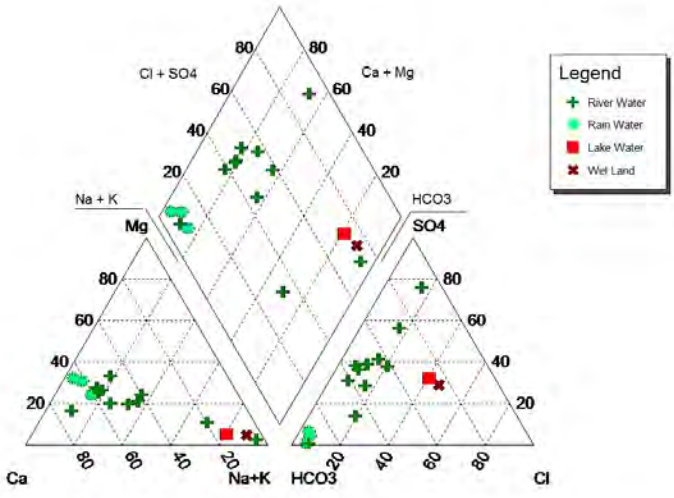

Figure 4.7 Hydrochemical representations of surface water: rainwater and wetland in the investigation area using piper plot. ***Note:*** *that all the river waters are originating from the escarpment and disappear in to the alluvium within 10-15 kilometers from the foot of Eastern Escarpment.*

4.4 CORRELATION OF MAJOR ION AND TOTAL DISSOLVED ION

Total dissolved ion (TDI) is the sum of major cations and anions. This method involves the plot of major ions (Ca^{+2}, Mg^{+2}, Na^{+} + K^{+}, $HCO3^{-}$, $SO4^{-2}$, Cl^{-}) against TDI in which both axes represent concentration in meq/l. This method is applied to detect the compositional differences (water types) in the sample set. In other words it is used to identify the major ions contributing to groundwater salinity.

On the TDI diagram, the data that plot in linear trends represent mixing of fresh and saline end members of groundwater. According to Mazor (2004) there are three possibilities for mixing lines (a) the line extrapolates to the zero points, indicating mixing of a saline water with a water that has negligible ion concentrations (dilution); (b) the line extrapolates to a point on the TDI axis, indicating the fresher end member contains significant concentrations of ions other than the ion under consideration; and (c) the line extrapolates to the ion axis, indicating both intermixing waters contain significant concentrations of the ion under consideration. For instance, mixing can be intermixing of water ascending from depth with seasonal recharge. Data that plot as more than one clusters indicate separate types of water that are not mixed. Random distributions of data indicate that many individual and unrelated water types exist or that the analytical quality of the data is poor (Mazor, 2004).

In this case, the Na+K, Cl and SO4 ions are extrapolated to a point on the TDI axis (Figure 4.8). This indicates the fresher end member contains significant concentrations of ions other than Na+K, Cl and SO4 while it is the reverse for the saline end member. In other words the major ions contributing to groundwater salinity are Na, Cl and SO4 ions. The diagram shows almost a clustering pattern for Ca, Mg and HCO3 ions against TDI.

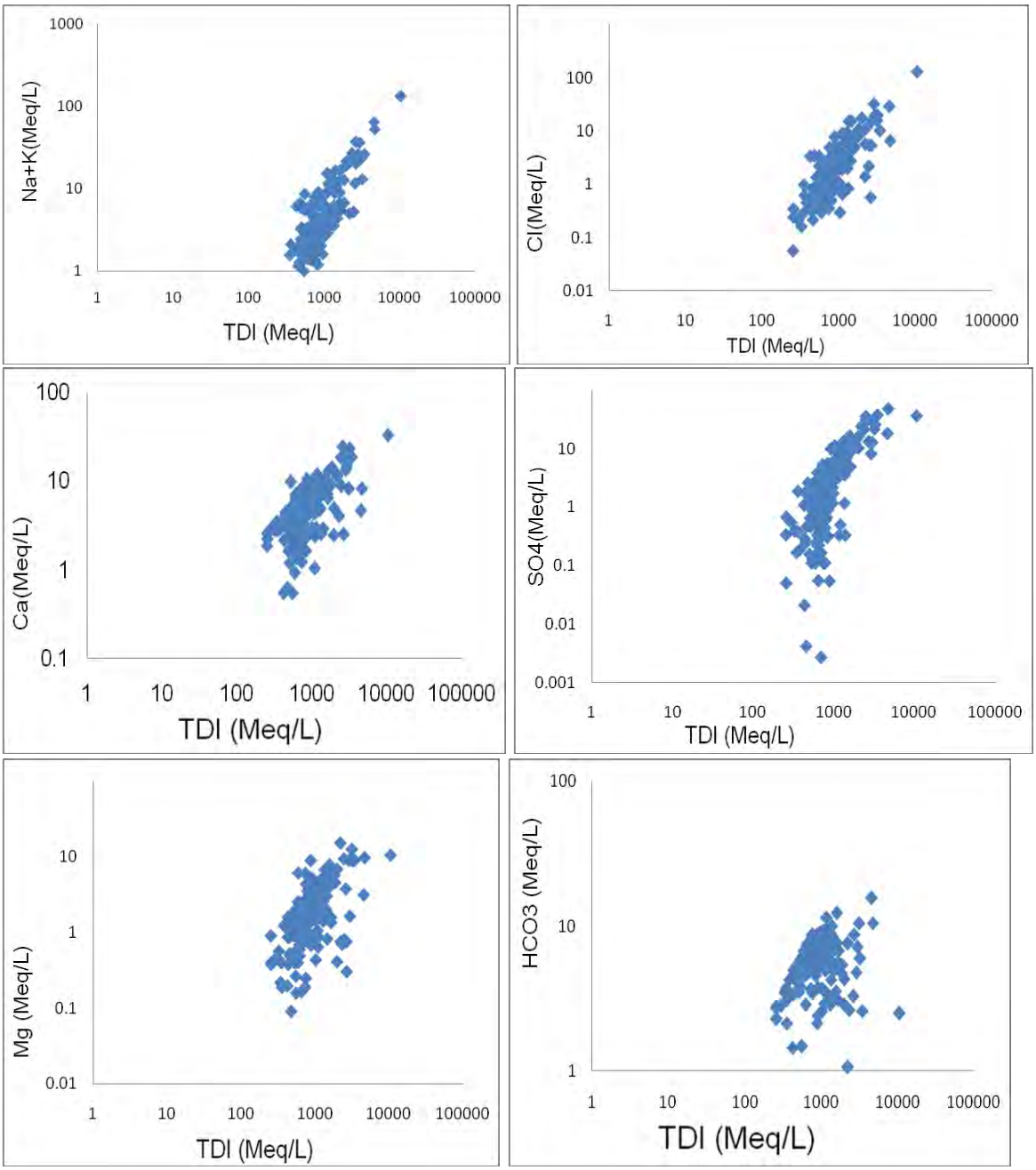

Figure 4.8 Composition diagrams of the major ions plotted against total dissolved ions (TDI) for the eastern lower Wash Basin

4.5 CORRELATION MATRICES

Correlation matrices help to identify the main elements contributing to the groundwater salinity and their tendency to follow a similar trend due to concentration by various processes such as evaporation, dissolution and cation exchange. It was used to find relationships between two or more variables (Swan and Sandilands, 1995). Samples showing $r > 0.70$ are considered to be strongly correlated whereas $r > 0.50–0.70$ shows moderate correlation.

Therefore, strong correlations exist among the major elements in Na, Cl, SO4 and TDS or EC between Na and Cl ions ($r > 0.70$) (Table 4.3). Moderate correlations $r > 0.50–0.7$ occurs between Ca, Mg, F and TDS, between SO4, F and Na, between Ca, Cl and SO4 and between Mg and SO4. These relations indicate that these ions tend to increase in concentration as the salinity of the water increases. The salinisation of the groundwater of the area resulted from increased ionic concentrations mainly due to evaporation of recharged water and dissolution effects of minerals.

The contributions of evaporitic salts are shown by the positive correlations between Ca, and SO4 (anhydrite), and between Na and Cl (halite). However, the negative and weak correlation between cations and HCO3 may reflect the precipitation of calcite minerals in the water. As evidence, travertine precipitate has been observed in the field in the eastern lower Awash Basin around Miesso, Afdem and Erer-Bona stream. The major exchangeable ions Na–Ca, Na–Mg, and K–Na all correlate positively. Any possible negative correlation brought about by cation exchange dependencies is not evident in the large and variable data set of the area. This may be due to masking of cation exchange by the other dominant processes.

Table 4.2 Correlation matrices for eastern lower Awash Basin groundwater data (for number of sample, n=179). All values in mg/l except for PH and EC (µs/cm)

	pH	TDS	Cond	K	Na	Ca	Mg	HCO3	Cl	SO4	F
pH	1	0.03	0.02	0.12	0.14	-0.33	-0.14	-0.32	0.02	0.06	0.2
TDS		1	0.99	0.17	0.93	0.7	0.54	-0.16	0.87	0.79	0.55
EC			1	0.16	0.93	0.69	0.53	-0.14	0.87	0.78	0.55
K				1	0.13	-0.05	-0.05	-0.11	0.11	0.18	0.41
Na					1	0.48	0.34	-0.17	0.88	0.65	0.62
Ca						1	0.49	-0.07	0.57	0.63	0.27
Mg							1	0.15	0.36	0.53	-0.02
HCO3								1	-0.14	-0.33	-0.25
Cl									1	0.42	0.46
SO4										1	0.48
F											1

Unlike the Awash Basin, the Aysha Basin correlation matrices show strong correlation r > 0.7 between all of the major ions (except K) and EC/TDS. However, moderate correlation r > 0.50-0.70 occurs only between EC or TDS and K, between Na and K, Na, Ca and HCO3, Ca and SO4, and between Cl and SO4 ions (Table 4.4).

From geological point of view (fig 2.8) Aysha Basin is characterized by all type of rocks: Precambrian basement, Mesozoic sedimentary succession and Quaternary volcanic rocks and alluvium. The Mesozoic succession contains gypsum intercalation between Aysha and Dewele, which is the source of raw material for Dire Dawa cement factory.

Therefore, the source of SO4 concentration in groundwater of the area is most likely gypsum dissolution and evaporation. Similarly, the strong correlation between Na and Cl may also reflect dissolution of halite.

Table 4.3 Correlation matrices for Aysha Basin groundwater data (for number of sample, n=14). All values in mg/l except for PH and EC (µs/cm)

	pH	EC	TDS	K	Na	Ca	Mg	HCO3	Cl	SO4	F
pH	1	0.09	0.08	-0.21	0.14	0.06	-0.05	-0.1	0.12	0	0.5
EC		1	0.99	0.56	0.99	0.92	0.89	0.71	0.92	0.84	-0.06
TDS			1	0.59	0.99	0.91	0.9	0.73	0.91	0.86	-0.04
K				1	0.53	0.29	0.74	0.81	0.3	0.83	-0.07
Na					1	0.89	0.87	0.64	0.93	0.82	0
Ca						1	0.73	0.56	0.91	0.64	-0.09
Mg							1	0.82	0.81	0.81	-0.22
HCO3								1	0.47	0.84	-0.1
Cl									1	0.57	-0.18
SO4										1	0.1
F											1

4.6 HIERARCHICAL CLUSTER ANALYSIS (HCA)

As it is defined in the methodology part Q-mode Hierarchical Cluster Analysis (HCA) is a powerful statistical tool which has been employed for objective clustering of the results of the groundwater data into hydrochemical facies based on their similarities in relation to compositional parameters. The classification of samples according to their parameters is termed Q-mode classification (Guler et al., 2002). This approach is commonly applied to water- chemistry investigations in order to define groups of samples that have similar chemical and physical characteristics because rarely is a single parameter is sufficient to distinguish between different water types.

In this research, Hierarchical Cluster Analysis (HCA) is performed using a Portable STATISTICA 8 soft ware. It is applied to test water quality data and determine whether samples are grouped into distinct populations (hydrochemical groups or sub groups) that are significant in the geologic and hydrogeologic context. For instance, the hydrochemical groups are assumed to have similar chemical characteristics, flow paths and processes. Prior to apply this method all the variables of water samples were log-transformed and standardized to a mean of zero and a variance of one. This restricts the influence of or the biases caused by the variables that have the greatest or the smallest variances or magnitudes on the clustering results.

The clustering technique is performed in a hierarchical way based on similarities in multidimensional space and Euclidean geometric distance between samples. Moreover, according to Euclidean principles only one line parallel to another given line may pass through a given point. The Ward's method was applied to agglomerate (link) similar samples using truncated parallel lines based on quantitative values of sample variables/parameters. The number of similar groups or sub-groups is chosen using a "phenoline" by visualization during analysis. Moving a phenoline (the broken line) toward increasing dissimilarity index causes to reduce the number of similar groups while moving it toward the descending dissimilarity index increases the number of similar groups or sub-groups. A total of 120 groundwater samples are used for eastern lower Awash Basin to group the groundwaters in to two major similar groups and eight sub-groups based on 10 (ten) parameters: TDS, EC, PH, Na, K, Ca, Mg, Cl, HCO3, and SO4 ions (fig. 4.9). For the case of Aysha Basin, 14 groundwater samples are used to classify the groundwater in to two major groups and five sub-groups based on the ten parameters (fig. 4.10).

The two major groups of the eastern lower Awash Basin are characterized by their distinct TDS, Na, SO4 and Cl anions. Both major groups comprised four (4) sub-groups each. The first group has TDS values ranging from 1,563 to 10,700 mg/l while group two has TDS values mainly varying from 190 to 1,660 mg/l.

However, the first major group of Aysha Basin contains 2 sub-groups containing a single sample each while the second group consists of 3 sub-groups. The first two sub-groups of Aysha Basin are characterized by a TDS of 2860 and 2780 mg/l respectively. But the ranges of TDS varies from 942 to 1140, 1296 to 1642 and 220 to 566 mg/l for sub-groups 3, 4, and 5 respectively.

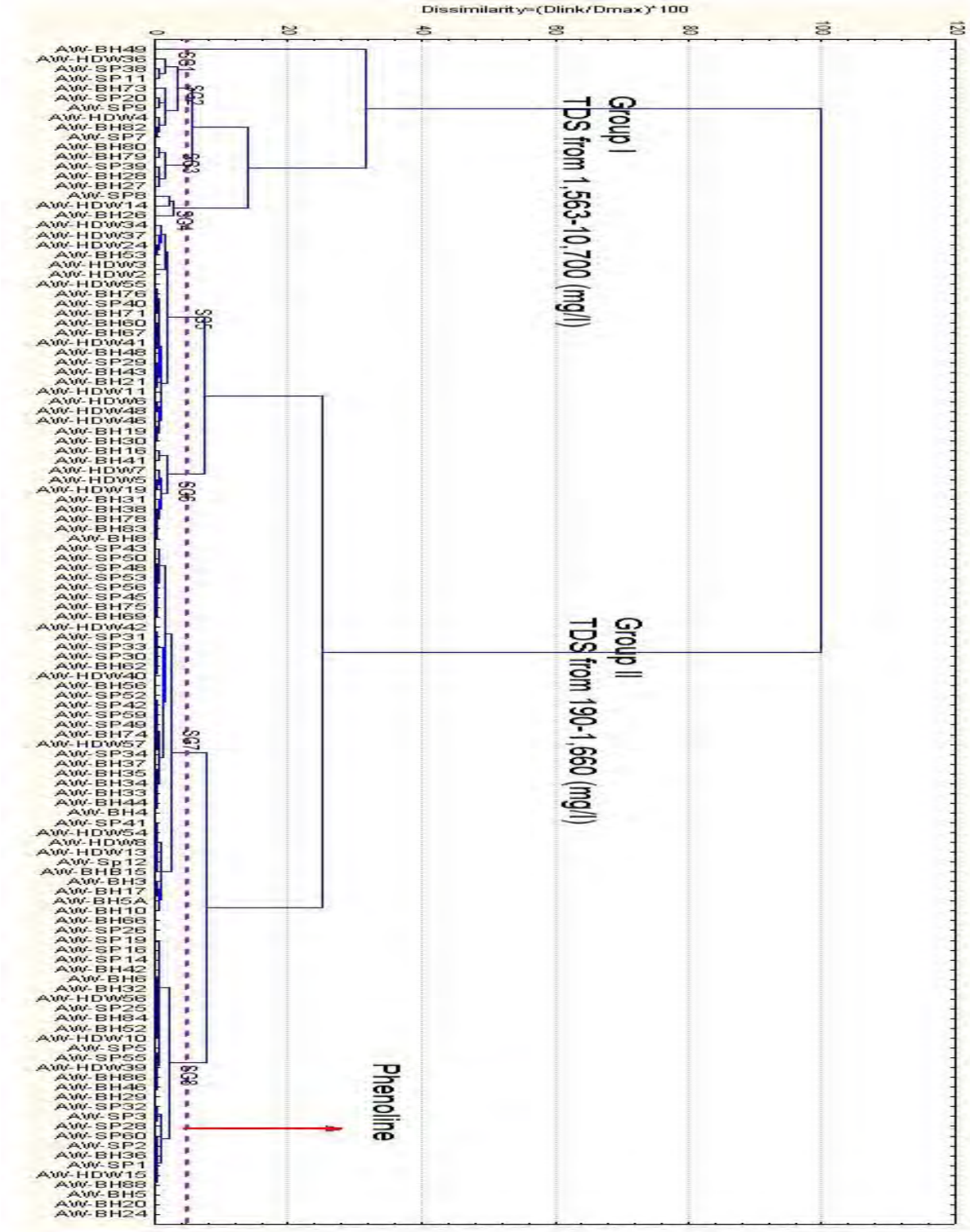

Figure 4.9 Dendrogram of Hierarchical Cluster Analysis (HCA) for Eastern Lower Awash Basin

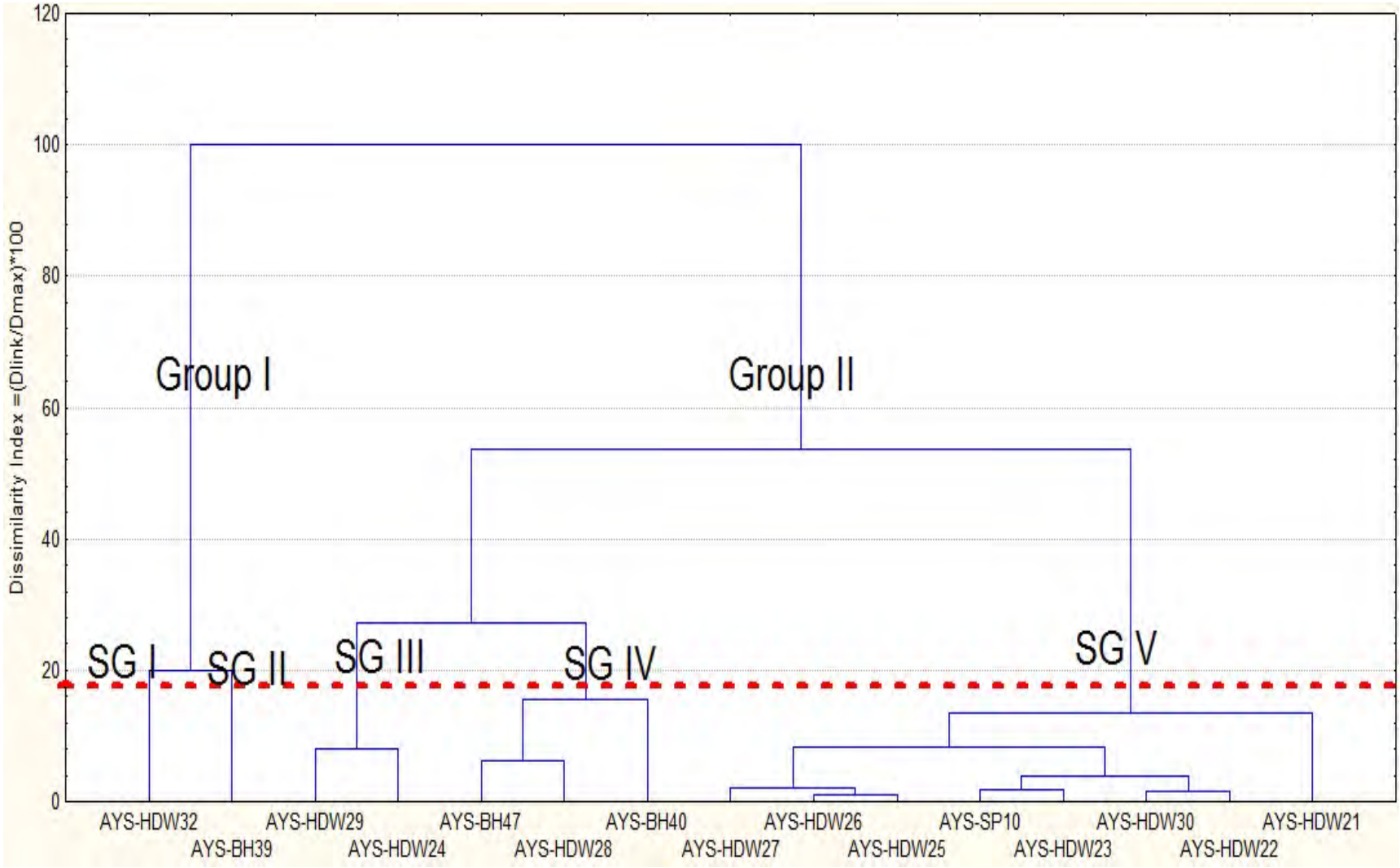

Figure 4.10 Dendrogram of Hierarchical Cluster Analysis (HCA) for Aysha Basin

The average physico-chemical compositions for each clustered sub-groups are summarized for simplicity and easy understanding of the dominant cations and anions for both Awash and Aysha Basins presented in tables (4.4) and (4.5) respectively. The mean values help to distinguish one cluster from the other easily based on physico-chemical properties and to conceptualize groundwater chemical evolution and dynamics along the flow paths. In addition, one can easily identify the recharge area groundwater from the discharge ones.

Table 4.4 Clusters Mean Values of parameters for eastern lower Awash Basin (in µs/cm for conductivity and mg/l for the rest parameters except PH), only the first 10 parameters were used for clustering

	Clusters Mean Values of Compositions (mg/l)										
Sub-Group	**TDS**	**COND**	**PH**	**Na**	**K**	**Ca**	**Mg**	**Cl**	**HCO3**	**SO4**	**F**
I^{1}	10,700.0	14,620.0	7.70	3,000.0	18.0	668.8	128.9	4,560.0	153.0	1,720.0	7.1
II^{9}	2,602.1	3,533.3	7.67	496.1	12.2	285.6	36.8	335.3	208.6	1,208.9	4.4
III^{5}	1,874.6	3,063.0	7.61	262.8	64.5	138.4	52.7	408.1	354.7	459.4	2.0
IV^{3}	4,031.3	5,963.3	7.91	1,093.3	5.8	214.1	89.7	537.4	584.8	1,630.6	1.7
V^{23}	895.0	1,294.1	7.49	91.2	3.6	148.1	27.8	119.5	422.2	154.7	0.9
VI^{10}	1,269.7	1,858.4	7.85	266.8	6.5	101.8	34.1	199.1	334.6	353.0	1.3
VII^{38}	653.7	896.6	7.75	63.1	3.9	100.1	25.9	49.6	381.4	83.1	0.7
$VIII^{31}$	413.4	635.5	7.64	42.0	3.7	77.9	15.5	23.4	321.6	33.3	0.6

$I^{1...}$ (the base roman no. indicate sub groups while the powers show no. of samples)

Table 4.5 Clusters Mean Values of Compositions for Aysha Basin (in µs/cm for conductivity and mg/l for the rest parameters except PH)

Sub-Group	**Clusters Mean Values of Parameters (mg/l)**									
	TDS	**COND**	**PH**	**Na**	**K**	**Ca**	**Mg**	**Cl**	**HCO3**	**SO4**
I^{1}	2860.0	4400.0	7.9	600.0	3.8	273.6	110.4	1130.5	292.1	388.6
II^{1}	2780.0	4060.0	7.6	515.0	33.0	167.2	154.1	551.0	642.1	1022.5
III^{2}	1041.0	1593.0	7.9	194.0	5.0	116.3	18.2	281.2	215.6	149.9
IV^{3}	1462.7	2136.3	7.9	275.3	7.4	144.4	23.6	222.9	280.5	482.9
V^{8}	357.8	533.3	7.7	41.7	4.6	63.6	5.6	21.3	195.0	74.3

Table 4.6 Descriptions for Eastern Lower Awash Basin groundwater clusters using (HCA)

Cluster	Descriptions
Subgroup I[1]	Contain a lonely saline water sample (AW-BH49) with the highest TDS (10,700 mg/l), Na cation (3,000 mg/l) and Cl anion (4,560 mg/l), which is characterized by Na-Cl-SO4 water type. This borehole is situated in the flat alluvium covered low land where flooding from the escarpment through Dire Dawa spread out and at down the catchment of brackish (TDS=4204 mg/l) Beyeas wet land (AW-SP8) which is concentrated with Na and Cl ion, 1480 and 1020 mg/l respectively. The saline behavior of this borehole is due to salt accumulation from evaporated flood water, dissolution and may be underground hydraulic linkage with the brackish Beyeas wet land due to NW running fault structure.
Subgroup II[9]	Comprised 5 hot springs, 2 boreholes and 2 dug wells. This group is characterized by an average TDS of 2,602 mg/l and dominated by Na cation and SO4 anion. The group water type is Na-Ca-SO4-Cl-HCO3. The high sodium and sulfate content reflects that the group represents deep circulating groundwater and evaporated/contaminated shallow groundwater (from alluvium). Erer palace hot spring (AW-SP7) emerging from conglomeratic upper sandstone, Biyman spring (AW-SP9) originating from tertiary basalt, Legahartu hot spring (AW-SP20) from lower Afar basalt, Arabi hot springs (AW-SP11 & AW-SP38) from the contact of upper Afar basalt and Kulen valley river bank (approximately about 5m thick travertine deposits observed around their eyes and on river bank), Hulabora borehole (AW-BH82) from tertiary basalt. All hot springs are fracture springs.
Subgroup III[5]	Consist of one hot spring and 4 boreholes. This group is characterized by an average TDS of 1875 mg/l and dominated by Na cation and SO4 or Cl anion. Their water type is Na-Ca-Cl-SO4-HCO3. The group represented a localized saline aquifer in the limestone formation in the recharge area due to fault structure (eg. Aubere BH) and in volcanic and alluvium around discharge area (Asbuli and Jama-Dere).
Subgroup IV3	This group represented the distinct evolution of subgroup 8 groundwater along two specific flow paths i.e. along Beyeas wet land and Aydora. This group is characterized by Na-SO4-Cl water type and has high average TDS of 4,031 mg/l. Aydora borehole (AW-BH26) is tapped from alluvium (250m) while Beyeas wet land water is emerging at the contact of alluvium and NW running ridge composed of rhyolitic/trachtic intrusion in basaltic rocks.

Subgroup V23	This group did not show a clear groundwater evolution from subgroup 8 and 7 at the southern part of the area but it showed relatively better evolution toward the center of the area. They are sourced mainly from alluvium and elluvium found at the foot of the highly faulted east-west running Escarpment constituted by Basement, Mesozoic and Volcanic rocks in the southern part of the area
Subgroup VI10	The group is relatively characterized by a higher average TDS (1270 mg/l) groundwater than subgroup 5, 7 and 8. This indicated the chemical evolution of subgroup 5, 7 or 8 to 6, except in the localized groundwater areas (e.g. Biyedidley-AW-BH41). The source of groundwater for this group is mainly from alluvium and some from talus bordering basaltic ridges.
Subgroup VII38	Characterized by an average TDS of 654 mg/l and Ca-Na-Mg-HCO3 water type. It represented shallow circulating groundwater near the recharge area and rapidly circulating low TDS regional groundwater (e.g. Mete-AW-BH10 and Gabi-AW-BH17 artesian well fields) in the rift. In other word, it represents transition zone groundwater. This group revealed a clear evolution from subgroup 8 as observed from spatial distribution map of clusters for eastern part of lower Awash Basin.
Subgroup VIII31	This group is characterized by the least average TDS of 413 mg/l and more of Ca-HCO3 water type. It indicated none evolved recharge area groundwater (on the Escarpment) or the least/none evolved groundwater in the lowland due to fast residence time (e.g. Biyobahay-Dure groundwater in Kulen valley). The geology of this group includes all rock types: Basement, Mesozoic sedimentary and Volcanic rock formations. However, the kulen valley surface geology is alluvium. The governing structures for the Kulen Valley groundwater may be explained by Red Sea trend faults (NW) (Shachnai, 1972).

Descriptions of Aysha Basin Groundwater Clusters Using HCA

Sub-group I and II of the Aysha Basin comprised only a single water sample each (Fig. 4.10). They are represented by their Na-Ca-Mg-Cl-SO4-HCO3 (AYS-HDW32, Dewelle) and Na-Ca-Mg-SO4-HCO3-Cl (AYS-BH39, Sanajif) water type and TDS of 2860 and 2780 mg/l respectively. The geology of Dewelle dug well is alluvium while that of Sanajif borehole is sedimentary plus basement rock.

Sub-group I II contains two samples: AYS-HDW24 and AYS-HDW29 which are distinguished by water types of Na-Ca-Cl-SO4-HCO3, Na-Ca-HCO3-Cl-SO4 and TDS of 942 and 1140 mg/l consecutively. The rock exposures that cover around the two dug wells are upper and lower Afar basalts even though the wells are supplied from river bank alluvium.

Sub-group IV characterized by a mean TDS of 1462 mg/l and Na-Ca-SO4-HCO3-Cl water type. It consists of two boreholes and one dug well. The surface geology of this sub-group is constituted by upper Afar basalt, lower Afar basalt and rhyolite/trachyte acidic rocks.

Sub-group V is represented by an average TDS of 358 mg/l and Ca-Na-HCO3 water type. This indicates that sub-group V represents shallow circulating as well as recharge area groundwater of the Basin. As it is indicated in fig 4.12 the origin of the recharging water is the water divide between the Awash Basin and Aysha Basin. The geological units of the group consist of gneiss and migmatites, upper and lower Afar basalts and rhyolitic/trachytic acidic rocks.

Therefore, the evaluation of the above sub-groups can help to arrive at the conclusions that evolution of groundwater in the Aysha basin is from sub-group V (Ca-Na-HCO3 water type) to sub-group III (Na-Ca-HCO3-Cl-SO4, Na-Ca-Cl-SO4-HCO3) and IV (Na-Ca-SO4-HCO3-Cl). However, sub-group I and II represented a localized brackish groundwater from alluvium and sedimentary rocks. This is due to salt accumulation because of evaporation and dissolution of sulfate containing sedimentary rocks.

Generally, the HCA of the eastern lower Awash basin indicated the groundwater flow direction to be; a) in the NW direction in the eastern part b) in the NS direction in the central part c) in the NE or NNE direction in the west almost following the seasonal stream flow directions (figure 4.11). Furthermore, the integration of geology, geomorphology and the groundwater evolutions identified with the help of HCA inferred the presence of at least three distinct regional structures i) from the high land along Kulen valley toward Gabi artesian wells ii) from the highland through Dire Dire Dawa toward Mete iii) from Chiro toward Afdem which results in fresh groundwater, similar to the recharge area groundwater, in the rift which have minimum water rock interaction.

The ability of HCA to classify groundwater chemistry into coherent groups that may be distinguished in terms of aquifer type, subsurface residence time and degree of human impact on water chemistry provides a good opportunity to conduct hydrogeochemical modeling and understand groundwater geochemical evolution among the different groups or subgroups (Seifu et al., 2004)

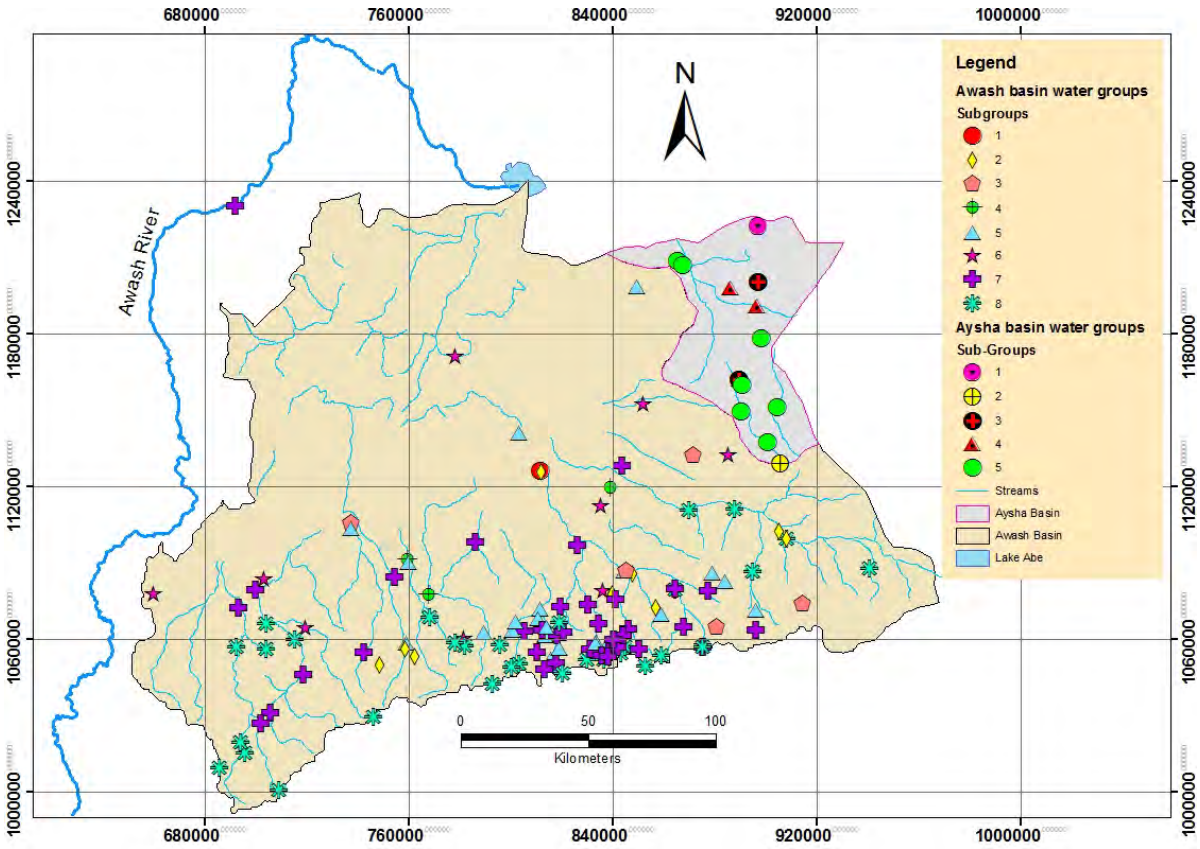

Figure 4.11 Spatial Distribution Map of Groundwater clusters for eastern lower Awash and Aysha Basins

4.7 INVERSE GEOCHEMICAL MODELING

As explained in the methodology chapter inverse geochemical modeling is commonly used to reconstruct geochemical evolution of groundwater from one point in an aquifer to another point along the groundwater flow path. Moreover, it is used to determine the type and amount in moles of minerals/phases that dissolve or precipitate along a groundwater flow path. Recent researchers (Addis, 2011; Bizuneh, 2011) also applied this technique and determined the phase mole transfers along the flow path.

The PHREEQC INTERACTIVE 2.8 computer program (Parkhurst and Appelo, 1999), which was built in Aquachem Version 4, is used to simulate the geochemical evolution between the two points. The initial and final members are selected along the groundwater flow path between different sub-groups of the HCA. Spring and dug well water categorized under subgroup 8 (recharge area water) are used as an initial member since there were no available boreholes data on the Escarpment (recharge zone). However, water from boreholes and hot spring are used as a final solution (in discharge area). Based on the HCA and groundwater evolution 5 flow paths and 1 flow path are accounted for the eastern lower Awash Basin and Aysha Basin respectively (Fig. 4.12).

The water chemistry data of the solutions used for the modeling are presented in (Table 4.7). The mineral phase selection during simulation is based on the knowledge of the area geology (fig. 2.9), the geological information from previous works in the area and field observation. The area under consideration comprises of Precambrian basement, Mesozoic sedimentary, Tertiary volcanics and Quaternary formations as well as recent basalts. Petro graphic analyses by WWDSE (2003) showing mineral compositions of some rocks in the area are summarized in (table 4.8).

Table 4.7 Groundwater chemistry data used for the Modeling

Models	Solution	ID	UTME	UTMN	Zone	PH	Na	K	Ca	Mg	F	Cl	CO3	HCO3	SO4	Water Type
	Initial	AW-HDW56	282512	1085869	38	7.8	25	5	80	16	0.45	22	0	303	24	CaMgHCO3
1	Final	AW-BH17	186047	1128116	38	7.6	200	11.5	33.44	21.12	0.62	133.78	0	278.16	145	Na-HCO3-Cl-SO4
	Initial	AW-SP55	200232	1053417	38	7.7	5	1	91	13	0.16	15	0	307	12	CaHCO3
2	Final	AW-BH49	811834	1126149	37	7.7	3000	18	668.8	128.8	7.1	4560	0	152.99	1720	Na-Cl-SO4
	Initial	AW-SP3	746448	1029765	37	7.1	20.5	0.1	70.4	2.64	0.48	10.01	0	224.48	8	CaNaHCO3
3	Final	AW-SP7	762457	1053520	37	7.7	460	7.3	380	9.2	5.6	188.1	0	56.12	1520.6	NaCaSO4
	Initial	AW-SP3	746448	1029765	37	7.1	20.5	0.1	70.4	2.64	0.48	10.01	0	224.48	8	CaNaHCO3
4	Final	AW-BH26	759581	1091435	37	7.5	600	9.7	380	110.9	0.82	358.2	0	158.6	1771	Na-Ca-SO4
	Initial	AW-SP3	746448	1029765	37	7.1	20.5	0.1	70.4	2.64	0.48	10.01	0	224.48	8	CaNaHCO3
5	Final	AW-BH27	737767	1106062	37	7.5	485	7.7	100	84	0.66	614.1	0	175.7	484.6	NaMg-Cl-SO4

Table 4.8 Summary of petrographic analysis of some rocks in the area (source: WWDSE, 2003)

Rock types	Percentage (%) and type of Mineral composition
Adigrat sandstone	30-39% quartz, up to 35% calcite, 15-62% potassium feldspar , 4% plagioclase, 2% muscovite, 2% zircon and 2% opaque minerals
Gray limestone	80-98% calcite, 2-17% quartz, 1-3% plagioclase and 0-1% opaque minerals
Brown limestone	84% calcite, 15% opaque and 1% plagioclase
Upper sanstone	40-90% quartz, up to 60% K- feldspar, 5-15% plagioclase feldspar, 3-13% clay cement, 5% calcite cement and 1% opaque
Alajae basalt	53-55% plagioclase, 25% pyroxene, 5-15% olivine, 3-8% devitrified glass, 10% oxides

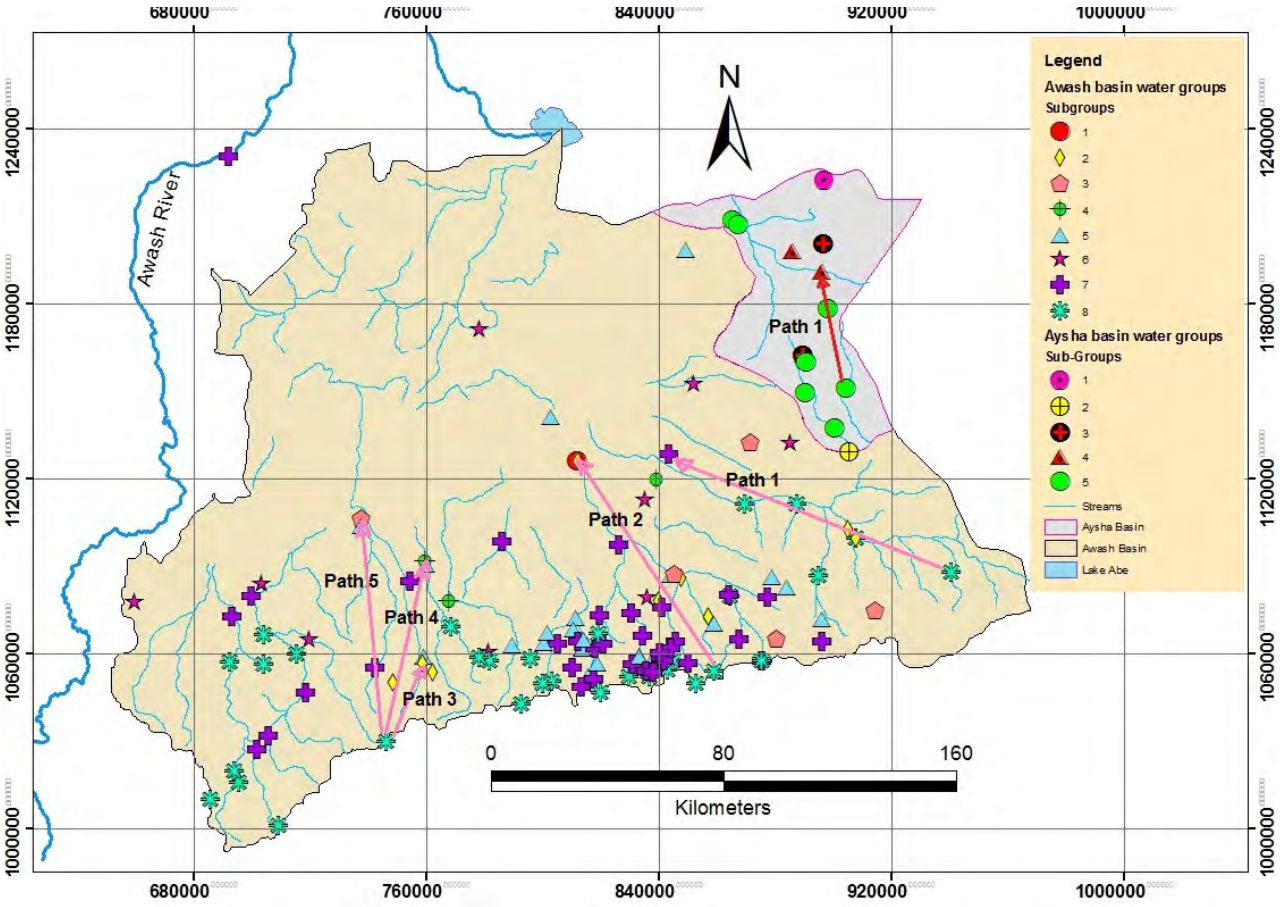

Figure 4.12 Selected flow paths for inverse geochemical modeling

A) Inverse geochemical modeling in the eastern part of lower Awash Basin;

Model 1- Flow path from Oberi to Gabi

This inverse geochemical modeling considered the groundwater flow along the potential Kulen valley. It is conducted by taking Deriwenega (Oberi) dug well (AW-HDW56) from subgroup 8 (with Ca-Mg-HCO3 water type) and Gabi artesian borehole (AW-BH17) from subgroup 7 (Na-HCO3-Cl-SO4 type) in the discharge area. The TDS of the initial solution (AW-HDW56) and final solution (AW-BH17) are 507 and 712 mg/l respectively. The BH aquifer is fractured basalt with alluvium as an upper confining layer. It is 250m deep.

Phase	mole transfers:	
Albite	4.361e-003	NaAlSi3O8
Anhydrite	1.271e-003	CaSO4
Calcite	-7.475e-003	CaCO3
CO2(g)	7.407e-003	CO2
Halite	3.187e-003	NaCl
K-feldspar	1.664e-004	KAlSi3O8
Pyroxene	3.560e-004	Mg0.5Ca0.5SiO3
Fluorite	4.480e-006	CaF2
Anorthite	5.918e-003	CaAl2Si2O8
Ca-Montmorillon	-7.023e-003	Ca0.165Al2.33Si3.67O10(OH)2

The result of the inverse geochemical modeling with uncertainties of 0.05 (5%) shows the main processes are calcite and Ca-montmorillon (typical clay mineral) precipitation and dissolution of albite, anorthite, halite, CO2 and anhydrite along this flow path.

Model 2- Flow path from SP55 to Harey

This inverse geochemical model is done for the groundwater flow from the top of the Escarpment along Jaldesa to Harey toward the rift. The model is conducted by considering a spring (AW-SP55) from subgroup 8 (with Ca-HCO3 water type) as initial solution and Harey borehole (AW-BH49) from subgroup 1 (with Na-Cl-SO4 water type) as final solution. This borehole is the most saline in the area. The TDS of the initial solution (AW-SP55) and final solution (AW-BH49) are 483 and 10,700 mg/l respectively.

Phase	mole transfers:	
Anorthite	2.639e-003	CaAl2Si2O8
Calcite	-8.517e-003	CaCO3
CaX2	2.519e-003	CaX2
CO2(g)	5.898e-003	CO2
Fluorite	1.846e-004	CaF2
Gypsum	1.797e-002	CaSO4:2H2O
Halite	1.295e-001	NaCl
K-feldspar	4.395e-004	KAlSi3O8
NaX	-5.037e-003	NaX
Olivine	2.409e-003	Mg2SiO4
Ca-Montmorillon	-2.453e-003	Ca0.165Al2.33Si3.67O10(OH)2

The result of the inverse geochemical model with uncertainties of 0.08 (8%) shows the main processes are calcite and Ca-montmorillon precipitation, cation exchange and dissolution of halite, gypsum, CO2, anorthite, olivine and K-feldspar along this flow path.

Model 3- Flow path from Hades to Kantras

This inverse geochemical model accounted the groundwater flow from Hades to Kantras (former Erer palace). The model is conducted by considering Hades cold spring (AW-SP3) from subgroup 8 (with Ca-Na-HCO3 water type) as initial solution and Kantras hot spring (AW-SP7) from subgroup 2 (with Na-Ca-SO4 water type) as final solution. The TDS of the initial solution (AW-SP3) and final solution (AW-SP7) are 230 and 2610 mg/l respectively. The cold spring originate from basalts while that of hot spring emerge from conglomeratic upper sandstone.

Phase	mole transfers:	
Calcite	-2.392e-002	CaCO3
K-feldspar	1.846e-004	KAlSi3O8
CO2(g)	1.997e-002	CO2
Fluorite	1.351e-004	CaF2
Pyroxene	5.416e-004	Mg0.5Ca0.5SiO3
Anorthite	9.545e-003	CaAl2Si2O8
Gypsum	1.656e-002	CaSO4:2H2O
Plagioclase	2.279e-002	Na0.62Ca0.38Al1.38Si2.62O8
Halite	5.037e-003	NaCl
Ca-Montmorillon	-2.177e-002	Ca0.165Al2.33Si3.67O10(OH)2

The result of the inverse geochemical model with uncertainties of 0.05 (5%) shows the main processes are calcite and Ca-montmorillon precipitation and dissolution of plagioclase, CO2, gypsum, anorthite and halite along this flow path.

Model 4- Flow path from Hades to Aydora

This inverse geochemical modeling carried out considering groundwater flow from Hades to Aydora. The model was conducted by considering Hades cold spring (AW-SP3) from subgroup 8 (with Ca-Na-HCO3 water type) as initial solution and Aydora borehole (AW-BH26) from subgroup 4 (with Na-Ca-SO4 water type) as final solution. The TDS of the initial solution (AW-SP3) and final solution (AW-SP7) are 230 and 3530 mg/l respectively. Aydora BH aquifer is alluvium from top to bottom. It is 250m deep.

Phase	mole transfers:	
Calcite	-3.966e+001	CaCO3
CaX2	1.327e+001	CaX2
Gypsum	2.021e-002	CaSO4:2H2O
CO2(g)	3.966e+001	CO2
Halite	9.654e-003	NaCl
Pyroxene	8.578e-003	Mg0.5Ca0.5SiO3
NaX	-2.655e+001	NaX
Plagioclase	4.284e+001	Na0.62Ca0.38Al1.38Si2.62O8
Anorthite	1.663e+001	CaAl2Si2O8
Ca-Montmorillon	-3.965e+001	Ca0.165Al2.33Si3.67O10(OH)2
Illite	4.075e-004	K0.6Mg0.25Al2.3Si3.5O10(OH)2

The result of the inverse geochemical modeling with uncertainties of 0.05 (5%) shows the main processes are calcite and Ca-montmorillon precipitation, cation exchange and dissolution of plagioclase, CO2, anorthite, gypsum, halite and illite (sediments) along this flow path.

Model 5- Flow path from Hades to Asbuli

This inverse geochemical modeling is done by considering groundwater flow from Hades to Asbuli. The model is conducted by taking Hades cold spring (AW-SP3) from subgroup 8 (with Ca-Na-HCO3 water type) as initial solution and Asbuli borehole (AW-BH27) from subgroup 3 (with Na-Mg-Cl-SO4 water type) as final solution. The TDS of the initial solution (AW-SP3) and final solution (AW-BH27) are 230 and 2174 mg/l respectively. Asbuli BH aquifer is basalts. It is 227m deep.

Phase	mole transfers:	
Calcite	-6.685e-003	CaCO3
Anorthite	2.260e-003	CaAl2Si2O8
Gypsum	4.971e-003	CaSO4:2H2O
CO2(g)	5.165e-003	CO2
K-feldspar	1.947e-004	KAlSi3O8
Halite	1.787e-002	NaCl
Olivine	1.677e-003	Mg2SiO4
Plagioclase	1.446e-003	Na0.62Ca0.38Al1.38Si2.62O8
Ca-Montmorillon	-2.880e-003	Ca0.165Al2.33Si3.67O10(OH)2

The result of the inverse geochemical modeling with uncertainties of 0.07 (7%) shows the main processes are calcite and Ca-montmorillon precipitation and dissolution of halite, CO2, gypsum, anorthite, olivine, and plagioclase along this flow path.

B) Inverse geochemical modeling in the Aysha Basin;

Model 1- Flow path from Biyegurgur to Aysha

This inverse geochemical modeling is approached by accounting groundwater flow from Beyegurgur to Aysha. The model is conducted by considering Beyegurgur shallow dug well (AYS-HDW25) from subgroup 5 (with Ca-HCO3 water type) as initial solution and Aysha borehole (AYS-BH47) from subgroup 4 (with Na-Ca- SO4-Cl-HCO3 water type) as final solution. The TDS of the initial solution (AYS-HDW25) and final solution (AYS-BH47) are 274 and 1450 mg/l respectively.

Phase	mole transfers:	
Calcite	-4.373e-002	CaCO3
Halite	5.582e-003	NaCl
K-feldspar	7.744e-006	KAlSi3O8
Plagioclase	4.409e-002	Na0.62Ca0.38Al1.38Si2.62O8
Pyroxene	2.577e-003	Mg0.5Ca0.5SiO3
CO2(g)	4.698e-002	CO2
Gypsum	4.355e-003	CaSO4:2H2O
CaX2	1.128e-002	CaX2
Ca-Montmorillon	-4.273e-002	Ca0.165Al2.33Si3.67O10(OH)2
Anorthite	1.936e-002	CaAl2Si2O8
NaX	-2.257e-002	NaX

The modeling result shows the dissolution of halite, gypsum, CO2 which is consumed during silicate hydrolysis and dissolution of silicate mineral. In addition, precipitation of calcite, Ca-montmorillon and cation exchanges are modeled along the flow path.

Generally, the inverse geochemical modeling revealed the existence of three main flow processes: precipitation, dissolution and cation exchange which control the groundwater chemistry of the basins. The calculations of saturation indices (SI) of groundwater in the area also supported the strong precipitation of carbonate minerals and dissolution of sulfate minerals and halite along the flow path (fig. 6.2 and 6.3). Especially, calcite precipitation is common in the Basins.

4.8 GOUNDWATER QUALITY

The data on chemistry of the groundwater have been used for the evaluation of quality of water for drinking, industrial and irrigation purposes in addition to its further application in the investigation of recharge processes and salinization processes.

4.8.1 DRINKING WATER QUALITY

The quality of water is very important to the mankind, because it has a direct link with human welfare. The water to be used for drinking purposes must meet very high standards of physical, chemical and biological purity. Certain minimum quality parameters for this requirement have been established by World Health Organization (WHO, 2011). The minimum recorded TDS in the area is 190 (Mg/L) which corresponds to the spring around the Escarpment (AW-SP32) and the maximum one is 10,700 (Mg/L) measured from a borehole drilled in the alluvium around Harey village (AW-BH49).

Table 4.9 Comparisons of min. and max. recorded parameters in the area with guidelines of WHO (2011)

S/N	Recorded Parameters (mg/l)	Eastern L/Awash		% > WHO out of 196 samples	Aysha Basin		% > WHO out of 14 samples	WHO (2011) guidelines
		Min.	Max.		Min.	Max.		
1	Turbidity (NTU)	1	9037.4		1	7		4 NTU
2	TDS	190	10700	24.5	220	2860	42.9	1000
3	PH	6.56	8.82	1	7.07	8.17	-	6.5-8.5
4	Na	4	3000	17.5	12.5	600	42.9	200
5	Fe	0	0.96	1	0	0.08	-	0.3
6	F	0.14	8.49	13.3	0.71	2.9	28.6	1.5
7	Cl	2	4560	12.8	5.7	1130.5	28.6	250
8	NO3	0.25	510.3	12.8	1.13	131.2	50	50
9	SO4	0.95	2260.8	20.9	25.89	1022.45	35.7	250
10	NH3	0.018	12.8		0.09	3.3		1.5
11	CaCO3 (TH)	85.5	2204		129.2	1140		500
12	Mn	0.02	0.15		0.02	0.03		0.1

4.8.1 IRRIGATION WATER QUALITY

The suitability of water for irrigation depends upon TDS (salinity) and the sodium content in relation to the amounts of calcium and magnesium or SAR (Alagbe, 2006). The suitability of groundwater for irrigation use is evaluated by calculating Sodium Adsorption Ratio (SAR).

$$SAR = \frac{Na^{+}}{\sqrt{\frac{Ca^{++} + Mg^{++}}{2}}}$$

The water having SAR values less than 10 are considered to be excellent, 10 to 18 as good, 18 to 26 as fair, and above 26 are unsuitable for irrigation use (USDA, 1954). In this research area, the SAR values are less than 10 for majority (85%) of groundwater of the eastern lower Awash Basin and be graded as an excellent for irrigation use (Fig.4.14). It is also greater than 26 mainly for some hot springs and some shallow groundwater in the study area (e.g Arabi hot spring). Hence, this water is unsuitable for irrigation purposes and constitutes only about 2% out of 190 groundwater samples. However, in the Aysha Basin water suitability for irrigation purpose mainly ranges from good to excellent (Fig.4.13) despite its low aquifer productivity.

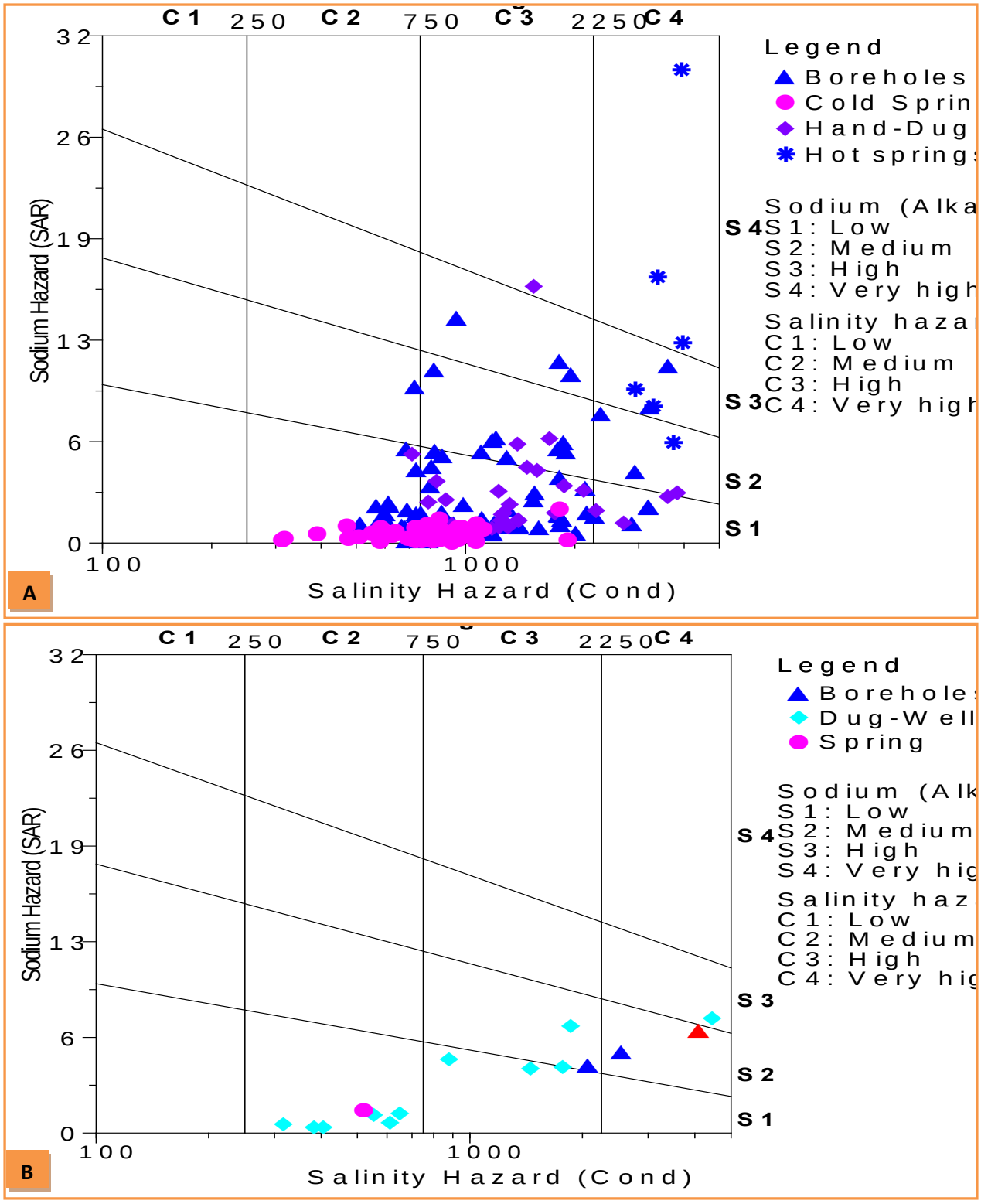

Figure 4.13 Wilcox diagram of Sodium Adsorption Ratio (SAR); A) Awash and B) Aysha groundwater in the investigation area

5. STABLE ISOTOPES OF WATER

A water molecule is composed of oxygen and hydrogen, which occurs with different isotopic combinations in its molecules. The isotopic composition of precipitation containing these two elements may be reflected directly or modified in the composition of groundwater. The modification of groundwater composition may be due to fractionation or separation of heavier and lighter isotopes because of evaporation processes (phase changes) prior to infiltration or isotopic exchange with aquifer matrixes (Mazor, 2004). The common practice is to plot water sample data on δ^2H versus $\delta^{18}O$ diagrams, along with the meteoric line of local precipitation as a reference line. The meteoric line is a convenient reference line for the understanding and tracing of local groundwater origins and movements using conservative isotopes of water molecules (deuterium and oxygen 18). Therefore, isotopic data of the Addis Ababa station monitored by International Atomic Energy Agency (IAEA) are used to drive a Local Meteoric Water Line for this specific research, since there is no other monitored station closer than Addis Ababa to the investigation area (fig 5.1). The data used are down loaded from GNIP isotopic data base web site (*http://isohis.iaea.org/*).

In order to trace the source and mechanism of groundwater recharge isotopic signature of deuterium and oxygen 18 in the groundwater sample are used. In order to get these signatures, 51 representative water samples are gathered from the eastern part of the lower Awash Basin during field work (Fig 5.2 and annex 2) from different sources (such as rain water, springs, dug wells, river water emanating from highlands, boreholes and a wet land) and analyzed at Addis Ababa University (AAU) isotope laboratory. But, 3 groundwater samples taken from Aysha Basin are excluded from the data set due to the unreliability of laboratory analysis result.

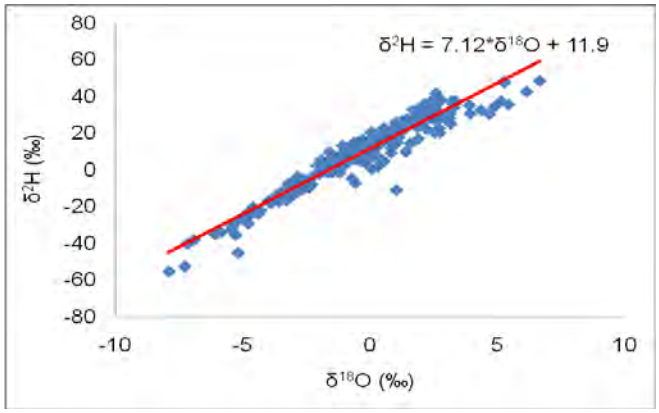

Figure 5.1 Scatter plot of deutrium (^2H) vs oxygen (^{18}O) monitored at Addis Ababa station by IAEA from 1961-2007

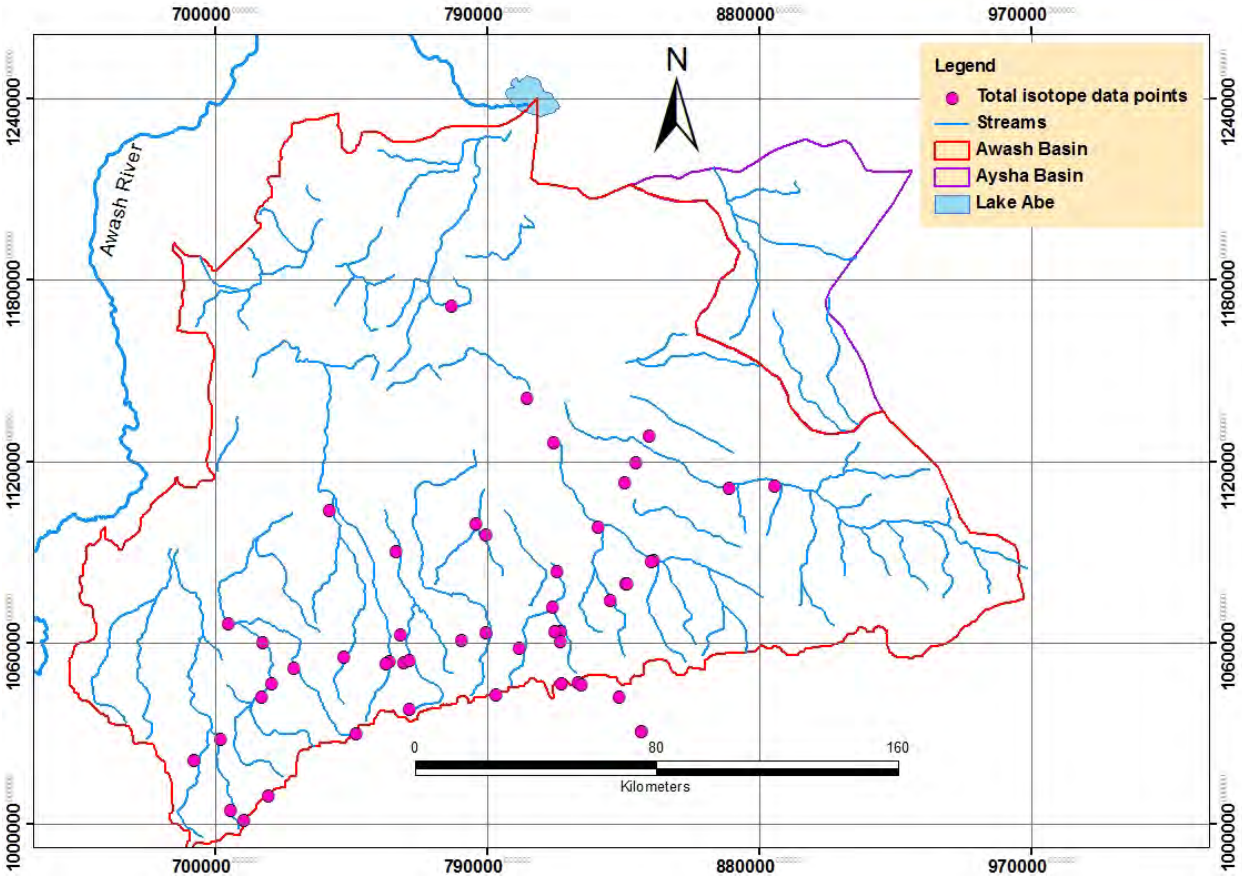

Figure 5.2 Location of sampling points for isotope data

5.1 ISOTOPIC COMPOSITION OF THE RESEARCH AREA RAIN WATER

The isotopic compositions of one month cumulative rainfall captured at 4 sites; 3 from the high land and 1 from the low land approaches the local meteoric water line of Addis Ababa. Just a one day light rainfall sampled at Chiro (at noon) shows high enrichment while that of Harar captured same day (at night) fall very close to the LMWL. The reason for the enrichment of chiro precipitation (AW-RAW6) is the amount effect (Fig. 5.3). The amount effect is due to the falling of light rain through a dry air column above the ground which can cause a kinetic fractionation (evaporation) on the drop (Clark and Fritz, 1997).

The global distribution pattern of stable isotope content in precipitation was reviewed (Dansgaard, 1964) during the first years of operation of the IAEA/WMO (World Meteorological Organization) network. In this evaluation, the spatial distribution of heavy isotope content was related to environmental parameters, such as altitude, latitude, amount of precipitation, air temperature and degree of continentality. All of these factors

reflect the degree of washout from the air mass, and to some extent, the water vapor history from the source to the site of precipitation.

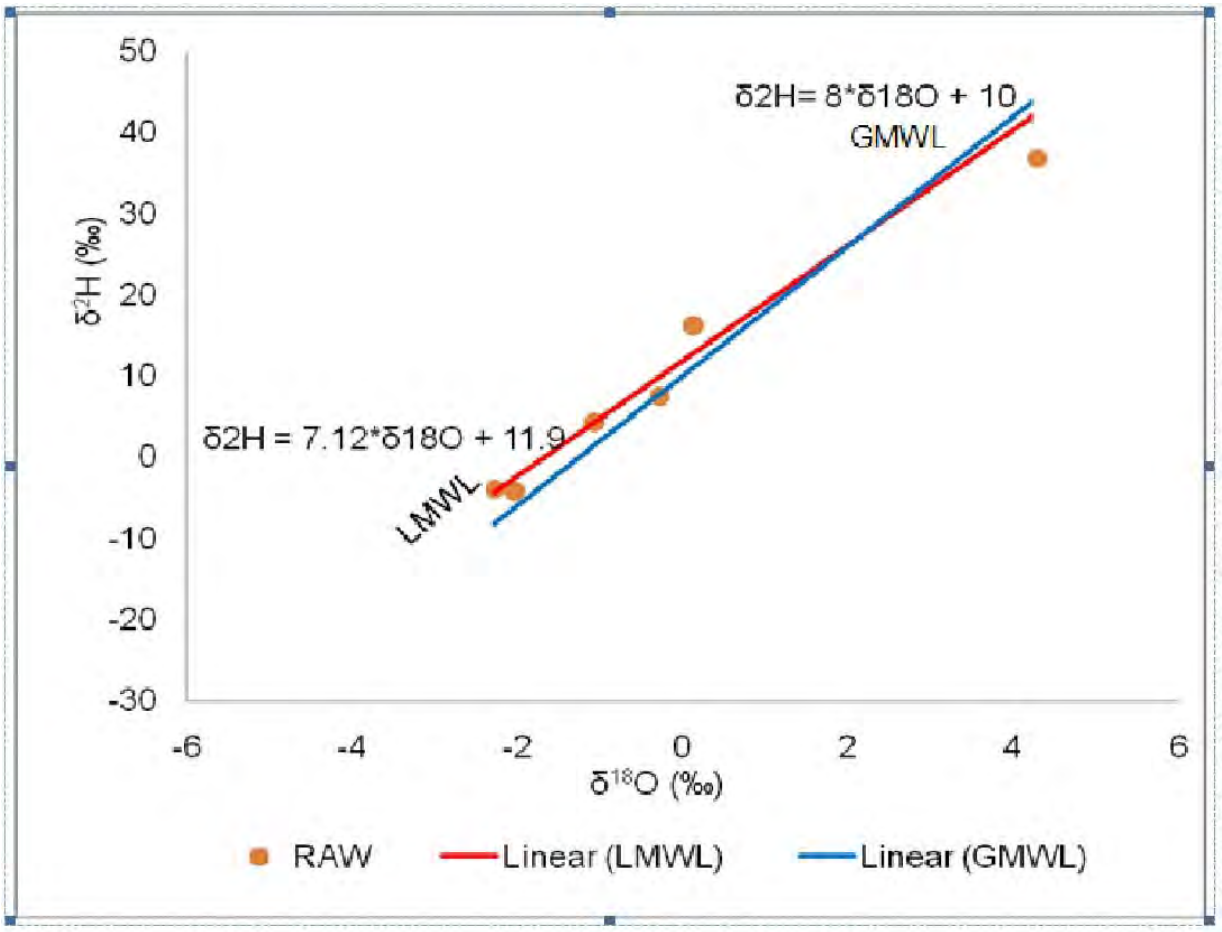

Figure 5.3 Plot of Isotopic signature of summer rainfall of 2011 from inside and around the investigation area

5.2 OXYGEN (δ18O) AND DEUTRIUM (δ2H) ISOTOPES

The most commonly employed stable isotopes are ^{18}O and ^{2}H, which are often used for assessment of the "genesis" (origin) of water, particularly in groundwater systems; processes involved in the replenishment (process-tracing); for estimating mixing proportions of different sources or component flows (component-tracing); and studying hydraulic interconnections between groundwater and surface waters or between different aquifer units within a given groundwater system (Yurtsever & Araguas, 1993). However, in this research the objective uses of stable isotopes are to identify recharge source, mechanism and to determine origin of salinity. One of the most important factors governing the use of these isotopes is the isotopic fractionation occurring during

phase changes, i.e. condensation or evaporation, which is mainly a temperature dependent phenomenon. The isotopic changes thus induced, is a conservative property of the isotope during its circulation in the hydrological systems, and it is a finger-print of the history of the processes involved in its formation and circulation.

The ^{18}O and ^{2}H variations in natural waters show a linear relation as a consequence of the fact that their behavior during the fractionation processes are similar. The equation derived in this regard was first given by Craig (1961) using annual average values of ^{18}O and ^{2}H as:

$$\delta^2H = 8*\delta^{18}O+10 \qquad \textbf{(GMWL equation)}$$

Craig's global meteoric water line is essentially a global average of many local meteoric water lines, each controlled by local climatic factors, including the origin of the vapour mass, secondary evaporation during rainfall and the seasonality of precipitation. These local factors affect both the deuterium excess and the slope (Clark and Fritz, 1997). Deuterium excess (d);

$$d = \delta^2H - Slope*\delta^{18}O, \qquad \text{(to calculate d for any precipitation)}$$

regionally varies due to variations in humidity, wind speed and sea surface temperature during primary evaporation. Whereas the slopes are affected by evaporation effects which occur after condensation.

For this investigation, surface water and groundwater isotopic data are compared with a local meteoric water line (LMWL) to identify the source and mechanism of recharge and the hydrological processes that took place. However, since there was no previous monitored stable isotope data over representative period of time (at least 1year) meteoric water line is borrowed from Addis Ababa monitored stable isotope data station, which is the closest:

$$\delta^2H= 7.12*\delta^{18}O*+11.9, \qquad \textbf{(LMWL of Addis Ababa precipitation),}$$

Where, 7.12 and 11.9 indicate the slope and deuterium excess of the LMWL

respectively.

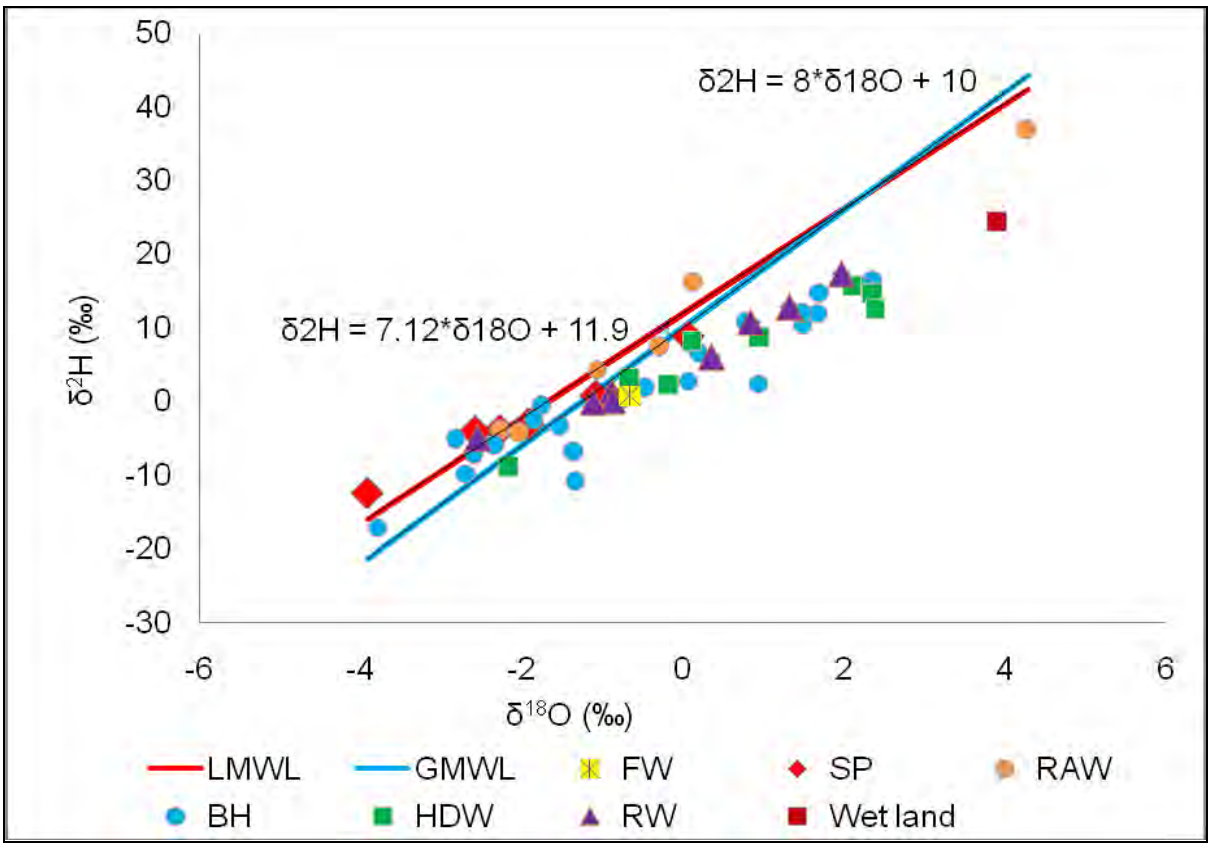

Figure 5.4 A plot of Deuterium (^2H) and Oxygen 18 isotopes of water samples

Majority of boreholes (BH), a few springs (SP), flood water (FW), the entire shallow groundwater (HDW), and river waters (RW), a wet land and one day light rainfall data (AW-RAW6) fall below the local meteoric water line (LMWL) (Fig. 5.4). This relation mainly revealed as secondary fractionation or evaporation after condensation or prior to recharge has occurred. The other factors that control the isotopic concentration of groundwater are distance from moisture source, isotopic exchange with aquifer matrices at high temperature and altitude of precipitation (Fig.5.5). This figure illustrates the increasing enrichment of the isotopic composition of groundwater from the highland toward the rift due to high evaporation effect in the rift.

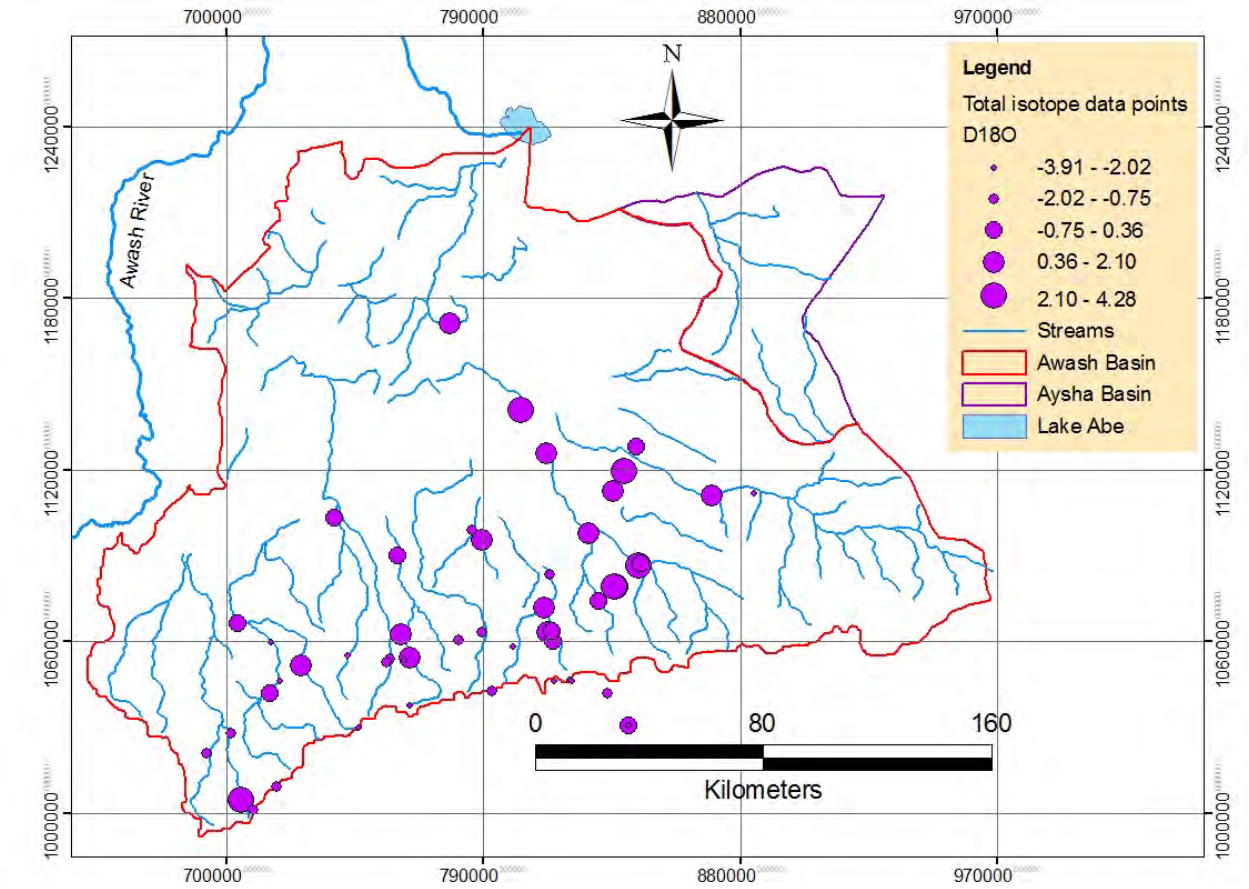

Figure 5.5 Spatial distribution map of d18O in the eastern lower Awash Basin over classified DEM

5.3 ISOTOPIC COMPOSITION OF GROUNDWATER

The isotopic signature of groundwater in the investigation area varies from -4 to 4 for $\delta^{18}O$ and -20 to 20 for $\delta^{2}H$. All of the shallow (dug wells) and intermediate groundwaters indicated enrichment of the isotopic composition. In this area, isotopic compositions of groundwaters are highly depleted on the escarpment and enriched in the rift. Similar to the escarpment area, some groundwater depletion is also evident in the rift where the source water is not affected by significant evaporation effect (Fig. 5.5). Among the springs sampled from the research area, Erer palace hot spring (AW-SP7) isotopic analysis result showed the highest depletion of $\delta^{18}O$ (-3.91‰) and $\delta^{2}H$ (-12.31‰) and plot above the LMWL. Cold springs of Dengego (AW-SP1), Kulubi (AW-SP2) and Hades (AW-SP3) gathered from top of the escarpment plotted very close to the meteoric water line. Whereas, cold springs of Wachu (AW-SP4), Arberekete (AW-SP5) and Deladu (AW-SP6) emerging from volcanic aquifers plot below the meteoric water

lines, indicating relative enrichment due to evaporation effect after condensation or secondary fractionation.

The other most important observation is the slight enrichment of isotopic composition of deep artesian groundwaters in the rift. The two sampled artesian groundwaters in the area are Gabi and Mete artesian wells. The isotopic composition of Gabi is 0.0697‰ $\delta^{18}O$ and 2.79‰ $\delta^{2}H$ and that of Mete is -1.34‰ $\delta^{18}O$ and -6.83‰ $\delta^{2}H$. Among the two wells Gabi artesian groundwater shows relatively higher enrichment.

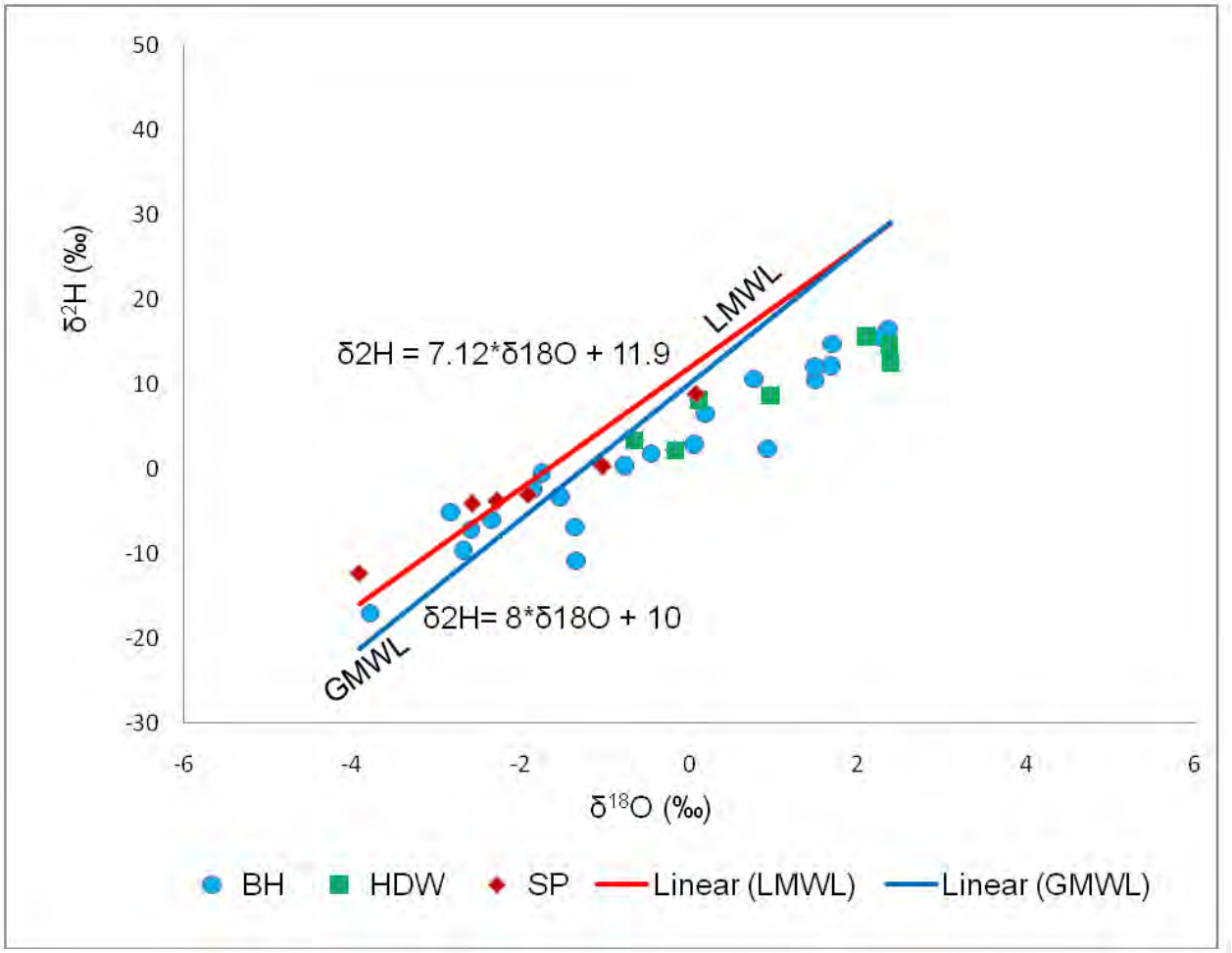

Figure 5.6 Graph showing Isotopic compositions of groundwater

5.4 ISOTOPIC SIGNATURE OF SURFACE WATER

The area under consideration is characterized by very limited surface water, due to the arid to semi-arid climatic condition and low annual rainfall of the area. All the sampled

river waters are emerging from the escarpment, which gets relatively good annual rainfall, as base flow of springs.

Except the isotopic compositions of Medisa river (AW-RW1) (with δ18O= -2.54‰ and δ2H= -4.92‰), sampled at the top of the escarpment on the way from Addis Ababa to Harar, all river waters sampled at the foot of the escarpment show enrichment and fall on river evaporation line with slope=5.052 and deuterium (d) excess=6.406, including the secondary isotope data of Awash river. The enrichment of the river water is due to secondary fractionation because of evaporation after condensation and while it flows down to the low land. Enrichment values vary from -0.88 to 1.97‰ for $\delta^{18}O$ and 0.13 to 17.43‰ for $\delta^{2}H$. Medisa River which is the base flow of spring emerging from around the water divide falls on LMWL and definitely reveals meteoric water (Fig. 5.7).

Beyeas wet land (AW-SP8) and flood water sampled from the area also depicted enrichment due to evaporation effect. The isotopic signatures of the wet land and flood water are ($\delta^{18}O$= 3.92‰, $\delta^{2}H$=24.29‰) and ($\delta^{18}O$= -0.66‰, $\delta^{2}H$= 0.77‰) respectively. The discharge of water to the wet land is along the contact of East-West running ridge, composed of associated silisic intrusion and basalts, and fine grained alluvium around Melo low land. The alluvium around the wet land seems wet during visualization although in reality it is dry. This may be due to the effect of capillary rise and high surface tension of the salty water which is evidenced by white and yellow salt stains over the area.

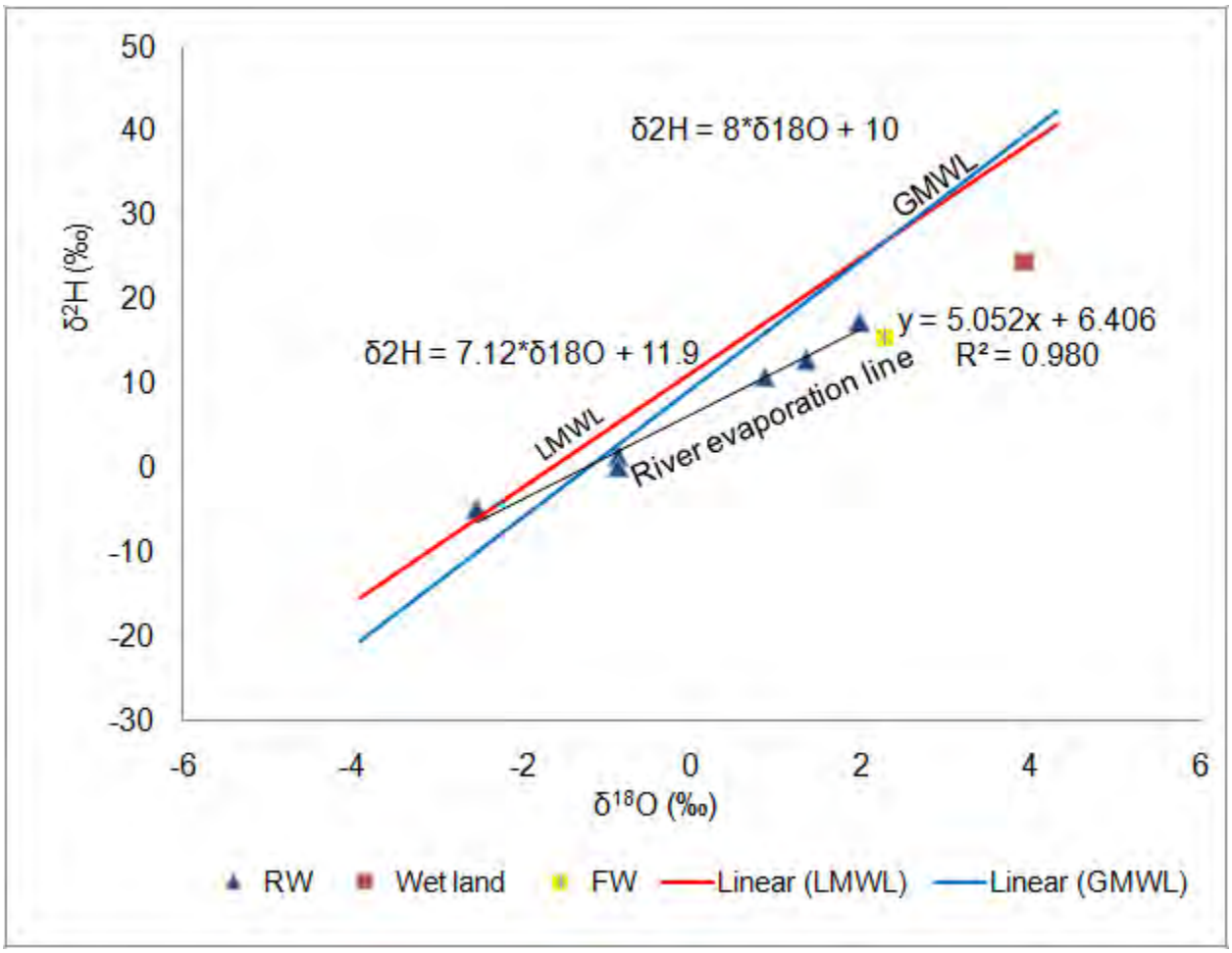

Figure 5.7 Graph showing isotopic compositions of surface water. (The entire river waters are originating from the escarpment and all are found west of Hurso. The flow of these river waters disappear in to the alluvium within 10-15 kilometers from the foot of the escarpment)

6. RECHARGE PROCESSES

6.1GENERAL

The concept of recharge is very essential in every groundwater resource studies. For instance, it is the scratching point in every groundwater resource studies, potential assessments, in groundwater modeling and the like.

Stable isotope (deuterium and Oxygen 18) and hydrogeochemical data are used to investigate the groundwater recharge and flow processes in the current research work. Knowledge of the local hydrogeological set up is the starting point for the detailed hydrogeochemical and isotopic investigation in the area. Because this has helped to define the recharge and discharge zones which in turn used to identify the groundwater flow paths as well as recharge sources and mechanisms. Recharge mechanisms are classified as direct, indirect and localized recharge by Lerner et al. (1990). These mechanisms can be influenced by various processes. The most important influential processes are the amount, frequency and distribution of precipitation and evaporation effect. Furthermore, the geological (availability and intensity of fractures and effective intergranular porosity), topographical and geomorphological features play an important role for the groundwater recharge mechanism.

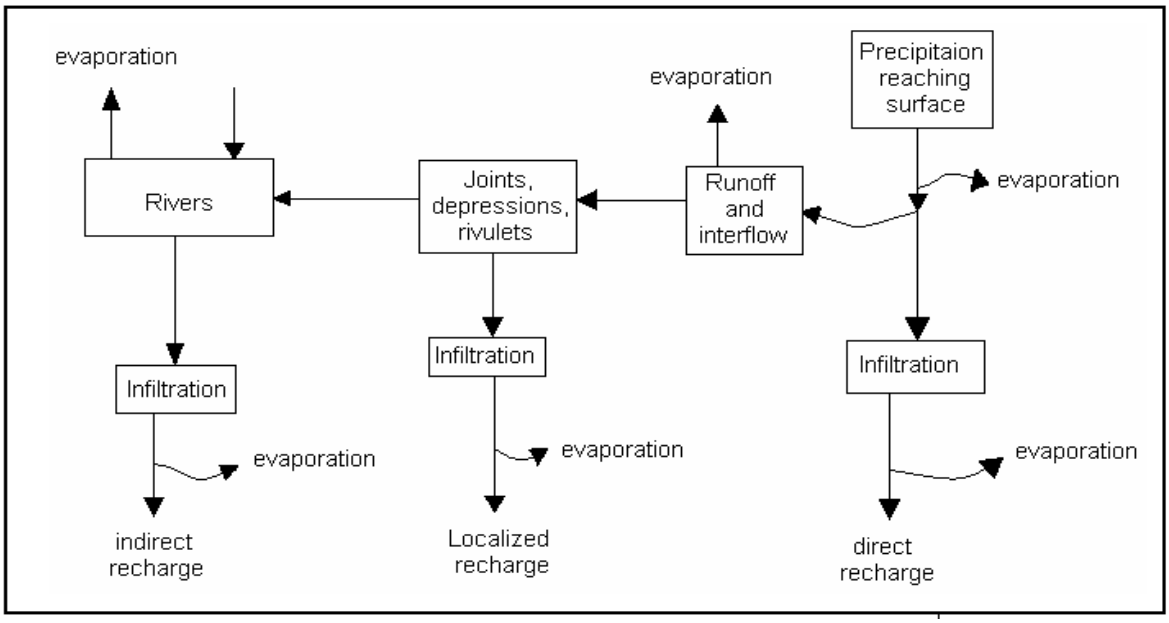

Figure 6.1 The various mechanisms of recharge in a (semi-)arid area (after Lerner, 1990).

In semiarid areas two of the mechanisms dominate according to the Author of this report. These are indirect and the local recharge. The indirect recharge includes the

percolation of rainwater to the groundwater table through the beds of surface water courses. The local one is an intermediate form of surface water in the absence of well-defined channels. The direct recharge, where water is added to the groundwater reservoir by direct vertical percolation through the vadose zone, is less important in these areas. Figure 6.1 shows a simplified representation of recharge mechanisms in semiarid areas.

6.2 HYDROGEOCHEMICAL EVIDENCES

6.2.1EQUILIBRIUM CONDITIONS OF GROUNDWATER

The hydrochemical equilibrium conditions of groundwater and mineral phases of the aquifer rocks can be evaluated using saturation indices (SI). SI is used to know the extent to which water chemistry is controlled by equilibrium of the solid phases. The saturation index (SImineral) of a certain mineral is defined as the logarithmic ratio of the ion activity product (IAP) in the water sample to the equilibrium constant (K). It is calculated using Aquachem version 4. The difference between equilibrium constant (K) and Ion Activity Product (IAP), is K stands for activities at equilibrium while IAP represents activities in the water sample different from equilibrium conditions.

$$\mathbf{SI_{mineral} = Log\ (IAP/K)}$$

When a mineral is in equilibrium with respect to a solution, the SI is equal to zero. Under saturation is indicated by a negative SI and super saturation by a positive SI. The concept is described briefly in Appelo and Postoma (2005).

The saturation indices of some common carbonate (aragonite, calcite and dolomite), sulfate (gypsum and anhydrite) and halite minerals of representative groundwater are shown in Fig. 6.2. The figure illustrates the saturation of groundwater with carbonate rocks while it flows from recharge to discharge area in the eastern lower Awash Basin.

Generally, the groundwaters from the Quaternary alluvial, Basalts, limestone and upper sandstone aquifers in the discharge area are moderately to strongly oversaturated with respect to the carbonate minerals (aragonite, calcite and dolomite) indicating their precipitation in the aquifer matrix along the flow path. These soluble carbonate minerals precipitate in the soil zone due to high evaporation rate and degassing of CO2. This can lead to increased saturation states of these minerals in the underlying groundwater. Few groundwaters are under-saturated with respect to carbonate minerals indicating

that these minerals can dissolve when contact with the aggressive groundwater. These under saturated groundwaters are recharge area groundwater and some fast flowing discharge area groundwater.

The groundwaters are also strongly under-saturated with respect to sulfate minerals (gypsum and anhydrite) and halite in both the aquifer formations (alluvium, basalts, limestone and upper sandstone) of recharge and discharge area in the eastern lower Awash Basin except in Harey borehole. This indicates that more sulfate and halite minerals will dissolve to increase their saturation states in groundwater along the flow path.

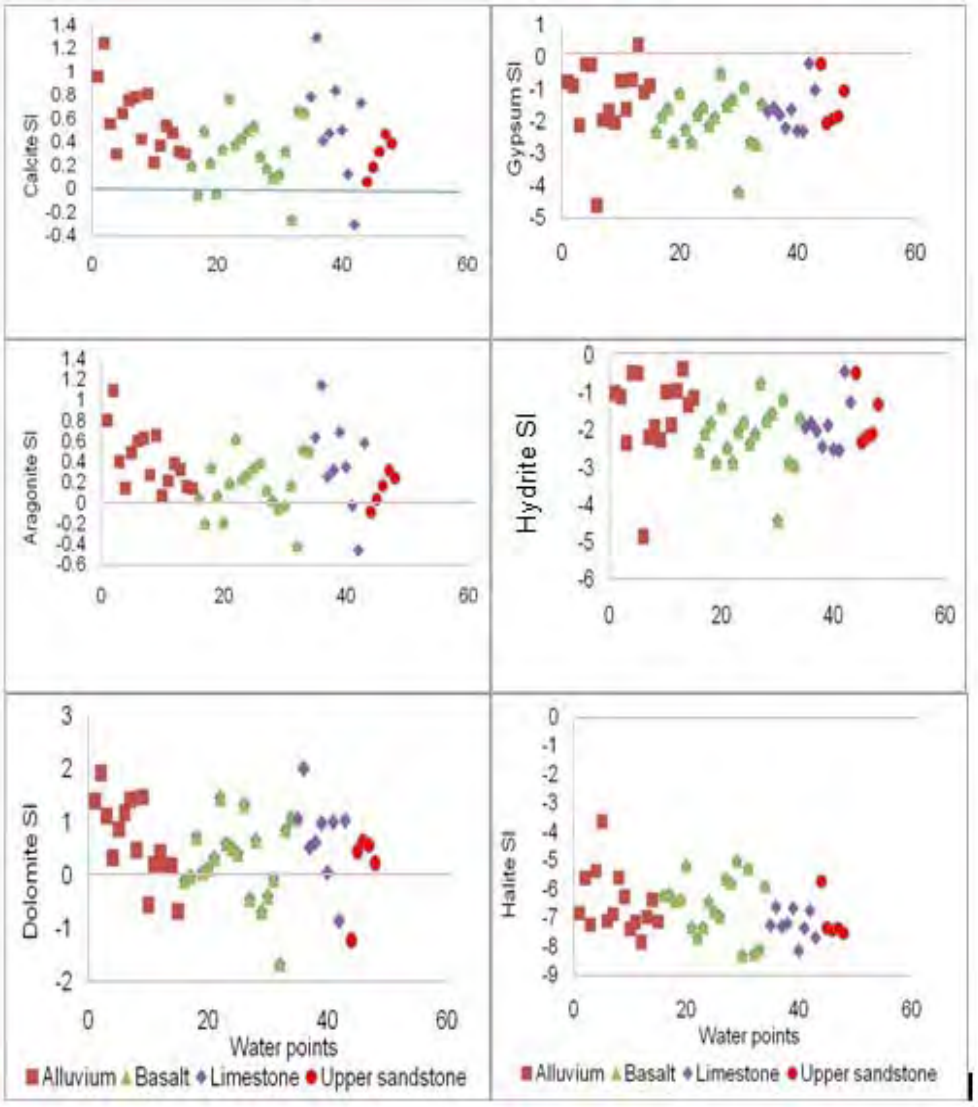

Figure 6.2 Graph of Saturation Indices (SI) of common minerals in eastern lower Awash Basin: carbonate (calcite, aragonite and dolomite), sulfate (gypsum and anhydrite) and halite minerals in the representative

groundwater samples from aquifers of alluvium, basalt, limestone and upper sandstone (The line of SI =0, for each scatter plot is the line of Equilibrium or Saturation line).

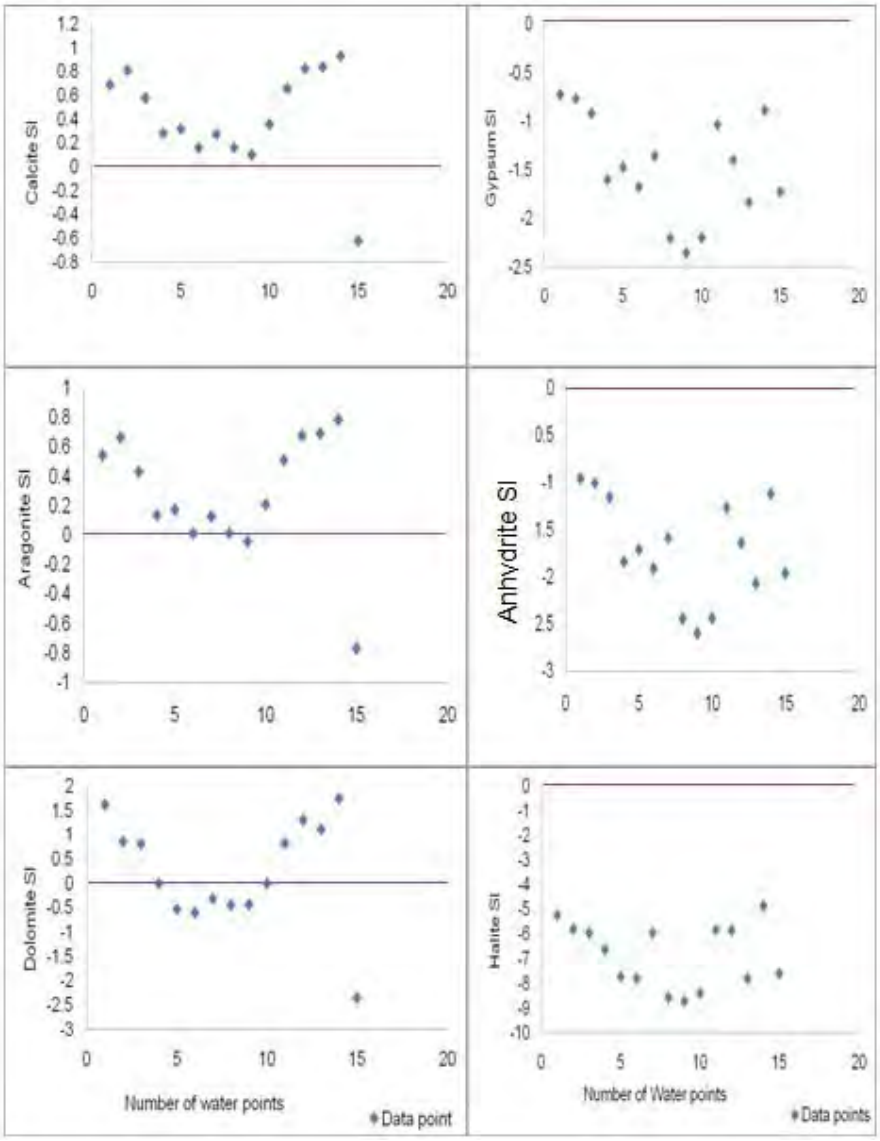

Figure 6.3 Graph of Saturation Indices (SI) of common minerals in Aysha Basin: carbonate (calcite, aragonite and dolomite), sulfate (gypsum and anhydrite) and halite minerals in the collected groundwater samples (The line of SI =0, for each scatter plot is the line of Equilibrium or Saturation line)

The saturation indices of Aysha Basin groundwater also revealed that a few groundwater samples gathered from the recharge area ranges from near saturation to under saturation with respect to carbonate minerals. However, the majority of groundwater from the discharge area indicated super saturation with respect to the common carbonate minerals (Fig.6.3). Similar to the Awash sub Basins the groundwater of the Aysha basin is strongly under saturated with respect to sulfate and halite minerals.

6.2.2 CALCIUM TO MAGNESIUM RATIO (Ca/Mg) IN GROUNDWATER

The spatial distribution map of Ca to Mg ratio in the groundwater indicated the presence of higher values in the recharge area and in some areas with local recharge (e.g. Aydora and Hore) as well as in hot springs where anorthite dissolution occur. However, there is also the occurrence of low values of Ca to Mg ratio in the recharge area which is dominated by limestone, where dolomite dissolution is expected.

In general, the Ca to Mg ratio decreases from the recharge to discharge area in the most part of the eastern lower Awash Basin (Fig. 6.4). This trend reflects that the precipitation of Ca in the form of carbonate minerals (like calcite, dolomite and aragonite) is significant as the groundwater moves toward the rift floor.

However, there is no clear distribution of the Ca to Mg ratio in the Aysha Basin as compared to the eastern lower Awash basin.

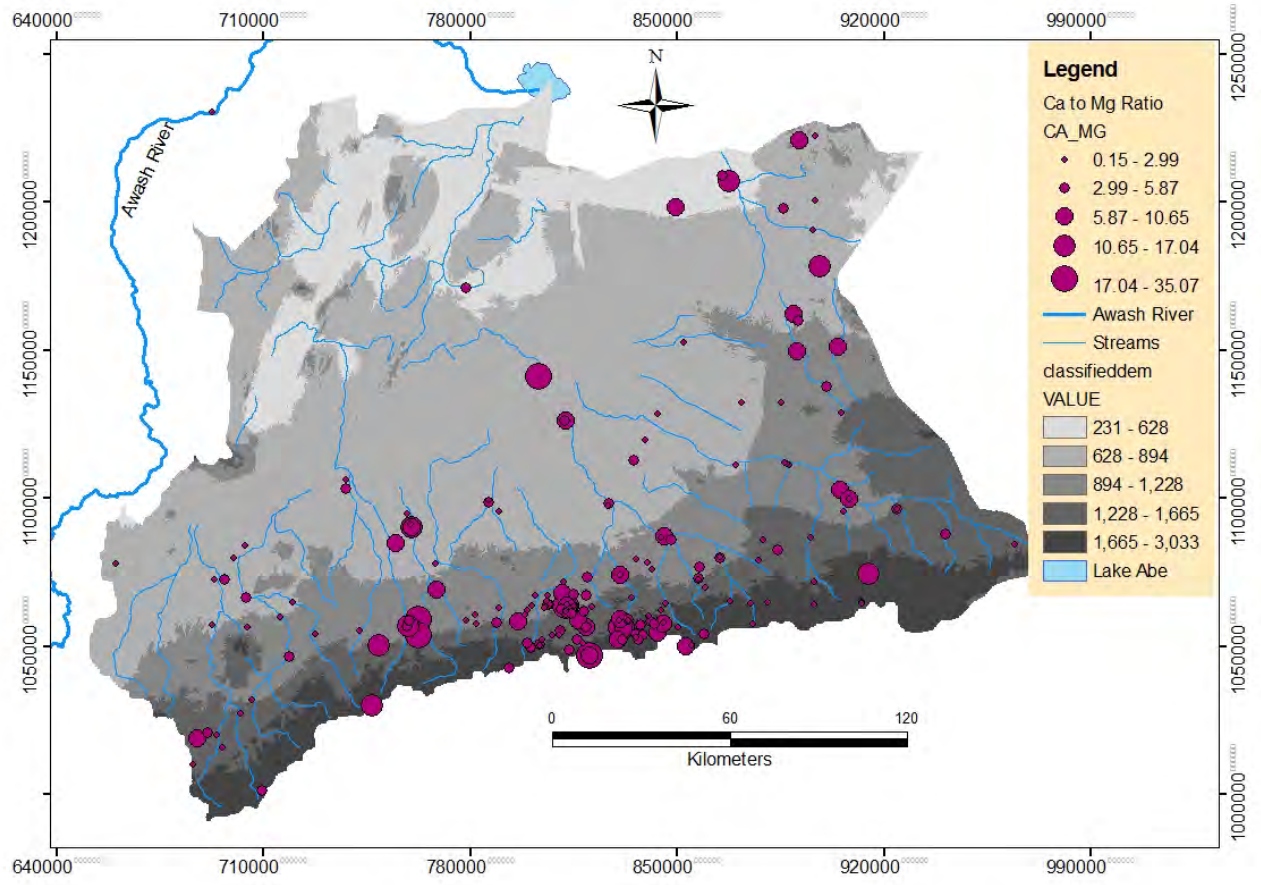

Figure 6.4 Spatial distribution map of Ca to Mg ratio in groundwater of the investigation area

6.3 ISOTOPIC EVIDENCES

6.3.1 DEUTRIUM (^{2}H) vs OXYGEN (^{18}O)

The plot of ^{2}H versus ^{18}O is used to assess the groundwater recharge sources and mechanisms of the area. This plot indicated rainfall as the major source of groundwater in the investigation area. In addition, the infiltration of the very limited surface water sources in to the alluvium in the western part of the eastern lower Awash Basin is also evident (e.g. around Erer). These surface water evaporation lines almost overlap with that of the groundwater except for Medisa River which falls on the LMWL (figure 5.4). This shows Medisa River is recharged by meteoric water.

The $\delta\ ^{2}H$ and $\delta\ ^{18}O$ scatter plot of groundwater in the investigation area is shown in Figure 6.5. Based on this scatter plot three mechanisms of recharge can be identified in the research area (Fig. 6.5):

a) Those groundwaters which plot above the local meteoric water line (LMWL) represent recharge from local rainfalls. This is evidenced by the groundwaters of the Escarpment (e.g. Dengego and Hades springs) which are plotted above the LMWL.
b) Those groundwaters which plot below the local meteoric water lines (LMWL) to the right are most likely recharged by evaporated meteoric waters (mainly evaporated flood waters) or mixing. This recharge mechanism mainly characterizes the shallow and intermediate groundwaters of the investigation area.
c) Those groundwaters which plot below the local meteoric water lines (LMWL) to the left shows regional groundwater mainly from deep and confined aquifers. Thus, groundwater in this group comes from lateral infiltration of meteoric recharge from the highland to the low land. These mechanisms occur where large regional fractures, dissections and solution openings in rocks exist on the highland (recharge area). This group also includes the artesian groundwaters of Gabi (0.0697‰ $\delta^{18}O$ and 2.79‰ $\delta^{2}H$) and Mete (-1.34‰ $\delta^{18}O$ and -6.83‰ $\delta^{2}H$) wells which are actually plotted to the right of the LMWL due to the horizontal

shifting of $\delta^{18}O$ because of higher groundwater temperature in the reservoir with no effect on $\delta^{2}H$ magnitude. This high temperature in the reservoir can facilitate the isotopic exchange between groundwater and aquifer matrices. The temperature of the groundwater of Gabi well is 40 ^{0}C while it is 44.9 ^{0}C for mete well when measured at the surface. The horizontal tracing back of the plot of these artesian wells most probably plots them between -4 and -2‰ $\delta^{18}O$.

Generally, isotope exchange is achieved by various mechanisms: dissolution and re-precipitation of the mineral, mineral alteration such as weathering of feldspars to clay minerals allows the exchange of oxygen between the alteration fluid and the silicate structure. A third isotope exchange process is the direct exchange of ^{18}O (or ^{2}H) between the water and the mineral crystal lattice. The kinetics of this diffusion-controlled reaction is temperature dependent and mineral specific. Oxygen exchange with hornblende takes place only at high temperature (Dodson, 1973), but occurs at decreasing temperatures for quartz > muscovite > biotite and finally feldspar. The loose lattice structure of feldspar allows ^{18}O to exchange, even at temperatures below 100 ^{o}C (O'Neil and Taylor, 1967).

$$CaAl_2Si_2O_7{}^{18}O + H_2O \longleftrightarrow CaAl_2Si_2O_8 + H_2{}^{18}O$$

Exchange with feldspar

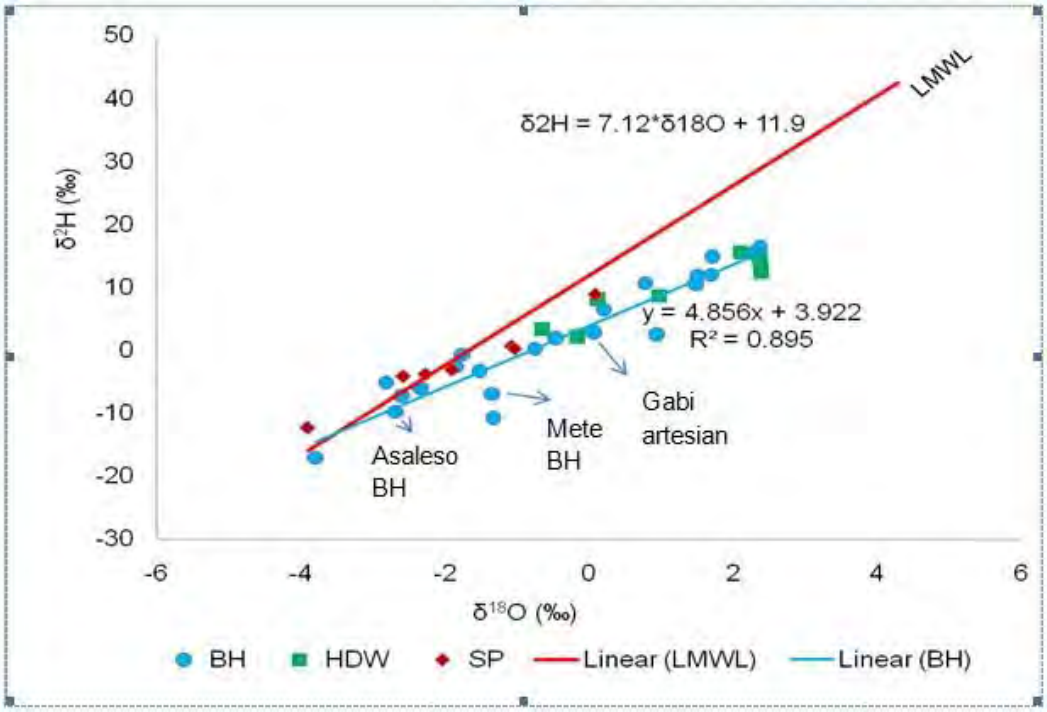

Figure 6.5 The plot of $\delta^{18}O$ vs $\delta^{2}H$ for the eastern part of lower Awash Basin groundwater

There are various factors that control the isotopic compositions of groundwater such as the temperature effect, amount effect, distance from moisture source, altitude effect and isotopic exchange with aquifer matrixes.

6.3.2 ALTITUDE EFFECT

Altitude effect is one of the factors controlling the isotopic compositions of groundwater. The altitude effect in the investigation area can be illustrated using figure 6.6. The figure presented the existence of a negative relationship between altitude and groundwater $\delta^{18}O$. As it is depicted on the illustration figure the recharge area or high altitude groundwater are depleted in $\delta^{18}O$ relative to the discharge zone groundwater which are enriched. However, the groundwater gathered from the foot of the Escarpment (including Asaleso well field and Kantras/the former Erer place hot spring) did not show the effect of altitude and it remains depleted regardless of altitude. This can confirm the groundwater of the Asaleso well field, Afdem town borehole and Kantras hot spring is a regional groundwater which was recharged at higher altitude through fractures and solution openings (lateral infiltration). Moreover, this relation also testifies as the source of the groundwater is probably delayed recharge or past recharged groundwater at different climatic conditions than today, especially for Erer/Kantras hot spring and Afdem town borehole.

The other evidence is the highest depletion in isotopic composition, salinity (TDS= 2610 mg/l), and temperature (39.6^0C) of Kantras hot spring (AW-SP7) can testify the existence of deep seated geological structures that guide deep groundwater circulation. For $\delta^{18}O$ the depletion varies between about -0.15 and -0.5‰ per 100m rise in altitude, with a corresponding decrease of about -1 to -4‰ for ^2H (Clark and Fritz, 1997). For the research area, the depletion of $\delta^{18}O$ per 100m rise in altitude is -0.1 (i.e. -0.1‰/100m) as derived from the equation of $\delta^{18}O = -0.001*h+1.516$. The work of Seifu (2004) also indicated as the depletion of $\delta^{18}O$ per 100m rise in altitude is -0.1‰ for Ethiopia.

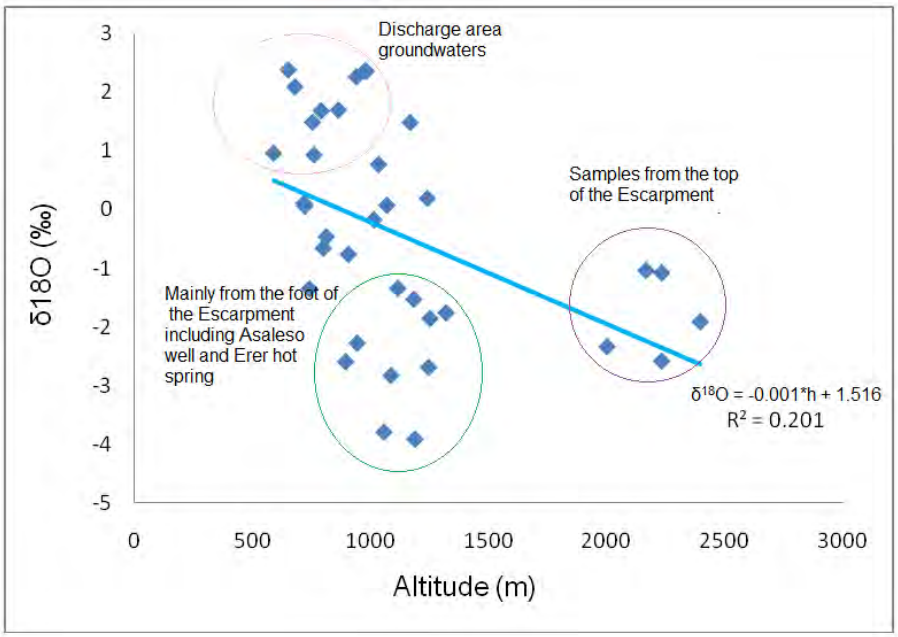

Figure 6.6 A scatter diagram showing a relationship between groundwater $\delta^{18}O$ and altitude

6.4 INTEGRATION OF STABLE ISOTOPE AND HYDROGEOCHEMISTRY

In studies dealing with salinization process identification, it is often common to consider both isotopic and hydrochemical evolution (IAEA, 1997). Such an approach will enable clear distinction to be made of the salinization processes (or processes), for cases where freshwater salinity may be caused by direct sea water intrusion, leaching of salt formations, mineral dissolution, or salt accumulation due to evaporation. During the processes of leaching salt formations or mineral dissolution, the stable isotope content of the water is not affected while the salinity of water increases. This is a unique feature which will enable identification of such processes based on isotopic and chemical data. The stable isotopes of $\delta^{18}O$ and $\delta^{2}H$ are the most conservative tracers during their transport in hydrological systems and their relationship with salinity changes is univocal.

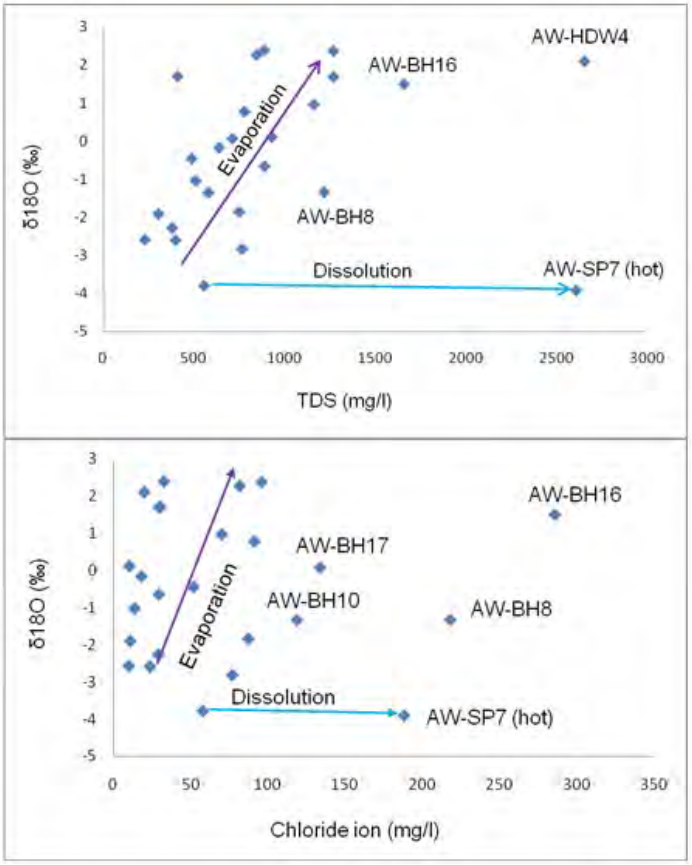

Figure 6.7 Relationship between salinity and stable isotope concentration for salinization processes identification in groundwater

Therefore, the relationship between salinity and stable isotope concentration revealed the presence of two distinct processes for the evolution of salinity in the eastern lower Awash Basin. These two processes are: salt accumulation due to evaporation and mineral dissolution (Fig.6.7). According to the diagram of salinity versus stable isotope the major cause and source of salinity in the basin is evaporation effect. Evolution of stable isotopic composition of water (deuterium vs oxygen-18 diagram) also support the evaporation effect.

6.5. GROUNDWATER RECHARGE ESTIMATION

6.5.1 CHLORIDE MASS BALANCE (CMB) METHOD

Chloride (Cl) is perhaps the most informative ion from a hydrochemical perspective, as it is common in groundwater. It has a limited number of identifiable sources, and is hydrochemically conservative (Mazor, 2004). Atmospheric deposition (wet fall plus dry

fall) is the only chloride source and is constant through time. These properties turn chloride into a most useful hydro chemical marker.

The CMB approach has been most widely used for estimating low recharge rates, largely because of lack of other suitable methods. Water fluxes as low as 0.05 to 0.1 mm/year have been estimated in arid regions in Australia and in the US (Allison and Hughes 1983; Cook et al. 1994; Prudic 1994; Prych 1998).

In this research, recharge rate estimation is also determined using the chloride mass balance (CMB) technique following the approach of Eriksson and Khunakasem (1969). The simplest expression of their model is:

$$R = \frac{P * Cl_P}{Cl_{GW}}$$

Where R and P represent the recharge and precipitation fluxes respectively (in mm/year); Cl_P and Cl_{GW} denote the chloride concentrations of precipitation and recharge/groundwater consecutively (in mg/l). Recharge is proportional to precipitation and the amount of chloride in the rain and it is inversely proportional to the chloride concentration in the groundwater.

This technique is a good first order estimate of recharge that may be refined by using other techniques in the future. The formulation assumes (1) steady state recharge and precipitation; (2) one dimensional (1-D) piston flow; (3) chloride in groundwater is derived only from atmospheric deposition and concentration occurs by evapotranspiration prior to recharge; (4) surface runoff from the catchment is negligible; (5) no sources or sinks of chloride or chloride behaves as a conservative tracer along its path i.e. it is not involved in any geochemical interactions and therefore is neither added to nor removed from water (Cook et al., 2002). This last assumption is generally valid in groundwater systems where saline and evaporite deposits such as halite are absent.

The mean wet chloride concentration in precipitation for the research area is 0.91mg/l and is used as Clp (rainfall + dry fall). Dry fallout of Chloride (Cl) is retained in the soil and leached during recharge and hence must be accounted for in the mass balance (Dettinger, 1989; Wood and Sanford, 1995a, 1995b). Dry deposition rates are quite variable, depending on distance from the ocean, wind patterns, and local sources of Cl

(Plummer, 1996; Davis et al., 1998). However, the chloride concentrations from dry deposition are not considered for this investigation area due to lack of data and the logical assumptions of the existence of deep groundwater table. In semi-arid areas like the research area, the chance of rising of groundwater table to the evaporation zone (root zone) is rare. Because of this fact, the leaching of residual chloride during recharge in the unsaturated zone to the water table is negligible.

Among the two areal depth of precipitation estimation applied for the area under consideration (fig 2.5 and 2.6), the one estimated using Isohyetal method is more preferable and accurate than Theisson polygon method. This is because the Isohyetal method accounts the physiographic effects of the area. Accordingly, the areal depth of precipitation averaged for the research area using this method is 662.81mm/year. This is the average precipitation amount considered for each springs, boreholes and hand dug wells to estimate the required annul recharge rates.

Totally, 99 groundwater samples gathered from springs, boreholes and hand dug wells from both basins (93 from Awash and 6 from Aysha) are used to estimate the recharge rate for the area under consideration (annex 5). Only groundwater samples with Cl concentration less 58 mg/l are used to minimize errors caused by evaporation effect. Recharge estimation is approached by calculating recharge rate, using the formulation of Eriksson and Khunakasem (1969), for each considered water points. The calculation is performed on Excel data base (annex 5) and then the data points are plotted on rainfall isohyetal map using Arc GIS 9.3.

According to the recharge rate computed for each springs, boreholes and hand dug wells the recharge is variable from place to place. This variation is mainly related to hydrologic cycle, topographic set up, geologic factors and climatic conditions of the area. The spatial distribution map of recharge rate (Fig. 6.8) clearly depicted that the highest rate is computed for recharge area groundwater in the southern part for the eastern lower Awash Basin (i.e the Escarpment area).

The exceptional highest rate is also computed for the Aysha Basin, in areas where fast selective recharge exists. This highest rate is observed in areas where rock fractures, solution openings, almost vertical dipping and contact between different rocks occur.

The fast selective recharge caused under estimation of groundwater chloride concentration and this resulted in over estimation of groundwater recharge rate in the basin. Whereas the high recharge rate is also mapped for the discharge area groundwater which are characterized by local recharge in the Awash Basin.

Basin wise average recharge rate computation is performed after analyzing the spatial distributions and recharge rates of each water points. Accordingly, the amount of average annual recharge rate calculated for the eastern lower Awash Basin is 29.15 mm/year. However, the average recharge rate is extremely over estimated for the Aysha Basin (i.e. 58.24mm/year). This is because of fast selective recharge which cause under estimation of the groundwater chloride concentration.

The major uncertainties that are suspected to violate the reliability of the quantified recharge rates for the research area may be: the negligence of dry fall out (D) of chloride concentration from the formula of Erikson and Khunakasem (1969),

$$R = \frac{P * Cl_p + D}{Cl_{GW}}$$

the evaporation effect, geological factors, the precision of the laboratory to determine chloride concentration in precipitation and groundwater, and the accuracy of the meteorological raw data recorded.

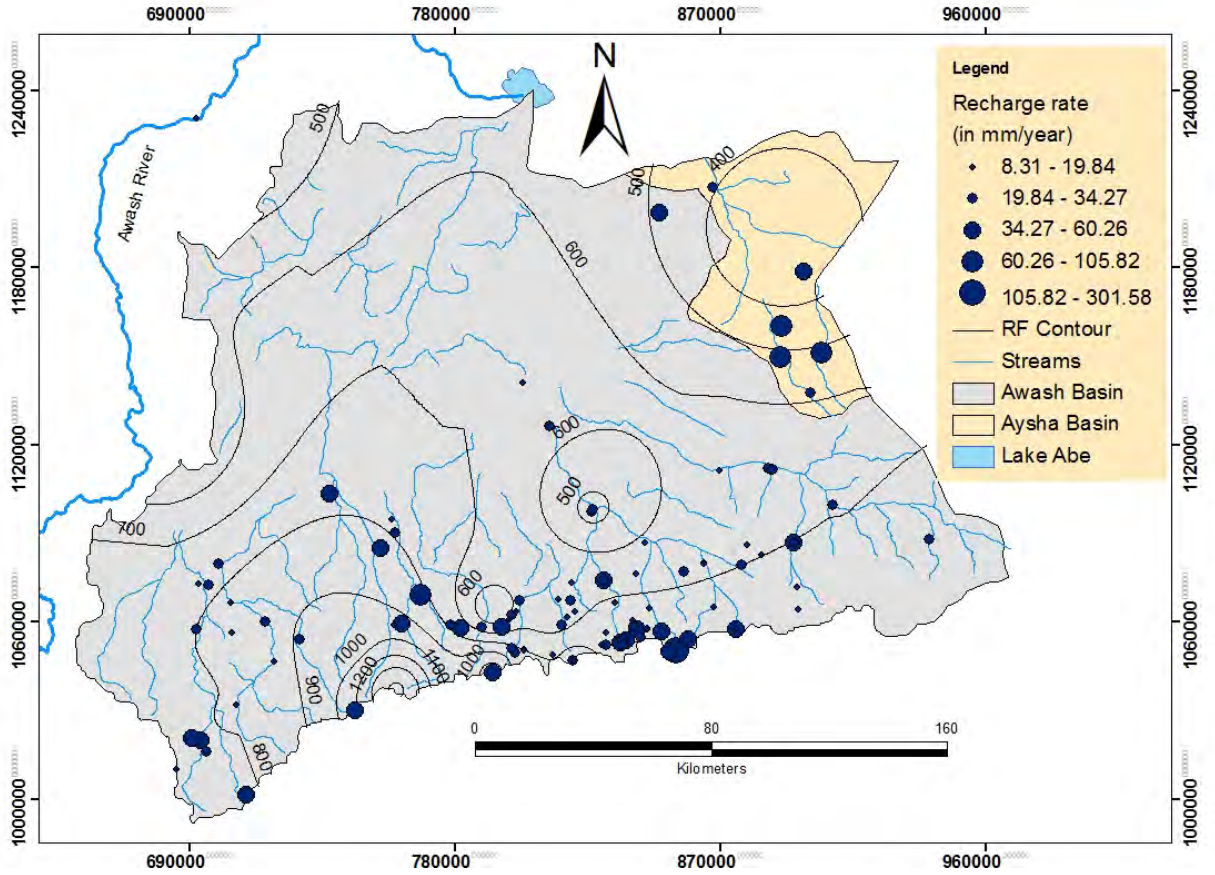

Figure 6.8 Spatial distribution map of Recharge rate estimated using Chloride Mass Balance (CMB) for Awash and Aysha Basins

6.5.2 RELATIONSHIP OF GROUNDWATER CHLORIDE AND RECHARGE RATE

According to the formula used to estimate the recharge rate, the amount of the rate is directly proportional to the precipitation and chloride amount in precipitation. But it is inversely proportional to the concentration of chloride in groundwater (Cl_{GW}). The graph of groundwater chloride concentration against recharge rate (Fig. 6.9) also depicts this fact. As observed from the curve the recharge amount becomes very high when the groundwater chloride concentration becomes underestimated (for instance, in the case of fast selective recharge mechanism). However, the recharge rate becomes very low when the groundwater chloride concentration increases. In general the groundwater recharge rate of the area becomes very sensitive for groundwater chloride concentrations less than 10mg/l.

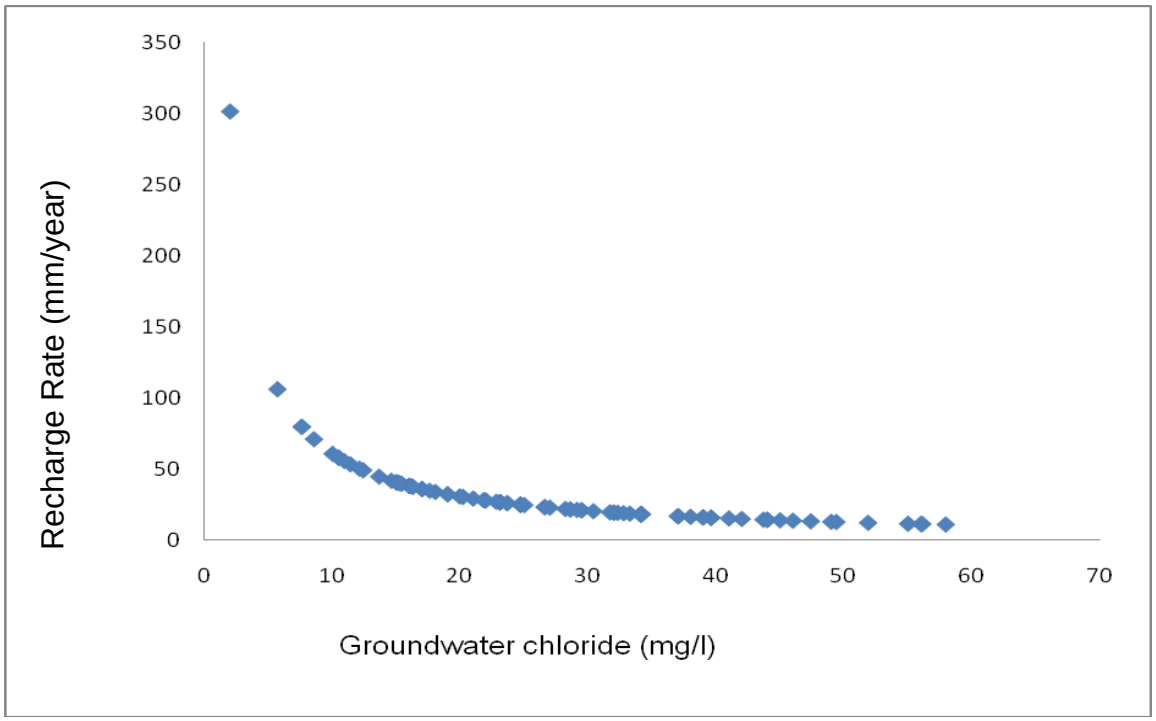

Figure 6.9 The curve showing the relationship between groundwater chloride and recharge rate

7. CONCLUSIONS AND RECOMMENDATIONS

Hydrochemical and stable isotope data of boreholes, springs, dug wells, rainwater and rivers water are used for recharge process investigations. All the isotope data are the primary generated data due to no availability of secondary data of isotope over the area. However, the hydrochemical data used include both the primary and secondary generated data. The major secondary data are obtained from OWWDSE, WWDSE and GSE. The raw data are organized, analyzed and interpreted with the help of statistical and geochemical methods. The results and findings are presented using various softwares.

The methodologies applied to arrive at the findings and results are: sampling and analysis; hierarchical cluster analysis (HCA); inverse geochemical modeling; stable isotopes (^{2}H vs ^{18}O); integration of stable isotopes with hydrogeochemistry and chloride mass balance (CMB).

Depending on the findings and results obtained, the following conclusions and recommendations are forwarded.

7.1 CONCLUSIONS

- Based on the major cation and anion analysis on piper diagram (after charge balance evaluation);
  - Four major water types are identified in the eastern lower Awash Basin and
  - Two major water types/groups are identified in the Aysha Basin
- Bicarbonate Ca-$HCO3^{-}$ or Na-$HCO3^{-}$ type waters occur mainly in topographically higher areas. However, rapidly circulating groundwaters which have not undergone a pronounced water-rock interaction have also a similar water types in the rift (e.g. Kulen valley groundwater).
- One of the most sulfates (SO4) rich route distinguished in the area is the Erer-Idora-Asbuli flow path.
- The entire hot springs plot on piper diagram as outliers relative to the cold springs due to the effect of structures. These structures cause deep circulation of

groundwater which brings the enrichment of Sodium (Na) and chloride (Cl) or sulfate (SO4) ions.

- The hierarchical cluster analysis (HCA) classified the eastern lower Awash Basin groundwaters in to two major similar groups and eight sub-groups based on 10 (ten) parameters: TDS, EC, PH, Na, K, Ca, Mg, Cl, HCO3, and SO4 ions. Similarly, HCA classified the groundwater of Aysha Basin in to two major groups and five sub-groups. The groundwaters in each sub-group are assumed to have similar or identical flow paths and evolution, residence time, reservoir or recharge history.

- The HCA of the eastern lower Awash basin indicated the groundwater flow direction to be; a) in the NW direction in the eastern part b) in the NS direction in the central part c) in the NE or NNE direction in the west almost following the seasonal stream flow directions. Furthermore, the knowledge of geology, geomorphology and groundwater evolutions inferred the presence of at least three distinct regional structures i) from the high land along Kulen valley toward Gabi artesian wells ii) from the highland through Dire Dire Dawa toward Mete iii) from around Chiro toward Afdem or Butuji which results in fresh groundwater, similar to the recharge area groundwater, in the rift which shows minimum water rock interaction.

- The advantage of HCA is its robustness for objective classification of groundwater in to distinct groups. These distinct groups clearly indicate groundwater flow direction which helps to select the initial and final solutions for inverse geochemical modeling.

- The results of inverse geochemical modeling revealed the dissolution of halite, anhydrite silicate minerals (pyroxene, olivine, k-feldspar and plagioclase), consumption of CO2 during silicate hydrolysis, cation-exchange, and precipitation of calcite and clay minerals along the flow path toward the rift in both basins.

- All the shallow dug wells, rivers (except Medisa river), intermediate and confined deep groundwater from the rift plot below the local meteoric water line to the right. This indicates the effect of evaporation and isotopic exchange with aquifer matrices.

- The plot of ^{2}H versus ^{18}O helped to identify three recharge mechanisms in the eastern lower Awash Basin: recharge from local rainfalls, recharge from evaporated

meteoric waters (mainly evaporated flood waters) or mixing, and regional groundwater which are most likely lateral infiltration of meteoric water from the highland to the low land.

- The high salinity, temperature, and depletion in isotopic composition of groundwater can testify the existence of deep seated geological structures that guide deep groundwater circulation e.g. Kantras (the former Erer palace) hot spring (AW-SP7).
- The relationship between salinity (TDS) and stable isotope concentration also reveals the presence of two distinct processes for the evolution of salinity in the eastern lower Awash Basin. These two processes are: salt accumulation due to evaporation and mineral dissolution. Moreover, the major cause and source of salinity in the basin is evaporation effect.
- The annual recharge rate computed using CMB method for the eastern lower Awash and Aysha Basins is 29.15 and 58.24 mm/year respectively. However, the figure is extremely over estimated for the Aysha Basin. This is because of fast selective recharge which cause under estimation of the groundwater chloride concentration. The average annual rainfall amount and average Cl concentration in rainfall accounted for the CMB method are 662.81mm/year and 0.91 mg/l respectively. Ninety nine (99) groundwater points (93 from Awash and 6 from Aysha basin) are used i.e. to obtain groundwater Cl (Cl_{GW}) concentrations.

7.2 RCOMMENDATIONS

- ✓ Q-mode Hierarchical Cluster Analysis (HCA) is a powerful statistical tool for objective clustering of the large data set and to identify the groundwater flow direction in areas where hydrogeological information are lacking but hydrochemical data are available.
- ✓ Inverse geochemical modeling is also helpful in determining the flow processes, if good conceptualization of the groundwater system and the geochemical processes are well done. Therefore, proper conceptualization must be made first.
- ✓ Isotope application techniques are recommended as powerful tools to identify the source and mechanism of groundwater recharge

- ✓ The isotopic signature of the salty Beyeas wet land revealed the highest enrichment due to extreme evaporation of the water during its rise to the surface. Therefore, tracing the accurate source of water to the wet land may require further detail isotopic investigation and the use of additional tracer elements like Tritium (^{3}H) and ^{14}C isotopes.

- ✓ Since this research is conducted at regional scale the future researchers are recommended to carry out their investigations at larger scale than the present in order to get more detailed and refined findings and results.

- ✓ Isotopic compositions of Aysha Basin groundwater are not included in this research due to unreliability of the laboratory results. Therefore, one should consider the isotopic compositions of Aysha basin groundwater to determine the recharge mechanisms.

- ✓ To determine the seasonal fluctuations of recharge processes monthly isotopic compositions and hydrochemistry of groundwater and rainfall should be monitored.

- ✓ The present work used shallow dug wells in some parts of the discharge area due to lack of deep wells, sealing and under construction of the newly drilled wells. Therefore, for the future investigation the deep wells should be considered. Because even at the present time more than 80 large size wells are designed for irrigation purpose and they are under construction in the investigation area.

REFERENCES

Adams, S., Tredoux, G., Harris, C., Titus, R., Pietersen, K., (2001). Hydrochemical characteristics of aquifers near Sutherland in the Western Karoo, South Africa. Journal of Hydrology 24, pp 91–103.

Addis Hailu (2011). Groundwater-Surface Water Interaction and Recharge Estimation Using Hydrogeochemistry and Isotope Hydrology, Unpublished M.Sc Thesis, Addis Ababa University, Ethiopia

Alagbe, S. A. (2006). Preliminary Evaluation of Hydrochemistry of the Kalambaina Formation, Sokoto Basin, Nigeria. Journal of Environmental geology, Vol. 51, pp 39-45.

Allison GB, Hughes MW (1983). The use of natural tracers as indicators of soil-water movement in a temperate semi-arid region. Journal of Hydrology 60, pp 157–173

Andarge Mekonen and Jiri Sima (2010). Hydrogeological and Hydrochemical Maps of Harar NC 38-9 and NC 38-10, First edition, Published Report

Anderson MP and Woessner WW (1992). Applied groundwater modeling. Academic Press, Inc. San Diego, California, pp 381

Appelo, C.A.J. and Postoma, D., (2005). Geochemistry, Groundwater and Pollution, 2nd edition, Amasterdam, the Netherlands, pp 182-186

Bizune Bekele (2011). Hydrogeochemical and Isotopic Characteristics of the Groundwater System in Alleydege Plain, Unpublished M.Sc Thesis, Addis Ababa University, Ethiopia

Canuti, N.S.P, Gregnanin, A, Piccirillo, E.M, Sagri, M, Tacconi, P. (1972). Volcanic Intercalation in the Mesozoic Sediments of the Kulubi Area, Geological Survey of Ethiopia, Addis Ababa

Clark, I & Fritz, P (1997), Environmental isotopes in hydrogeology, Lewis, New York. pp 328

Craig, H. (1961b). Isotopic variations in meteoric waters, Science, 133, pp 1702-1703.

Cook, P. G., W. M. Edmunds, and C. B. Gayes (1994). Estimating paleo recharge and paleoclimate from unsaturated zone profiles, Water Resource Research., 28, pp 2721– 2731

Dansgaard, W. (1964). Stable isotopes in precipitation. Tellus 16, pp 436-468.

Davis, S. N., D. Cecil, M. Zreda, and P. Sharma (1998), Chlorine-36 and the initial value problem, Hydrogeology Journal, 6, pp 104– 114.

Dettinger, M. D. (1989), Reconnaissance estimates of natural recharge to desert basins in Nevada, U.S.A., by using chloride mass balance calculations, Journal of Hydrology, 106, pp 55–78,

Donson, M.H., 1973. Closure temperature in cooling geochronological and petrological systems. Contributions to Mineral Petrology, 40, pp 259-274.

Eriksson, E & Khunakasem, V (1969). Chloride concentration in groundwater, recharge rate and rate of deposition of chloride in the Israel Coastal Plain. Journal of Hydrogeology, 7, pp 178-197.

Fetter (1994). Applied Hydrogeology, 4th edition, Prince-Hall, inc. Upper Saddle River, Newjersy, PP 654

Greitzer Y., (1970). Stratigraphy, Hydrogeology and Jurassic Ammonites of the Harar and Dire Dawa Area, Ethiopia, PhD Thesis, Jerusalem

Guler, C., Thyne,G. McCray, J.E., and Turner, A.K. (2002). Evaluation of graphical and multivariate statistical methods for classification of water chemistry data. Hydrogeology Journal 10, pp 455–474.

Guler, C and Thyne, G.D. (2004), Delineation of hydrochemical facies distribution in a regional groundwater system by means of fuzzy c-means clustering, Water Resources Research, Vol. 40, W12503, Colorado, USA

Hem, J. D (1985). Study and Interpretation of the Chemical Characteristics of Natural Water, Third Edition, USGS, pp 58-69

Hidalgo, M.C., and Cruz-Sanjulian, J. (2001). Ground water composition, hydrochemical evolution and mass transfer in a regional detrital aquifer (Baza Basin, southern Spain). Applied Geochemistry 16, pp 745–758.

Jiri S. and Habteab Z. (1986). Hydrogeology and Hydrochemistry of the Dire Dawa Area, NC 37-12 Sheet, Ministry of Mines and Energy, EIGS, Note No. 276

Joseph A, Frangi, P, Aranyossy, JF. (1992). Isotopic composition of Meteoric water and groundwater in the Sahelo-Sudanese Zone. Journal of Geophysical research 97, pp 7543-7551.

Katema Tadesse (1982). Hydrogeology of Dire Dawa Area, Ministry of Mines and Energy, Addis Ababa, EIGS, Note No. 174

Kirchner, J.O.G., (1994). Investigation of the contribution of ground water to the salt load of the Breede River, using natural isotopes and chemical tracers. Report No. 344/1/95. Water Research Commission, Pretoria.

Lerner DN, Issar AS, and Simmers I, (1990). Groundwater Recharge: A guide to understanding and estimating natural recharge. International contributions to Hydrogeology, Vol. 8, pp 345

Mazor, E. (2004). Chemical and Isotopic Groundwater Hydrology, Third Edition, Weizmann Institute of Science, Rehovot, Israel, pp 114-152

Mengesha T., Tadiwos C., and Workineh H. (1996). Explanation of the Geological Map of Ethiopia, 1:2,000,000 scale, Geological Survey of Ethiopia, Addis Ababa, Bulletin No. 3, 2Nd edition

Mezmure Hailemeskel (1964). Report on Geology of Eastern Harar Sheet, Hydrogeological Division, Geological Survey of Ethiopia, Unpublished Report

O'Neil, J.R. and Taylor, H.P., 1967. The oxygen isotope and cation exchange chemistry of feldspars. American Mineralogist, 52, pp 1414-1437

OWWDSE (2011). Shinille Groundwater Resource Potential Assessment, Inception Report

OWWDSE (2011). Geology and Geomorphology of Shinille Zone and Adjoining Areas, Somali Region Project Office, Addis Ababa

Ophori, D.U., Toth, J., (1988). Patterns of ground-water chemistry, Ross Creek Basin, Alberta, Canada. Ground Water 27 (1), pp 20–55.

Paul .A. Mohr, (1962). The Ethiopian Rift System Reprinted from the Bulletin of Addis Ababa College of Geophysical Observatory, Vol. III, No. 1, pp 33-62.

Paul .A. Mohr (1973). Structural Geology of the African Rift System, Center for Astrophysics, Harvard College Observatory and Smithsonian Astrophysical Observatory, Cambridge, Massachusetts 02138

Parkhurst, D.L. and Appelo, C.A.J. (1999). User's guide to PHREEQC (version 2) - A computer Program for Speciation, Reaction-Path, Advective-Transport, and Inverse Geochemical Calculations. USGS Water-Resources Investigations Report 95-4227.

Piper, A.M., (1944). A Graphic Procedure in the Geochemical Interpretation of Water Analyses. Trans. Am. Geophys. Union 25,914–923.

Plummer, L.N., Busby, J.F., Lee, R.W., Hanshaw, B.B., (1990). Geochemical modeling of Madison aquifer in parts of Montana, Wyoming, and South Dakota. Water Resource Research 26 (9), pp 1981–2014.

Plummer, M. A.(1996). Secular variation of cosmogenic nuclide production from chlorine– 36 in fossil pack rat middens, Masters thesis, N. M. Inst. Of Mining and Technol., Socorro, N. M..

Prudic DE (1994). Estimates of percolation rates and ages of water in unsaturated sediments at two Mojave Desert sites, California- Nevada. USGS 94–4160:19

Prych EA (1998). Using chloride and chlorine-36 as soil-water tracers to estimate deep percolation at selected locations on the US Department of Energy Hanford Site, Washington. USGS Water-Supply paper 2481:67

Seife Michael Berhe, (1985). Geological Map of the Dire Dawa Sheet (NC 37-12), 1:250,000 scale, GSE, Addis Ababa.

Seifu K., Tenalem A., Tamiru A. and Yves T. (2005), Groundwater recharge circulation and geochemical evolution in the source region of the Blue Nile River, Applied Geochemistry, pp 1658–1676, www.siencedirect.com

Seifu Kebede (2004), Environmental Isotopes and Geochemistry in Investigating Groundwater and Lake Hydrology: Cases from the Blue Nile basin & the Ethiopian Rift, Ethiopia, PhD dissertation, University of Avignon, Paris, France, pp 74-95,

Shachnai (1972). The Geology of Sheets NC37-12 and NC38-9, Harar Province, Progess Report

Sidle, W. C., (1998). Environmental isotopes for resolution of hydrology problems. Journal of Environmental Monitoring and Assessment, 52(3), pp 389-410. http://www.springerlink.com

Swanson SK, Bahr JM, Schwar MT, and Potter KW (2001). Two-way cluster analysis of geochemical data to constrain spring source waters. Elsevier Science B.V., Chemical Geology 179Z2001, pp. 73–91

Swan, A.R.H., Sandilands, M., (1995). Introduction to Geological Data Analysis.

Tadesse Belachew (1972). Preliminary Hydrogeological Survey of the Issa Lowland-Hararghe Province, Hydrogeological note no. 1972/2, Unpublshed Report

Tenalem A., Shimeles F., Frank W., Molla D. and Stefan W. (2009). Hierarchical Cluster Analysis of Hydrochemical Data as a Tool for Assessing the Evolution and Dynamics of Groundwater across the Ethiopian Rift, International Journal of Physical Sciences Vol. 4 (2), pp 076-090, http://www.academicjournals.org/IJPS

Tesfamikael Keleta (1974). Hydrogeology of Dire Dawa Area-A Statement of Present Knowledge, Unpublished report No. 11, Addis Ababa

USDA (1954). Diagnosis and improvement of saline and alkali soils. U.S.Salinity Laboratory Staff, Government Printing Office, Washington, D.C.

WHO (2011). Guidelines for Drinking-Water Quality, 4th edition, WHO Library Cataloguing-in-Publication Data, http://www.who.int/

WWDSE (2003). Dire Dawa Adminstrative Council Integrated Resource Development Master Plan Study Project, Part-2 Hydrogeology Report, Addis Ababa, Ethiopia

WWDSE (2008). Harar Water Supply and Sanitation project Water Wells Drilling and Construction Completion Report, Addis Ababa, Ethiopia

Wood, W. W., and W. E. Sanford (1995a), Chemical and isotopic methods for quantifying groundwater recharge in a regional, semiarid environment, Ground Water, 33(3), pp 456– 468

Wood, W. W., and W. E. Sanford (1995b). Eolian transport, saline lake basin, and groundwater solutes, Water Resource Research, 31(12), pp 3121– 3129

Yurtsever, Y. & Payne, B.R. (1978). Application of environmental isotopes to groundwater investigations in Qatar. Proceedings of a Symposium, IAEA, Vienna. Vol. 2, pp 465-490,

Yurtsever, Y. & Araguas-Araguas, L. (1993). Environmental isotope applications in hydrology: An overview of the IAEA's Activities, Experiences and Prospects. In: Tracers in Hydrology, IAHS, Publication, 215, pp 3-20

Zhu, C., Anderson, G., 2002. Environmental Application of Geochemical Modeling. Cambridge University Press, Cambridge.

ANNEXES

Annex 1 Mean monthly and annual precipitation at selected sattions

Station	UTME	UTMN	Elv	Mean Monthly Precipitation (mm)												Annual PPT (mm)
				Jan	Feb	Mar	Apr	May	Jun	Jul	Aug	Sep	Oct	Nov	Dec	
Dire Dawa	812546	1063671	1194	21.52	32.50	65.36	93.09	41.51	24.66	92.17	120.24	64.92	24.63	12.73	12.64	605.98
Dengego	820992	1046567	2087	15.57	12.06	68.62	107.91	80.87	90.11	109.74	168.70	109.78	34.97	15.83	10.83	824.98
Kulubi	792886	1042580	2394	37.08	38.22	96.99	151.04	93.37	67.44	128.50	207.56	134.27	48.04	15.90	19.67	1038.07
Kara Mile	760039	1036822	2298	28.26	23.84	192.32	174.96	107.22	88.78	180.65	285.08	149.24	18.54	10.90	54.10	1313.89
Mieso Mission	692992	1021059	1319	14.14	25.16	68.67	82.43	47.90	52.50	124.15	134.35	89.87	47.52	35.51	13.13	735.32
Mullu	702038	1027095	1256	16.14	42.76	84.27	125.23	80.28	43.23	126.54	162.18	84.06	9.28	18.93	17.08	809.98
Aysha	890419	1190118	724	22.40	15.13	23.31	26.48	19.32	29.82	64.59	66.48	39.37	2.33	0.78	0.32	310.32
Hurso	793297	1064546	1110	13.23	54.23	56.93	108.98	42.09	13.08	63.36	95.66	49.21	9.96	8.96	9.55	525.24
Harewa	826718	1098359	787	23.94	47.28	59.91	48.24	29.32	5.86	63.51	120.29	38.33	17.45	19.39	10.24	483.77
Teferi Ber	963039	1085545	1595	13.38	1.17	28.77	263.40	57.38	28.67	103.73	148.63	48.50	26.87	45.35	0.00	765.83
Lange	806996	1044023	2001	30.23	6.27	55.10	75.97	40.70	85.40	109.90	198.80	88.18	86.60	27.50	0.00	804.64
Bike	739049	1055797	1121	33.22	78.43	108.13	140.62	56.35	33.03	136.10	155.80	115.20	19.31	23.84	18.94	918.97
Adaitu	692104	1229636	506	14.29	14.65	44.03	55.58	30.01	2.90	60.41	88.98	27.36	7.16	8.29	0.35	354.01
Gewane	682063	1123271	629	11.41	42.13	66.58	56.51	24.30	8.50	93.36	103.48	35.21	23.67	7.56	8.70	481.43

Annex 2: Primary Stable Isotope Data Generated for the Research from Eastern part of lower Awash Basin

S/No	Locality	Sample code	Source	UTME	UTMN	Elv	Zone	d18O	d2H	Temp
1	Harmukale	AW-FW1	Flooding	186934	1087015	924	38	-0.66	0.77	Cold
2	Dengego	AW-SP1	Spring	820233	1046649	943	37	-2.27	-3.85	Cold
3	Wachu	AW-SP4	Spring	717479	1009200	2231	37	-1.07	0.76	Cold
4	Arberekete	AW-SP5	Spring	709494	1001112	2165	37	-1.03	0.32	Cold
5	Hades	AW-SP3	Spring	746448	1029765	2231	37	-2.58	-4.09	Cold
6	Kulubi	AW-SP2	Spring	792886	1042580	2394	37	-1.91	-3.02	Cold
7	Deladu	AW-SP6	Spring	715356	1042092	1069	37	0.08	8.89	Cold
8	Erer Palace	AW-SP7	Spring	762444	1053535	1188	37	-3.91	-12.31	Hot
9	Beyeas	AW-SP8	Wetland	181554	1119422	719	38	3.92	24.30	Cold
10	Madisa	AW-RW1	River	764111	1037740	2057	37	-2.54	-4.92	Cold
11	Afdem (Keraba)	AW-RW2	River	726094	1051660	1036	37	1.97	17.43	Cold
12	Bona	AW-RW3	River	761167	1062461	1007	37	0.86	10.85	Cold
13	Erer-Gota	AW-RW4	River	757441	1053834	1146	37	-0.88	1.45	Cold
14	upper Erer	AW-RW5	River	764404	1054223	1153	37	1.34	12.85	Cold
15	Hurso	AW-RW6	River	789393	1063182	1114	37	-0.87	0.13	Cold
16	Dire Dawa	AW-RAW4	Rainfall	814153	1063604	1167	37	0.14	16.13	Cold
17	Chiro (1 day)	AW-RAW6	Rainfall	705141	1004512	1763	37	4.29	36.92	Cold

18	Harar	AW-RAW1	Rainfall	181812	1030392	2001	38	-0.28	7.48	Cold
19	Haramaya Univ	AW-RAW2	Rainfall	174552	1041922	2016	38	-1.06	4.39	Cold
20	Harar (1 day)	AW-RAW5	Rainfall	181812	1030392	2001	38	-2.02	-4.24	Cold
21	Dengego	AW-RAW3	Rainfall	820999	1046116	2087	37	-2.27	-3.85	Cold
22	Miesso	AW-BH2	Borehole	692992	1021059	1319	37	-1.75	-0.62	Cold
23	Kersa	AW-BH1	Borehole	814690	1046395	2000	37	-2.33	-5.98	Cold
24	Bike	AW-BH5A	Borehole	742453	1055082	1087	37	-2.82	-5.06	Cold
25	Mulutown	AW-BH3	Borehole	701694	1027855	1252	37	-1.85	-2.54	Cold
26	Afdem Town	AW-BH4	Borehole	718771	1046429	1057	37	-3.79	-17.02	Thermal
27	Afdem TW	AW-BH5B	Borehole	715616	1059980	895	37	-2.59	-7.15	Cold
28	Salademer	AW-BH6	Borehole	704217	1066296	813	37	-0.46	1.83	Thermal
29	Erer Gota	AW-BH7	Borehole	756327	1052914	1183	37	-1.52	-3.35	Cold
30	Megaladi	AW-BH8	Borehole	781567	1060757	1115	37	-1.34	-10.82	Cold
31	Mete village	AW-BH9	Borehole	789746	1095557	761	37	0.94	2.45	Thermal
32	Mete (artesian)	AW-BH10	Borehole	786144	1099148	742	37	-1.34	-6.83	Thermal
33	Gad	AW-BH11	Borehole	813117	1083494	906	37	-0.76	0.29	Cold
34	Asaleso	AW-BH12	Borehole	800539	1058263	1245	37	-2.68	-9.72	Cold
35	D/Dawa	AW-BH13	Borehole	812425	1063533	1168	37	1.49	10.50	Cold
36	D/Dawa	AW-BH14	Borehole	814324	1060392	1240	37	0.2	6.56	Cold
37	Harawa	AW-BH15	Borehole	826858	1098077	791	37	1.69	12.07	Cold
38	Melo	AW-BH16	Borehole	177681	1112656	755	38	1.5	11.92	Cold
39	Gabi	AW-BH17	Borehole	186047	1128116	722	38	0.07	2.79	Thermal
40	Kalebed	AW-BH18	Borehole	177628	1079208	981	38	2.37	16.31	Cold
41	Harmukale	AW-BH19	Borehole	186263	1086565	940	38	2.27	15.46	Cold
42	Dure	AW-BH20	Borehole	212061	1110383	864	38	1.71	14.81	Cold
43	Shinile	AW-BH21	Borehole	811445	1071714	1034	37	0.78	10.70	Cold
44	Idora	AW-HDW2	Dugwell	759979	1089986	800	37	-0.65	3.36	Cold
45	Asbuli	AW-HDW3	Dugwell	737775	1103513	718	37	0.11	8.10	Cold
46	Harey	AW-HDW4	Dugwell	812012	1126022	680	37	2.1	15.60	Cold
47	Beyobahay	AW-HDW1	Dugwell	227134	1110915	967	38	-2.15	-8.97	Cold
48	Kalebed	AW-HDW7	Dugwell	177701	1079157	976	38	2.37	14.57	Cold
49	Degajebis	AW-HDW8	Dugwell	172107	1074032	1014	38	-0.17	2.19	Cold
50	Hore	AW-HDW6	Dugwell	803160	1140980	652	37	2.39	12.48	Cold
51	Hareso	AW-HDW5	Dugwell	778353	1171256	590	37	0.97	8.65	Cold

Annex 3: **Primary Physico-chemical data Generated for the Research from the Eastern part of Lower Awash Basin**

	Primary Water Chemistry Data Generated for the Research from Eastern part of Lower Awash Basin																				
S/N0.	**Location**	**Sample ID**	**Source**	**UTME**	**UTMN**	**Elv**	**Zone**	**EC**	**TDS**	**PH**	**Na**	**K**	**Ca**	**Mg**	**Fe**	**F**	**Cl**	**NO3**	**CO3**	**HCO3**	**SO4**	
1	Hareso	AW-HDW5	Dugwell	778353	1171256	590	37	1681	1162	7.46	270	19	97	17.4	0.07	0.89	70.08	33.22	0	395.28	400	Na-Ca-SO4-HCO3
2	Hore	AW-HDW6	Dugwell	803160	1140980	652	37	1244	888	7.16	94	23	189	5.28	0.06	0.06	32.76	29.74	0	353.8	310	Ca-Na-SO4-HCO3
3	Dengego	AW-SP1	Spring	820233	1046649	943	37	578	380	6.56	37	2.9	88	6.34	0	0.58	29.12	34.8	0	259.62	22	Ca-Na-HCO3
4	Kulubi	AW-SP2	Spring	792886	1042580	2394	37	503	304	7.22	17	0.1	90	10.6	0	0.55	10.92	10.44	0	312.32	0.2	Ca-HCO3
5	Hades	AW-SP3	Spring	746448	1029765	2231	37	386	230	7.05	20.5	0.1	70	2.64	0.01	0.48	10.01	5.3	0	224.48	8	Ca-Na-HCO3
6	Salademer	AW-BH6	Borehole	704217	1066296	813	37	726	488	8.02	122	6.2	42	5.81	0.01	0.57	51.88	32.48	0	268.4	50	Na-Ca-HCO3
7	Arberekete	AW-SP5	Spring	709494	1001112	2165	37	621	510	7.67	22	1.7	106	18.5	0	0.56	13.65	42.81	0	361.12	6	Ca-Mg-HCO3
8	Beyeas	AW-SP8B	Wetland	181554	1119422	719	38	6390	4204	8.5	1480	5.4	95	38.5	0.01	2.56	1020	6.4	216	956.48	860	Na-Cl-SO4-HCO3
9	Afdem TW	AW-BH5	Borehole	715616	1059980	895	37	612	398	7.72	75	6	51	12.1	0.01	0.73	23.66	17.19	0	292.8	31	Na-Ca-HCO3
10	Gabi	AW-BH17	Borehole	186047	1128116	722	38	1205	712	7.61	200	12	33	21.1	0.01	0.62	133.8	6.3	0	278.16	145	Na-HCO3-Cl-SO4
11	Medisa	AW-RW1	River	764111	1037740	2057	37	484	280	8.11	13	1.1	79	10.6	0	0.54	12.74	6.2	0	302.56	1	Ca-HCO3
12	Harar town	AW-RAW-01	Rainfall	181812	1030392	2001	38	49	26	6.66	0.3	0.2	6.1	1.82	0.18	0.55	0.91	0.94	0	25.62	0.1	Ca-Mg-HCO3
13	Dengego	AW-RAW-03	Rainfall	820999	1046116	2087	37	38	24	6.02	0.3	1.3	3.8	0.91	0.12	0.49	0.91	0.56	0	28.18	1	Ca-HCO3
14	Dire Dawa	AW-RAW-04	Rainfall	814153	1063604	1167	37	60	34	6.2	0.4	1.3	7.6	2.28	0.22	0.47	0.91	1.16	0	35.87	1.9	Ca-Mg-HCO3

Annex 4: Secondary physico-chemical data gathered for the research from various sources

S/N	Easten Lower awash Basin																				Water Type
	Locality	ID	Source	UTME	UTMN	Elv	Zone	EC	TDS	PH	Na	K	Ca	Mg	Fe	F	Cl	NO3	CO3	HCO3	SO4	
1	Biyobahay no7	AW-BH22	OWWDSE	228536	1110869	965	38	564	388	7.82	71	5.1	32.8	21.12	0.01	1.25	23.66	19.29	0	264.25	72.04	Na-Mg-Ca-HCO3-SO4
2	Biyobahay no5	AW-BH23	OWWDSE	229175	1110571	971	38	597	414	7.79	63	6	44.8	24	0.01	1.15	21.84	27.43	0	289.75	77.6	Na-Ca-Mg-HCO3-SO4
3	Biyobahay no6	AW-BH24	OWWDSE	229915	1110283	979	38	594	406	7.78	57	4.7	64	14.4	0	0.93	28.21	17.59	0	287.43	66.12	Ca-Na-HCO3
4	Mete no3	AW-BH25	OWWDSE	786149	1099151	741	37	719	452	8.61	140	3.8	11.2	2.4	0	1.77	117.8	0.4	24	87.84	51.19	Na-Cl-HCO3
5	Mete no2	AW-BH10	OWWDSE	786138	1098605	738	37	938	580	8.64	196	3.8	11.2	1.92	0.02	6.81	118.77	0.51	21.6	90.28	121.23	Na-Cl-SO4
6	Harawa TW	AW-BH15B	OWWDSE	826331	1097377	790	37	965	672	7.78	101	4.6	72.8	30.2	0.018	0.7	27	20.9	0	222	249.6	Na-Ca-SO4-HCO3
7	Aydora	AW-BH26	OWWDSE	759581	1091435	792	37	5070	3530	7.47	600	9.7	380	110.9	0.012	0.82	358.2	43.4	0	158.6	1771	Na-Ca-SO4
8	Asbuli	AW-BH27	OWWDSE	737767	1106062	711	37	3190	2174	7.5	485	7.7	100	84	0.006	0.66	614.1	44.5	0	175.7	484.6	Na-Mg-Cl-SO4
9	Jama-Dere	AW-BH28	OWWDSE	214296	1131593	831	38	2910	1902	7.33	284	10.7	184	69.6	0.96	0.76	381.41	20.72	0	287.92	584.29	Na-Ca-Mg-SO4-Cl
10	Magala-Adi	AW-BH8	OWWDSE	781594	1060728	1117	37	1874	1218	7.82	250	3.3	92.7	28.98	0.02	0.63	218.2	198.2	0	378.2	185.16	Na-Ca-HCO3-Cl-SO4
11	Alcho	AW-BH29	OWWDSE	782134	1057523	1193	37	681	448	7.56	9.4	1	19	74.9	0.06	0.58	10.5	0.39	0	414.8	52.6	Mg-HCO3
12	Hurso	AW-BH30	OWWDSE	789629	1062713	1120	37	1390	910	7.25	66	0.7	144.4	57.5	0.03	0.7	79.8	41.48	0	573.4	180	Ca-Mg-HCO3-SO4
13	Aydora1	AW-HDW9	OWWDSE	759959	1090176	797	37	1381	900	7.61	78	0.6	184.7	17.9	0.05	1.24	31.4	20.99	0	158.6	528.6	Ca-Na-SO4
14	Aydora2	AW-HDW2	OWWDSE	759968	1090121	796	37	1275	890	7.5	60	0.8	187.7	9.7	0	1.11	29.5	42.6	0	146.4	466.8	Ca-SO4
15	Girmame-Maras	AW-HDW10	OWWDSE	778533	1058777	1107	37	786	510	7.78	35	5.3	87.4	27.6	0.13	0.35	24.7	3.76	0	312.3	146.4	Ca-Mg-HCO3-SO4
16	Asbuli	AW-HDW3	OWWDSE	737763	1103347	1185	37	1295	930	7.63	58	4.8	190	23	0.09	0.63	10.45	4.99	0	226.9	508.6	Ca-SO4-HCO3
17	Dimtu	AW-HDW11	OWWDSE	759331	1058654	1064	37	1168	760	7.38	52	0.8	155.8	29.9	0.01	0.8	38	16.38	0	402.6	185.2	Ca-Mg-HCO3-SO4
18	Khelwine	AW-HDW12	OWWDSE	758665	1094670	780	37	2690	1942	7.67	110	8.2	231.8	186.3	0.13	1.02	49.4	0.5	0	463.6	1123.6	Mg-Ca-SO4-HCO3
19	Oerdela	AW-HDW13	OWWDSE	754872	1084824	813	37	906	598	7.62	52	0.4	121.6	11.5	0.06	1.33	16.15	63.6	0	300.12	162.3	Ca-Na-HCO3-SO4
20	Tabi	AW-HDW14	OWWDSE	768100	1077704	846	37	6430	4360	7.75	1200	2.4	167.2	119.6	0.07	1.73	233.7	16.3	0	639.3	2260.8	Na-SO4
21	Sedit	AW-HDW15	OWWDSE	768587	1069065	917	37	575	380	7.56	26	0.4	85.1	5.98	0.02	1.08	7.6	26.8	0	268.4	58.6	Ca-HCO3-SO4
22	Gode	AW-HDW16	OWWDSE	762251	1059159	1056	37	806	530	7.51	41	3.7	133	2.3	0.01	0.65	12.4	2.1	0	475.8	56.8	Ca-HCO3

23	Kantras-HSP	AW-SP7	OWWDSE	762457	1053520	1190	37	3680	2610	7.65	460	7.3	380	9.2	0	5.6	188.1	0.84	0	56.12	1520.6	Na-Ca-SO4
24	Keleme	AW-SP8A	OWWDSE	789029	1057941	1219	37	789	528	7.7	20	1.5	129.2	16.1	0	0.84	24.7	8.6	0	419.7	78.3	Ca-HCO3
25	Bona	AW-RW3	OWWDSE	761206	1062468	993	37	3870	2748	7.62	320	4.7	411.9	100.3	0	1.45	238.5	1.6	0	219.6	1546.2	Ca-Na-SO4
26	upper Erer	AW-RW5	OWWDSE	764416	1054223	1159	37	736	480	7.99	28	1.9	89.7	26.2	0	1.03	22.8	22	0	305	120.3	Ca-Mg-HCO3-SO4
27	Girmame	AW-RW7	OWWDSE	771686	1055856	1153	37	1383	920	7.48	84	2.9	162.6	34.9	0	1.5	86.45	9.7	0	419.7	310.8	Ca-Na-HCO3-SO4
28	Halcho	AW-RW8	OWWDSE	782321	1057930	1186	37	1098	722	7.96	48	1.7	125.4	35.9	0	0.8	69.35	2.1	0	405.6	161.5	Ca-Mg-HCO3-SO4
29	Biyman	AW-HDW17	OWWDSE	758548	1056732	1085	37	1554	1030	7.6	192	15.5	107.9	12.88	0.01	1.06	95.95	58.6	0	217.89	428.6	Na-Ca-SO4-HCO3
30	Biyman	AW-SP9	OWWDSE	758909	1056571	1103	37	3240	2190	7.52	500	10.1	235.6	9.2	0.06	7.5	199.5	2.8	0	64.9	1168.3	Na-Ca-SO4
31	Bike	AW-BH5A	OWWDSE	742434	1055100	1008	37	1177	766	7.93	196	10	48.64	11.5	0.01	1.3	76.95	1.48	0	294.39	212.3	Na-Ca-HCO3-SO4
32	Erer town river	AW-RW9	OWWDSE	763074	1057045	1096	37	627	400	8.12	27	2.8	64.6	26.68	0	0.61	22.8	17.1	0	227.16	118.6	Ca-Mg-HCO3-SO4
33	Sisilu	AW-BH31	OWWDSE	719876	1064805	887	37	1937	1360	8.14	385	4.1	59.28	23.92	0.03	1.05	96.9	210.3	0	507.64	326.2	Na-HCO3-SO4
34	Afdem	AW-BH4	OWWDSE	718770	1046429	1047	37	854	556	7.88	78	10.1	88.92	14.26	0.12	1.75	57.95	30.54	0	370.88	69.9	Ca-Na-HCO3
35	Sala'a	AW-BH32	OWWDSE	704353	1056263	809	37	682	470	8.56	129	6.4	24.32	6.44	0.017	0.18	47.4	56.8	14.4	214.11	71.11	Na-HCO3
36	Alijir	AW-BH33	OWWDSE	699990	1079698	745	37	793	520	7.94	115	7.3	53.2	12.88	0.012	1.19	26.6	7.47	0	463.6	0.13	Na-Ca-HCO3
37	Komiye	AW-BH34	OWWDSE	705842	1031637	1219	37	800	520	8.18	129	5.6	38	9.2	0.047	1.19	34.2	6.43	0	454.33	26.8	Na-Ca-HCO3
38	Afase	AW-BH35	OWWDSE	693369	1072568	777	37	857	558	8.4	142	3.7	30.4	11.5	0	1.54	37.05	0.35	9.6	314.27	111.67	Na-HCO3-SO4
39	Butuji	AW-BH36	OWWDSE	692621	1057125	863	37	509	332	8.22	40	4.7	44.08	19.32	0	0.73	19	0.25	4.8	279.99	13.89	Ca-Na-Mg-HCO3
40	Adayitu	AW-BH37	OWWDSE	692408	1230522	459	37	817	534	8.18	138	6.5	27.36	8.74	0	0.77	38.95	51.3	0	331.47	80.1	Na-HCO3
41	Gedamayitu	AW-BH38	OWWDSE	660081	1077855	793	37	1798	1170	8.17	340	11.2	48.64	10.58	0	1.59	314.41	78.5	0	178.49	177.5	Na-Cl-SO4
42	Mulutown	AW-BH3	OWWDSE	702038	1027095	1256	37	1097	750	8.26	178	5.9	51.68	11.5	0.05	1.48	87.4	123	9.6	223.87	168.12	Na-Ca-HCO3-SO4-Cl
43	Sisilu (Keraba)	AW-RW10	OWWDSE	719468	1064329	873	37	708	500	7.94	69	5.1	74.48	21.62	0.02	0.51	19.95	43.8	0	254.98	139.08	Ca-Na-Mg-HCO3-SO4
44	Afdem (Keraba)	AW-RW2	OWWDSE	726111	1051504	1036	37	550	390	8.58	52	4.9	53.2	19.32	0.04	0.63	46.55	1.39	12	161.04	113.6	Ca-Na-Mg-HCO3-SO4
45	Adayitu (Awash)	AW-RW11	OWWDSE	692368	1230572	452	37	614	400	8.43	106	7.8	27.36	8.74	0.11	1.77	44.65	5.3	14.4	262.79	41.89	Na-HCO3
46	Der Ela	AW-HDW18	OWWDSE	727546	1053854	1003	37	780	510	8.03	90	16.5	60.8	16.56	0.07	1.57	26.6	2.03	0	421.88	70.64	Na-Ca-HCO3
47	Asili	AW-HDW19	OWWDSE	703512	1084032	706	37	1522	1066	8.5	345	2.4	21.28	7.82	0.02	1.92	67.45	168.3	36	448.35	187.16	Na-HCO3-SO4
48	Afase	AW-HDW20	OWWDSE	696625	1072311	776	37	821	550	7.81	117	1.4	53.2	8.28	0.02	1.11	24.7	53.6	0	282.79	144.79	Na-Ca-HCO3-SO4

49	Biyedidley	AW-BH41	OWWDSE	227735	1131358	970	38	2120	1420	6.99	208	8.4	182.4	49.62	0.02	1.37	285.95	1.6	0	317.57	501.7	Ca-Na-SO4-Cl-HCO3
50	Arabi	AW-BH42	OWWDSE	250011	1098123	1114	38	686	460	7.78	73	4.3	53.2	19.78	0	1.33	24.7	36.4	0	296.7	96.34	Na-Ca-Mg-HCO3-SO4
51	Keranle	AW-BH43	OWWDSE	225663	1081638	1354	38	1056	688	7.25	45	2.8	159.6	19.32	0	2.04	43.7	27.9	0	509.96	114.04	Ca-HCO3
52	Semekab	AW-BH44	OWWDSE	219016	1078318	1322	38	828	542	7.52	53	2.2	98.8	25.3	0	1.92	24.7	19.7	0	452.01	73.01	Ca-Na-Mg-HCO3
53	Arabi (hot)	AW-SP11	OWWDSE	250011	1098123	1114	38	3870	2520	7.48	825	36	51.68	3.68	0.01	7.2	551	2.4	0	533.14	627.6	Na-Cl-SO4-HCO3
54	Hagarwein	AW-BH45	OWWDSE	265999	1094497	1242	38	1541	1050	7.6	154	8.2	129.2	25.3	0.02	0.94	182.4	282.6	0	229.48	148	Na-Ca-Cl-HCO3-NO3
55	Derega	AW-HDW31	OWWDSE	248250	1094041	1144	38	1307	852	7.18	122	6.6	117.8	39.1	0	1.4	110.2	29.3	0	431.15	177.3	Ca-Na-Mg-HCO3-SO4-Cl
56	Dembel town	AW-BH46	OWWDSE	236715	1085654	1317	38	677	440	7.43	38	3	68.4	23	0	1.09	11.4	30.5	0	366.2	41.3	Ca-Mg-Na-HCO3
57	Shinile Town	AW-BH21	OWWDSE	811477	1071736	1029	37	1191	780	7.19	69	1.3	140.6	36.8	0.01	1.46	91.2	62.3	0	468.24	128.6	Ca-Mg-Na-HCO3
58	Mermarsa	AW-BH48	OWWDSE	810949	1067896	1078	37	1261	822	7.45	68	1.7	184.7	11.5	0.02	1.29	116.85	94.4	0	447.37	102.6	Ca-Na-HCO3-Cl
59	Harewa existing	AW-BH15A	OWWDSE	826859	1098079	797	37	1803	1270	8.12	218	7	161.9	26.22	0.01	0.97	29.45	57	0	259.62	610.3	Na-Ca-SO4-HCO3
60	Melo	AW-BH16	OWWDSE	177686	1112659	754	38	2340	1660	8.59	380	3.3	131.5	19.32	0.01	1.88	285.95	96.1	24	189.95	610.3	Na-Ca-SO4-Cl
61	Mete (old)	AW-BH9	OWWDSE	789759	1095378	751	37	1845	1200	8.09	258	15.5	91.2	19.32	0.01	1.59	290.7	50.5	0	208.62	245.6	Na-Ca-Cl-SO4
62	Harey	AW-HDW4	OWWDSE	812228	1126012	679	37	3560	2656	7.4	260	5.7	494	46	0.07	2.93	19.95	53.6	0	199.35	1548.6	Ca-Na-SO4
63	Harey	AW-BH49	OWWDSE	811834	1126149	678	37	14620	10700	7.7	3000	18	668.8	128.8	0.32	7.1	4560	510.3	0	152.99	1720	Na-Cl-SO4
64	Kalebed	AW-HDW7	OWWDSE	177702	1079158	975	38	1740	1270	7.57	120	4.4	178.6	66.7	0.01	1.64	95.95	20.3	0	192.39	628.3	Ca-Mg-Na-SO4
65	Degajebis	AW-HDW8	OWWDSE	172107	1074025	1002	38	947	640	7.29	19	3	161.9	15.18	0	0.92	18.05	22.8	0	336.11	225.6	Ca-HCO3-SO4
66	Tome	AW-BH50	OWWDSE	815089	1067392	1089	37	1182	778	7.16	36	1.6	182.4	27.6	0.06	1.19	33.25	30.94	0	440.42	219.9	Ca-HCO3-SO4
67	Barak	AW-Sp12	OWWDSE	819664	1073154	1000	37	1033	688	7.73	26	2.4	159.6	31.28	0.01	1	32.3	14.6	0	299.02	263.7	Ca-Mg-SO4-HCO3
68	Dure	AW-BH20	OWWDSE	212061	1110383	864	38	609	410	8.18	75	5.3	34.2	18.4	0	1.12	30.4	41.2	0	266.6	63.8	Na-Ca-Mg-HCO3
69	Harmukale	AW-BH19	OWWDSE	186261	1086563	940	38	1291	846	7.69	188	3	60.8	17.48	0	1.32	81.7	12.3	0	472.87	164.2	Na-Ca-HCO3-SO4
70	Hurso	AW-BH51	OWWDSE	789718	1062924		37	1829	1296	7.45	100	1	208	65.66	ND	0.51	188.1	ND	ND	466.04	448.4	Ca-Mg-Na-SO4-HCO3-Cl
71	Cheremiti-#2	AW-BH52	WWDSE	864535	1079607		37	758	466	7.88	55	2.8	88	14.11	ND	0.47	39.6	ND	ND	363.56	73.8	Ca-Na-HCO3
72	Rail way station	AW-BH53	WWDSE	813936	1061662		37	1582	1092	8.08	60	2.2	214	29.5	ND	0.71	165.9	ND	16.8	322	56.7	Ca-HCO3-Cl
73	D/Dawa food com	AW-BH54	WWDSE	814520	1063426		37	1996	1060	7.59	40	1.3	188.8	36.5	ND	0.67	144.1	ND	ND	319.64	92.3	Ca-Mg-HCO3-Cl

74	Hafcat #2	AW-BH55	WWDSE	814941	1063539		37	2250	1583	7.29	125	1.8	264	68.1	ND	0.69	331.1	ND	ND	412.36	448.5	Ca-Mg-Na-SO4-Cl-HCO3
75	Melka Jebdu #2	AW-BH56	WWDSE	805241	1063341		37	957	598	7.27	30	2.5	128	34.1	0.01	0.51	67.1	ND	ND	441.64	47.5	Ca-Mg-HCO3
76	Palace	AW-BH57	WWDSE	814172	1061499		37	2140	1570	7.46	125	3.2	240	41.34	ND	0.49	314.6	ND	ND	414.8	23.7	Ca-Na-Cl-HCO3
77	Hafcat #1	AW-BH58	WWDSE	814865	1063384		37	1810	1245	7.69	80	1.1	240	44.75	ND	0.55	215.6	ND	ND	353.8	221.5	Ca-Mg-Cl-HCO3-SO4
78	Cement Factory	AW-BH59	WWDSE	812378	1061804		37	994	532	7.43	30	1.7	116	28.7	ND	0.65	83.6	ND	ND	373.32	18.46	Ca-Mg-HCO3-Cl
79	Ras Hotel # 2	AW-BH60	WWDSE	813870	1061350		37	1393	946	7.6	60	1.5	200	20.92	0.03		149.6	ND	ND	378.2	50	Ca-Na-HCO3-Cl
80	East Afri Bot#2	AW-BH61	WWDSE	814020	1061049		37	1137	834	7.27	40	1.2	152	30.16	ND	0.39	80.6	ND	ND	373.32	39.56	Ca-Mg-HCO3-Cl
81	Medekedjima	AW-SP13	WWDSE	804366	1052194		37	1081	644	7.56	50	1.3	148	31.62	ND	0.46	94.6	ND	ND	461.16	47.5	Ca-Mg-HCO3-Cl
82	Gende Boru	AW-SP14	WWDSE	803501	1050527		37	746	426	7.57	20	1.3	128	19.46	ND	0.32	34.1	ND	ND	419.68	2.64	Ca-HCO3
83	D/DEdible oil f	AW-HDW33	WWDSE	812941	1061925		37	1084	650	7.73	60	1.1	140	24.32	ND	0.42	100	ND	ND	397.72	31.65	Ca-Na-HCO3-Cl
84	Jelobelina	AW-HDW34	WWDSE	815939	1052060		37	1844	560	7.6	200	4	188	21.89	ND	0.99	298.1	ND	ND	610	15.8	Ca-Na-HCO3-Cl
85	HARAWATU	AW-SP15	WWDSE	803522	1050333		37	774	462	7.74	20	1.3	120	24.32	0.01	0.16	39.6	ND	ND	419.68	10.6	Ca-Mg-HCO3
86	Borte	AW-SP16	WWDSE	800391	1049534		37	749	432	7.25	9	1.3	140	17.02	0.01	0.45	17.6	ND	ND	427	7.9	Ca-HCO3
87	Fechase	AW-SP17	WWDSE	831945	1055546		37	1056	686	7.41	6	0.9	160	9.73	ND	0.65	94.6	ND	ND	402.6	7.9	Ca-HCO3-Cl
88	Cement Factory	AW-SP18	WWDSE	812255	1061280		37	908	526	7.6	4	1.9	132	17.02	ND	0.57	94.6	ND	ND	356.24	7.9	Ca-HCO3-Cl
89	Eftua	AW-SP19	WWDSE	843185	1054557		37	719	408	7.37	8	1.4	144	9.73	ND	0.39	23.1	ND	ND	405.04	10.6	Ca-HCO3
90	Legahrtu(hotsp)	AW-SP20	WWDSE	847988	1085780		37	3330	2414	8.03	600	31.5	82.3	8.5	ND	2.35	412.3	ND	7.2	161	1000.5	Na-SO4-Cl
91	Legemeda	AW-SP21	WWDSE	807621	1053559		37	1890	1268	7.4	14	2.9	184	60.8	ND	0.14	281.6	ND	ND	427	290.2	Ca-Mg-Cl-HCO3-SO4
92	Halobusa(Legego	AW-SP22	WWDSE	810084	1053690		37	1797	1270	7.6	140	7.3	172	82.67	ND	0.81	226.6	ND	ND	524.6	168.8	Ca-Mg-Na-HCO3-Cl
93	Keche	AW-SP23	WWDSE	820449	1046854		37	546	408	7.1	35	3.1	200	4.86	0.01	0.56	34.1	ND	ND	231.8	5.27	Ca-HCO3
94	Adada	AW-SP24	WWDSE	819112	1056268		37	810	480	7.4	40	3.5	128	7.29	ND	0.37	83.6	ND	ND	324.52	15.8	Ca-Na-HCO3-Cl
95	Serkama	AW-SP25	WWDSE	845129	1057387		37	800	468	7.65	30	3.9	140	12.16	0.01	0.29	34.1	ND	ND	392.84	13.2	Ca-HCO3
95	Awale Roresa	AW-SP26	WWDSE	836775	1052144		37	730	408	7.43	12	1.7	128	19.46	0.01	0.23	28.6	ND	ND	412.36	15.8	Ca-HCO3
96	Bishambaye	AW-SP27	WWDSE	830595	1058862		37	1062	680	7.44	60	1.2	152	9.73	0.01	0.51	105.6	ND	ND	390.4	5.27	Ca-Na-HCO3-Cl
97	Biyoawale	AW-SP28	WWDSE	829794	1052057		37	466	270	7.3	35	1.2	64	4.86	ND	0.39	34.1	ND	ND	187.88	18.2	Ca-Na-HCO3-Cl
98	Gende kurto	AW-SP29	WWDSE	837595	1057243		37	1108	752	7.61	50	4.5	176	24.32	ND	0.76	78.1	ND	ND	429.44	31.6	Ca-HCO3

99	Legehare	AW-SP30	WWDSE	818219	1061625		37	966	570	7.38	50	6.1	140	24.32	ND	0.22	56.1	ND	ND	507.52	15.8	Ca-Na-HCO3
100	Mudi Anano	AW-SP31	WWDSE	820995	1063252		37	890	559	7.68	20	0.9	200	109.4	ND	0.37	39.6	ND	ND	480.68	2.6	Ca-Mg-HCO3
101	Jarso-Gendelege	AW-SP32	WWDSE	852823	1049830		37	314	190	7.9	9	3.7	52	4.86	ND	0.15	12.1	ND	ND	165.92	2.4	Ca-HCO3
102	Legedomirga	AW-SP33	WWDSE	813438	1048587		37	966	570	7.38	50	6.1	140	24.32	ND	0.22	56.1	ND	ND	507.52	15.8	Ca-Na-HCO3
103	Sabian Pw-1	AW-BH62	WWDSE	812491	1063930		37	1057	622	7.19	50	1.3	136	30.16	ND	0.65	105.6	ND	ND	424.56	44.8	Ca-Mg-HCO3-Cl
104	Sabian Pw-4	AW-BH63	WWDSE	812527	1063543		37	1060	670	7.01	50	1.4	160	15.57	0.01	0.76	105.6	ND	ND	407.48	29	Ca-HCO3-Cl
105	Sabian Pw-5	AW-BH64	WWDSE	812362	1063793		37	1017	618	7.02	40	1.3	159	3	ND	0.96	75.7	ND	ND	407.5	47.5	Ca-HCO3-Cl
106	Jelobelina	AW-SP34	WWDSE	817946	1051086		37	882	544	7.62	20	1.4	128	26.75	ND		94.6	ND	ND	295.24	50.1	Ca-Mg-HCO3-Cl
107	Koriso	AW-SP36	WWDSE	799366	1051072		37	835	554	7.23	12	1.8	152	21.89	ND	0.55	23.1	ND	ND	400.16	81.6	Ca-HCO3
108	Elfora	AW-BH65	WWDSE	810907	1062360		37	1080	650	7.16	50	1.6	151.2	21.5	ND	0.37	83.4	ND	ND	446	56.7	Ca-HCO3-Cl
109	Bore TW4(2002)	AW-BH66	WWDSE	796050	1058100		37	704	415	7.49	15	1.5	134	11.5	ND	0.64	14.6	ND	ND	392.8	43.5	Ca-HCO3
110	Amdael well #1	AW-BH67	WWDSE	814356	1064666		37	1302	790	7.09	100	2	112	31.13	0.01	0.54	160.6	ND	ND	383.08	14.5	Ca-Na-Mg-HCO3-Cl
111	Dechatu	AW-BH68	WWDSE	816294	1058832		37	784	470	7.33	10	3	140	8.27	0.01	0.27	28.6	ND	ND	400.16	12.1	Ca-HCO3
112	Jeldesa	AW-HDW35	WWDSE	841574	1075928		37	890	526	7.61	40	3	120	27.86	0.01	0.51	61.6	ND	ND	297.68	147.7	Ca-Mg-HCO3-SO4
113	Garba Anano	AW-HDW36	WWDSE	857203	1072551		37	3780	3110	7.48	300	1.5	472	109.4	0.04	1.19	694.1	ND	ND	363.56	1213	Ca-Na-SO4-Cl
114	Kalicha	AW-HDW37	WWDSE	833527	1059032		37	1250	882	7.74	80	1	180	24.32	ND	0.77	533.1	ND	ND	441.6	55.4	Ca-Cl-HCO3
115	Tsehay Hotel	AW-HDW38	WWDSE	813009	1061596		37	1380	878	6.97	80	4.3	180	19.46	ND	0.56	133.1	ND	ND	700.28	15.8	Ca-Na-HCO3-Cl
116	Mudi Anano	AW-HDW39	WWDSE	819238	1066909		37	704	446	8.09	130	2.1	32	4.86	0.01	1.4	23.1	ND	ND	378	5.3	Na-Ca-HCO3
117	Kenchera #1	AW-HDW40	WWDSE	810272	1055328		37	964	610	7.67	50	2.2	150	17.02	ND	0.65	78.1	ND	ND	439.2	42.2	Ca-Na-HCO3-Cl
118	Ejaneni	AW-HDW41	WWDSE	819113	1056268		37	1245	884	6.68	80	1.9	184	19.46	0.01	0.45	160.6	ND	ND	431.88	55.4	Ca-Na-HCO3-Cl
119	Belewa#1	AW-HDW42	WWDSE	840894	1058278		37	890	508	7.35	9	1	160	24.32	0.02		23.1	ND	ND	531.92	5.3	Ca-Mg-HCO3
120	Gende Sur	AW-HDW43	WWDSE	799308	1062084		37	872	532	7.87	100	1.1	68	17.02	0.01	0.67	23.1	ND	ND	524.6	21.1	Na-Ca-HCO3
121	Bore	AW-HDW44	WWDSE	798554	1060531		37	1218	804	7.92	140	1.4	88	29.18	ND	1.07	34.1	ND	ND	563.64	200.4	Na-Ca-HCO3-SO4
122	Grba Anano	AW-HDW45	WWDSE	857182	1072675		37	2260	1710	7.64	150	4.7	288	55.94	ND	0.83	325.6	ND	ND	327	685	Ca-Na-SO4-Cl
123	Koran Goga	AW-HDW46	WWDSE	800714	1063496		37	1373	872	7.79	220	0.9	60	19.46	0.04	1.12	72.6	ND	ND	549	208.4	Na-Ca-HCO3-SO4
124	Melka Jebdu	AW-HDW47	WWDSE	805579	1065086		37	1457	974	7.2	240	1	136	31.62	0.08	0.76	127.6	ND	ND	549	184.6	Na-Ca-HCO3-SO4

125	Goladeg	AW-HDW48	WWDSE	802030	1067013		37	1257	862	7.41	100	0.8	128	41.34	0.01	0.87	23.1	ND	ND	470.92	329.7	Ca-Na-Mg-HCO3-SO4
126	Arsho Adele	AW-HDW49	WWDSE	806000	1067040		37	2090	1416	7.42	200	0.9	144	75.39	0.01	1.21	248.6	ND	ND	463.6	448.4	Na-Ca-Mg-SO4-HCO3-Cl
127	Melka(Fuad Haji	AW-SP37	WWDSE	805106	1062727		37	720	412	6.67	40	2.5	80	24.32	ND	0.27	78.1	ND	ND	275.72	39.56	Ca-Mg-Na-HCO3-Cl
128	Gende Alo	AW-HDW50	WWDSE	805943	1064012		37	1223	808	7.3	60	1.9	188	31.62	0.01	0.5	138.6	ND	ND	446.52	81.8	Ca-HCO3-Cl
129	Gende Rige	AW-HDW51	WWDSE	806316	1064129		37	1068	670	7.31	40	1.7	168	24.32	0.09	0.5	83.6	ND	ND	461.16	42.24	Ca-HCO3-Cl
130	Chirmite	AW-BH69	GSE	206067	1079400	1170	38	920	777	7.68	55	2.4	25	74	ND	0.35	32	20	0	464	72	Mg-Na-HCO3
131	Harmukale	AW-BH70	GSE	186257	1086571	943	38	978	862	7.88	98	0.9	45	43	ND	0.74	45	18	0	432	111	Na-Mg-Ca-HCO3-SO4
132	Harwato	AW-BH71	GSE	220858	1085139	1285	38	1101	950	7.5	75	3.1	83	48	ND	0.63	56	38	0	533	64	Ca-Mg-Na-HCO3
133	Dembel	AW-BH72	GSE	236714	1085653	1319	38	727	627	7.85	63	2.5	48	26	ND	0.74	21	19	0	377	39	Na-Ca-Mg-HCO3
134	Jaldesa	AW-BH73	GSE	181505	1077975	1049	38	2850	2445	7.26	110	15	375	115	ND	0.96	77	0.039	0	60	1686	Ca-Mg-SO4
135	Dini	AW-BH74	GSE	175896	1066152	1380	38	809	669	7.93	31	2.2	100	30	ND	0.39	55	32.8	0	342	48	Ca-Mg-HCO3
136	Gende Geboba	AW-BH75	GSE	172475	1056298	1613	38	894	743	7.49	48	1	98	2	ND	0.52	44	48.7	0	428	21	Ca-Na-HCO3
137	Kalicha	AW-BH76	GSE	174701	1058490	1615	38	1267	1014	7.4	58	11	148	35	ND	0.44	101	102	0	459	64	Ca-Mg-HCO3-Cl
138	Agar Wene	AW-BH77	GSE	265998	1094498	1239	38	1526	999	8.12	130	7	76	53	ND	0.46	172	222	0	211	88	Na-Mg-Ca-Cl-HCO3-NO3
139	Tulu Gubel	AW-BH78	GSE	253803	1062973	1884	38	1788	1231	7.72	108	5	155	60	ND	0.71	294	8.42	0	343	235	Ca-Mg-Na-Cl-HCO3-SO4
140	Lefeisa/Aubere	AW-BH79	GSE	221953	1064058	1723	38	3162	1622	7.41	150	8	148	95	ND	0.83	179	3.5	0	750	232	Mg-Ca-Na-HCO3-Cl-SO4
141	Jara/Aubere	AW-BH80	GSE	256115	1073010	1885	38	3163	1563	7.68	125	6	210	10	ND	0.54	537	15.06	0	299	243	Ca-Na-Cl-SO4-HCO3
142	Tulu Guled	AW-BH81	GSE	253916	1063159	1882	38	1795	1284	7.67	108	5	170	60	ND	0.71	326	6.2	0	323	263	Ca-Mg-Na-Cl-SO4-HCO3
143	Gerba Aneno	AW-HDW52	GSE	199173	1076201	1139	38	825	752	7.77	56	0.5	110	14	ND	0.77	25	8	0	383	105	Ca-Na-HCO3-SO4
144	Kalebed	AW-HDW53	GSE	177703	1079158	972	38	2100	1574	7.7	128	3.2	145	95	ND	0.75	164	11.5	0	217	782	
145	Jaldesa	AW-HDW54	GSE	182964	1075763	1081	38	894	733	7.56	40	3	90	30	ND	0.47	44	14.2	0	339	144	Ca-Mg-HCO3-SO4
146	Lowenage/Dembel	AW-HDW55	GSE	237645	1070414	1539	38	1238	984	7.76	73	3	110	48	ND	0.6	71	4.43	0	558	81	Ca-Mg-Na-HCO3
147	Deriwenega/Oberi	AW-HDW56	GSE	282512	1085869	1433	38	752	507	7.81	25	5	80	16	ND	0.45	22	15.1	0	303	24	Ca-Mg-HCO3

148	Oberi	AW-HDW57	GSE	305640	1081977	1572	38	870	641	7.9	30	3.2	100	28	ND	0.67	94	18.6	0	282	61	Ca-Mg-HCO3-Cl
149	Kore/Jarso	CS-4	GSE	196016	1049740	2540	38	309	305	7.66	7	4	38	11	ND	0.23	2	6.2	0	171	16	Ca-Mg-HCO3
150	GSE (hot)	AW-SP38	GSE	247112	1101347	1077	38	3910	2978	7.66	840	0.1	300	20	ND	8.49	686	1.3	0	438	605	Na-Ca-Cl-SO4
151	GSE (hot)	AW-SP39	GSE	187241	1086821	933	38	2890	2112	8.12	270	290	50	5	ND	7.08	329	0.039	0	261	753	Na-K-SO4-Cl
152	GSE	AW-SP40	GSE	200737	1069302	1356	38	1093	893	7.7	43	1.4	98	48	ND	0.54	81	31	0	401	161	Ca-Mg-HCO3-SO4
153	GSE	AW-SP41	GSE	172099	1074021	1004	38	948	810	7.58	15	22	133	28	ND	0.56	17	6.2	0	328	235	Ca-Mg-HCO3-SO4
154	GSE	AW-SP42	GSE	187458	1064006	1384	38	732	607	8.15	41	2.6	70	31	ND	0.51	49	9.3	0	301	81	Ca-Mg-Na-HCO3-SO4
155	GSE	AW-SP43	GSE	185651	1061658	1477	38	724	971	7.41	53	1.8	103	65	ND	0.56	60	59.8	0	505	89	Mg-Ca-HCO3
156	GSE	AW-SP44	GSE	172562	1051954	1887	38	635	562	7.25	29	2.2	84	11	ND	0.36	19	24.4	0	333	22	Ca-HCO3
157	GSE	AW-SP45	GSE	177143	1053899	1798	38	865	758	7.71	35	1	128	15	ND	0.34	37	22.6	0	461	31	Ca-HCO3
158	GSE	AW-SP46	GSE	177395	1052611	1924	38	798	667	7.38	10	1.4	108	23	ND	0.23	17	31	0	445	16	Ca-Mg-HCO3
159	GSE	AW-SP47	GSE	171756	1058542	1541	38	1064	869	7.62	55	1	110	25	ND	0.49	78	79.7	0	414	53	Ca-Na-HCO3-Cl
160	GSE	AW-SP48	GSE	183313	1057139	1777	38	802	721	7.52	10	1.5	125	25	ND	0.24	16	25.3	0	462	24	Ca-Mg-HCO3
161	GSE	AW-SP49	GSE	181739	1059937	1519	38	808	676	7.87	20	1.4	86	30	ND	0.32	32	21.1	0	409	48	Ca-Mg-HCO3
162	GSE	AW-SP50	GSE	179491	1053509	2014	38	808	729	7.4	9	0.9	146	20	ND	0.19	15	35.4	0	473	15	Ca-HCO3
163	GSE	AW-SP51	GSE	186359	1057417	1760	38	941	788	7.85	45	2.2	98	33	ND	0.47	42	50.9	0	437	57	Ca-Mg-HCO3
164	GSE	AW-SP52	GSE	191460	1056168	1713	38	687	590	7.75	14	2	93	22	ND	0.32	15	15.5	0	378	27	Ca-Mg-HCO3
165	GSE	AW-SP53	GSE	237635	1062805	1723	38	906	799	7.68	30	2.4	120	32	ND	0.36	41	26.6	0	445	66	Ca-Mg-HCO3
166	GSE	AW-SP55	GSE	200232	1053417	2136	38	575	483	7.74	5	1	91	13	ND	0.16	15	23.9	0	307	12	Ca-HCO3
167	GSE	AW-SP56	GSE	209138	1064329	1570	38	839	725	7.51	15	2	118	26	ND	0.27	39	26.6	0	438	36	Ca-Mg-HCO3
168	GSE	AW-SP57	GSE	216065	1063479	1610	38	838	735	7.7	61	3	81	22	ND	0.81	81	20.4	0	392	49	Ca-Na-HCO3-Cl
169	GSE	AW-SP59	GSE	216753	1056626	1974	38	774	676	8.82	48	1.3	88	20	ND	0.54	46	39.9	0	379	25	Ca-Na-HCO3
170	GSE	AW-SP60	GSE	216753	1056626	2457	38	471	435	7.67	11	2	60	15	ND	0.22	16	19.9	0	259	9	Ca-Mg-HCO3
171	Chirmite/Obely	AW-RW12	GSE	189693	1085777	951	38	5380	4213	8.36	1248	4.7	40	15	ND	4.32	337	0.03	0	966	1546	Na-SO4-HCO3
172	Yelba Temer	AW-RW13	GSE	182590	1076236	1072	38	1110	904	7.73	43	2.3	125	33	ND	0.56	55	0.03	0	387	237	Ca-Mg-HCO3-SO4
173	Hula Bora	AW-BH82	OWWDSE	748960	1050023	1226	37	3580	2496	8.58	570	2.3	180	9.76	0.03	1.72	189.6	4.55	12	1.22	1510.6	Na-Ca-SO4

174	Adigala town	AW-BH83	OWWDSE	195029	1152220	745	38	1784	1140	7.57	262	3.7	52	56.16	0.02	0.82	261.68	12.32	0	395.28	278.95	Na-Mg-Cl-HCO3-SO4
175	Waruf lake	AW-LW1	OWWDSE	160248	1152564	660	38	1245	780	7.94	224	12.6	36	7.2	0.01	0.71	179.6	8.38	0	207.4	188.14	Na-Cl-SO4-HCO3
176	Tutuftu	AW-BH84	OWWDSE	685854	1009744	1528	37	748	468	7.47	69	21	63.7	17.6	0.23	0	31.7	10	0	397.1	50.88	Ca-Na-HCO3
177	Fa'o	AW-BH85	OWWDSE	691053	1020494	1341	37	726	446	7.62	70	9.1	80.1	14.8	0.02	0.8	16.3	7	0	468.8	14.3	Ca-Na-HCO3
178	Huse Sodoma	AW-BH86	OWWDSE	695877	1015842	1418	37	662	424	7.65	44	5.6	84.6	19.2	0	1	20.2	10.5	0	399.7	6.6	Ca-Na-Mg-HCO3
179	Gulufa	AW-BH87	OWWDSE	687371	1018850	1376	37	812	526	8.49	152	2.8	12.7	1.1	0.11	0	120.9	67.5	4.8	54.3	123.7	Na-Cl-SO4
180	Ganda Aliware	AW-BH88	OWWDSE	694136	1019853	1329	37	576	404	7.48	50	8.2	57.3	15.95	0	0.8	15.4	16.25	0	333.1	7.43	Ca-Na-Mg-HCO3
181	Umerguluf	AW-HDW23	OWWDSE	193397	1197910	449	38	546	380	7.56	41	3.5	72.2	4.6	0	1.05	15.2	50.6	0	206.3	83.5	
		Aysha Basin Secondary Data																				
	Locality	**ID**	**Source**	**UTME**	**UTMN**	**Elv**	**Zone**	**EC**	**TDS**	**PH**	**Na**	**K**	**Ca**	**Mg**	**Fe**	**F**	**Cl**	**NO3**	**CO3**	**HCO3**	**SO4**	
1	Durdur	AYS-HDW21	OWWDSE	209433	1208169	483	38	566	869	8.04	130	4.4	41.8	5.98	0	1.15	73.15	1.13	0	173.85	181.64	Na-Ca-SO4-HCO3-Cl
2	Gerbale	AYS-HDW22	OWWDSE	241656	1176996	709	38	420	642	7.52	48	3.2	90.44	3.22	0.05	1.46	15.2	2.42	0	268.89	111.09	Ca-Na-HCO3-SO4
3	Sanajif	AYS-BH39	OWWDSE	248057	1127633	1203	38	2780	4060	7.55	515	33	167.2	154.1	0.08	1.11	551	1.34	0	642.09	1022.5	Na-Mg-SO4-Cl-HCO3
4	Degago	AYS-BH40	OWWDSE	232637	1161153	858	38	1642	2520	7.81	284	10.1	179.4	16.56	0	1.54	247	42.3	0	338.43	548.3	Na-Ca-SO4-Cl-HCO3
5	Kebrehauso	AYS-HDW24	OWWDSE	235399	1219589	748	38	942	1436	7.75	180	6.4	115.5	8.28	0.01	1.32	271.7	50.59	0	129.81	147.9	Na-Ca-Cl-SO4
6	Biyegurgur	AYS-HDW25	OWWDSE	247310	1149757	929	38	274	400	7.68	13.5	4.9	60.8	5.52	0	1.32	7.6	60.4	0	171.53	25.89	Ca-HCO3
7	Meramedobes	AYS-HDW26	OWWDSE	233951	1158904	861	38	246	378	7.54	12.5	5	57	6.9	0.01	0.71	5.7	22.8	0	213.3	18.6	Ca-HCO3
8	Biyekebobe	AYS-HDW27	OWWDSE	233272	1148331	937	38	220	313	8.08	17.5	4.6	45.6	4.6	0	1.09	8.55	34.6	0	139.08	31.98	Ca-Na-HCO3
9	Anajog	AYS-HDW28	OWWDSE	229718	1196777	676	38	1296	1839	8.17	300	7	101.8	17.48	0.01	2.9	216.6	90.6	0	173.85	456.9	Na-Ca-SO4-Cl
10	Durdur	AYS-SP10	OWWDSE	211558	1206305	498	38	360	514	7.07	44	7	57	2.3	0.01	1.2	21.85	58.3	0	130	88.6	Ca-Na-HCO3-SO4
11	Adele (Motorized)	AYS-HDW29	OWWDSE	240662	1199109	717	38	1140	1750	7.97	208	3.5	117	28.06	0	1.72	290.7	94.8	0	301.34	151.8	Na-Ca-Cl-HCO3
12	Helele	AYS-HDW30	OWWDSE	243177	1136277	1077	38	396	604	8.1	27	4.1	83.6	11.96	0	2.04	22.8	58.6	0	257.29	53.4	Ca-HCO3
13	Dewele	AYS-HDW32	OWWDSE	241131	1221097	807	38	2860	4400	7.86	600	3.8	273.6	110.4	0	0.78	1130.5	14.85	0	292.07	388.6	Na-Ca-Cl
14	Ayisha Town	AYS-BH47	OWWDSE	239677	1189512	708	38	1450	2050	7.64	242	5.2	152	36.8	0.01	1.28	205.2	131.2	0	329.16	443.6	Na-Ca-SO4-Cl-HCO3

Remark: ND is to mean Not Determined

Annex 5: Recharge rate computed for the eastern part of lower Awash Basin and Aysha Basin

S/No.	Location Name	ID	UTME	UTMN	Elv	Zone	Aver.P (mm/year)	Clp (mg/l)	ClGW (mg/l)	Recharge rate (mm/Year)
1	Biyobahay no7	AW-BH22	228536	1110869	965	38	662.81	0.91	23.66	25.49
2	Biyobahay no5	AW-BH23	229175	1110571	971	38	662.81	0.91	21.84	27.62
3	Biyobahay no6	AW-BH24	229915	1110283	979	38	662.81	0.91	28.21	21.38
4	Harawa TW	AW-BH15	826331	1097377	790	37	662.81	0.91	27	22.34
5	Alcho	AW-BH29	782134	1057523	1193	37	662.81	0.91	10.5	57.44
6	Aydora2	AW-HDW2	759968	1090121	796	37	662.81	0.91	29.5	20.45
7	Girmame-Maras	AW-HDW10	778533	1058777	1107	37	662.81	0.91	24.7	24.42
8	Asbuli	AW-HDW3	737763	1103347	1185	37	662.81	0.91	10.45	57.72
9	Dimtu	AW-HDW11	759331	1058654	1064	37	662.81	0.91	38	15.87
10	Khelwine	AW-HDW12	758665	1094670	780	37	662.81	0.91	49.4	12.21
11	Oerdela	AW-HDW13	754872	1084824	813	37	662.81	0.91	16.15	37.35
12	Sedit	AW-HDW15	768587	1069065	917	37	662.81	0.91	7.6	79.36
13	Gode	AW-HDW16	762251	1059159	1056	37	662.81	0.91	12.4	48.64
14	Keleme	AW-SP8	789029	1057941	1219	37	662.81	0.91	24.7	24.42
15	Afdem	AW-BH4	718770	1046429	1047	37	662.81	0.91	57.95	10.41
16	Sala'a	AW-BH32	704353	1056263	809	37	662.81	0.91	47.4	12.72
17	Alijir	AW-BH33	699990	1079698	745	37	662.81	0.91	26.6	22.68
18	Komiye	AW-BH34	705842	1031637	1219	37	662.81	0.91	34.2	17.64
19	Afase	AW-BH35	693369	1072568	777	37	662.81	0.91	37.05	16.28
20	Butuji	AW-BH36	692621	1057125	863	37	662.81	0.91	19	31.75
21	Adayitu	AW-BH37	692408	1230522	459	37	662.81	0.91	38.95	15.49
22	Der Ela	AW-HDW18	727546	1053854	1003	37	662.81	0.91	26.6	22.68
23	Afase	AW-HDW20	696625	1072311	776	37	662.81	0.91	24.7	24.42
24	Arabi	AW-BH42	250011	1098123	1114	38	662.81	0.91	24.7	24.42
25	Keranle	AW-BH43	225663	1081638	1354	38	662.81	0.91	43.7	13.80
26	Semekab	AW-BH44	219016	1078318	1322	38	662.81	0.91	24.7	24.42
27	Dembel town	AW-BH46	236715	1085654	1317	38	662.81	0.91	11.4	52.91
28	Harewa existing	AW-BH15	826859	1098079	797	37	662.81	0.91	29.45	20.48
29	Harey	AW-HDW4	812228	1126012	679	37	662.81	0.91	19.95	30.23
30	Degajebis	AW-HDW8	172107	1074025	1002	38	662.81	0.91	18.05	33.42
31	Tome	AW-BH50	815089	1067392	1089	37	662.81	0.91	33.25	18.14
32	Barak	AW-Sp12	819664	1073154	1000	37	662.81	0.91	32.3	18.67
33	Dure	AW-BH20	212061	1110383	864	38	662.81	0.91	30.4	19.84
34	Cheremiti-#2	AW-BH52	864535	1079607		37	662.81	0.91	39.6	15.23

35	Gende Boru	AW-SP14	803501	1050527		37	662.81	0.91	34.1	17.69
36	HARAWATU	AW-SP15	803522	1050333		37	662.81	0.91	39.6	15.23
37	Borte	AW-SP16	800391	1049534		37	662.81	0.91	17.6	34.27
38	Eftua	AW-SP19	843185	1054557		37	662.81	0.91	23.1	26.11
39	Keche	AW-SP23	820449	1046854		37	662.81	0.91	34.1	17.69
40	Serkama	AW-SP25	845129	1057387		37	662.81	0.91	34.1	17.69
41	Awale Roresa	AW-SP26	836775	1052144		37	662.81	0.91	28.6	21.09
42	Biyoawale	AW-SP28	829794	1052057		37	662.81	0.91	34.1	17.69
43	Legehare	AW-SP30	818219	1061625		37	662.81	0.91	56.1	10.75
44	Mudi Anano	AW-SP31	820995	1063252		37	662.81	0.91	39.6	15.23
45	Jarso-Gendelege	AW-SP32	852823	1049830		37	662.81	0.91	12.1	49.85
46	Legedomirga	AW-SP33	813438	1048587		37	662.81	0.91	56.1	10.75
47	Koriso	AW-SP36	799366	1051072		37	662.81	0.91	23.1	26.11
48	Bore TW4(2002)	AW-BH66	796050	1058100		37	662.81	0.91	14.6	41.31
49	Dechatu	AW-BH68	816294	1058832		37	662.81	0.91	28.6	21.09
50	Mudi Anano	AW-HDW39	819238	1066909		37	662.81	0.91	23.1	26.11
51	Belewa#1	AW-HDW42	840894	1058278		37	662.81	0.91	23.1	26.11
52	Gende Sur	AW-HDW43	799308	1062084		37	662.81	0.91	23.1	26.11
53	Bore	AW-HDW44	798554	1060531		37	662.81	0.91	34.1	17.69
54	Goladeg	AW-HDW48	802030	1067013		37	662.81	0.91	23.1	26.11
55	Chirmite	AW-BH69	206067	1079400	1170	38	662.81	0.91	32	18.85
56	Harmukale	AW-BH70	186257	1086571	943	38	662.81	0.91	45	13.40
57	Harwato	AW-BH71	220858	1085139	1285	38	662.81	0.91	56	10.77
58	Dembel	AW-BH72	236714	1085653	1319	38	662.81	0.91	21	28.72
59	Dini	AW-BH74	175896	1066152	1380	38	662.81	0.91	55	10.97
60	Gende Geboba	AW-BH75	172475	1056298	1613	38	662.81	0.91	44	13.71
61	Gerba Aneno	AW-HDW52	199173	1076201	1139	38	662.81	0.91	25	24.13
62	Jaldesa	AW-HDW54	182964	1075763	1081	38	662.81	0.91	44	13.71
63	Deriwenega/Oberi	AW-HDW56	282512	1085869	1433	38	662.81	0.91	22	27.42
64	Kore/Jarso	CS-4	196016	1049740	2540	38	662.81	0.91	2	301.58
65	GSE	AW-SP41	172099	1074021	1004	38	662.81	0.91	17	35.48
66	GSE	AW-SP42	187458	1064006	1384	38	662.81	0.91	49	12.31
67	GSE	AW-SP44	172562	1051954	1887	38	662.81	0.91	19	31.75
68	GSE	AW-SP45	177143	1053899	1798	38	662.81	0.91	37	16.30
69	GSE	AW-SP46	177395	1052611	1924	38	662.81	0.91	17	35.48
70	GSE	AW-SP48	183313	1057139	1777	38	662.81	0.91	16	37.70
71	GSE	AW-SP49	181739	1059937	1519	38	662.81	0.91	32	18.85
72	GSE	AW-SP50	179491	1053509	2014	38	662.81	0.91	15	40.21
73	GSE	AW-SP51	186359	1057417	1760	38	662.81	0.91	42	14.36
74	GSE	AW-SP52	191460	1056168	1713	38	662.81	0.91	15	40.21

75	GSE	AW-SP53	237635	1062805	1723	38	662.81	0.91	41	14.71
76	GSE	AW-SP55	200232	1053417	2136	38	662.81	0.91	15	40.21
77	GSE	AW-SP56	209138	1064329	1570	38	662.81	0.91	39	15.47
78	GSE	AW-SP59	216753	1056626	1974	38	662.81	0.91	46	13.11
79	GSE	AW-SP60	216753	1056626	2457	38	662.81	0.91	16	37.70
80	Hore	AW-HDW6	803160	1140980	652	37	662.81	0.91	32.76	18.41
81	Dengego	AW-SP1	820233	1046649	943	37	662.81	0.91	29.12	20.71
82	Kulubi	AW-SP2	792886	1042580	2394	37	662.81	0.91	10.92	55.23
83	Hades	AW-SP3	746448	1029765	2231	37	662.81	0.91	10.01	60.26
84	Salademer	AW-BH6	704217	1066296	813	37	662.81	0.91	51.88	11.63
85	Arberekete	AW-SP5	709494	1001112	2165	37	662.81	0.91	13.65	44.19
86	Afdem TW	AW-BH5	715616	1059980	895	37	662.81	0.91	23.66	25.49
87	Tutuftu	AW-BH84	685854	1009744	1528	37	662.81	0.91	31.7	19.03
88	Fa'o	AW-BH85	691053	1020494	1341	37	662.81	0.91	16.3	37.00
89	Huse Sodoma	AW-BH86	695877	1015842	1418	37	662.81	0.91	20.2	29.86
90	Ganda Aliware	AW-BH88	694136	1019853	1329	37	662.81	0.91	15.4	39.17
91	Umerguluf	AW-HDW23	193397	1197910	449	38	662.81	0.91	15.2	39.68
	Average									**29.15**
	Aysha Basin									
1	Gerbale	AYS-HDW22	241656	1176996	709	38	662.81	0.91	15.2	39.68
2	Biyegurgur	AYS-HDW25	247310	1149757	929	38	662.81	0.91	7.6	79.36
3	Meramedobes	AYS-HDW26	233951	1158904	861	38	662.81	0.91	5.7	105.82
4	Biyekebobe	AYS-HDW27	233272	1148331	937	38	662.81	0.91	8.55	70.54
5	Durdur	AYS-SP10	211558	1206305	498	38	662.81	0.91	21.85	27.60
6	Helele	AYS-HDW30	243177	1136277	1077	38	662.81	0.91	22.8	26.45
	Average									**58.24**